Investigating the impact of early-life adversity on perineuronal nets in the human brain

Claudia Belliveau

Integrated Program in Neuroscience

Faculty of Medicine and Health Sciences

McGill University, Montreal

January 2024

A thesis submitted to McGill University in partial fulfillment of the requirements of the degree of

Doctor of Philosophy

Table of Contents

Abstract

Severe child abuse experienced during the critical period of developmental brain plasticity significantly increases the risk of depression and suicide later in life. Perineuronal nets (PNNs), a condensed form of extracellular matrix (ECM), play a pivotal role in dampening the critical period of plasticity. These nets selectively enwrap specific neurons in the brain through a process that remains inadequately understood. Comprising primarily chondroitin-sulfate (CS) proteoglycans from the lectican family, PNNs consist of CS glycosaminoglycan (GAG) side chains attached to a core protein. CS disaccharides (CS-d) can manifest in various isoforms with distinct sulfation patterns, influencing the function and labeling of PNNs. The aim of this thesis was to investigate the impacts of child abuse on PNNs in the postmortem human brain.

We first examined the ventromedial prefrontal cortex (vmPFC), a brain area involved in emotion regulation and impulsivity. Our findings revealed a child-abuse associated increased density and maturity of PNNs in individuals who died by suicide during a depressive episode. Significantly, we implicated oligodendrocyte precursor cells for the first time in the genesis of PNN components—a process also altered by child abuse. We then explored PNN composition using liquid chromatography tandem mass spectrometry (LC-MS/MS) to read the sulfation code across various brain regions and species. Intriguingly, we found that early-life stress (ELS) does not exert a long-lasting impact on PNN composition. Lastly, we implicated a dampened microglia response to the persistent increased density of PNNs, by investigating matrix metalloproteinases (MMPs) and various factors implicated in microglial ECM degradation.

In conclusion, the findings presented in this thesis unveil enduring effects of child abuse on cortical PNNs and neuroplasticity in the human vmPFC, with glial cells likely contributing to this phenomenon. We posit that these alterations in PNN development and regulation may underlie

heightened vulnerability to psychopathologies and suicide, frequently observed in individuals who have experienced childhood maltreatment.

Resumé

La maltraitance infantile subie au cours de la période critique de la plasticité cérébrale augmente considérablement le risque de dépression et de suicide plus tard dans la vie. Les filets périneuronaux (FPN), une forme condensée de matrice extracellulaire (MEC), jouent un rôle essentiel dans l'atténuation de la période critique de plasticité. Ces filets enveloppent sélectivement des neurones spécifiques dans le cerveau par un processus qui reste mal compris. Composés principalement de protéoglycanes à base de chondroïtine-sulfate (CS) de la famille des lecticans, les FPN sont constitués de chaînes latérales de glycosaminoglycanes (GAG) CS attachées à une protéine centrale. Les disaccharides CS (CS-d) peuvent se manifester sous différentes isoformes avec des schémas de sulfatation distincts, influençant la fonction et le marquage des FPN. L'objectif de cette thèse était d'étudier les impacts de la maltraitance infantile sur les FPN dans le cerveau humain post-mortem.

Nous avons d'abord examiné le cortex préfrontal ventromédian (vmPFC), une région cérébrale impliquée dans la régulation des émotions et de l'impulsivité. Nos résultats ont révélé une augmentation de la densité et de la maturité des FPN associée à l'abus d'enfants chez les personnes décédées par suicide au cours d'un épisode dépressif. De plus, nous avons impliqué pour la première fois les cellules précurseurs d'oligodendrocytes dans la genèse des composants des FPN, un processus également altéré par la maltraitance infantile. Nous avons ensuite exploré la composition des FPN en utilisant la chromatographie liquide avec spectrométrie de masse en tandem (LC-MS/MS) pour lire le code de sulfatation dans différentes régions du cerveau et chez différentes espèces. Nous avons ensuite constaté (avec surprise) que le stress au début de la vie n'exerce pas d'impact durable sur la composition du FPN. Enfin, nous avons mis en évidence une réponse atténuée de la microglie à l'augmentation persistante de la densité des FPN, en étudiant

les métalloprotéinases matricielles et divers facteurs impliqués dans la dégradation de la MEC par la microglie.

En conclusion, les résultats présentés dans cette thèse révèlent des effets persistants de la maltraitance infantile sur les FPN corticaux et la neuroplasticité au sein du vmPFC humain, les cellules gliales contribuant probablement à ce phénomène. Nous postulons que ces altérations dans le développement et la régulation des FPN puissent être à l'origine d'une vulnérabilité accrue aux psychopathologies et au suicide, tous deux plus fréquents chez les individus ayant subi de la maltraitance au cours de l'enfance.

Acknowledgements

I would like to extend my profound gratitude to Dr. Naguib Mechawar whose immeasurable support has been instrumental in shaping my academic journey. Thank you for recognizing my intrinsic value as a researcher and entrusting me with the freedom to explore my ideas. I express my deepest appreciation to my advisory committee, Dr. Claire Dominique Walker and Dr. Cecilia Flores, your invaluable suggestions and insights have significantly enriched my research. I hold a special place in my heart for the Douglas MCMP, thank you to Melina Jaramillo Garcia and Dr. Bita Khadivjam for helping me discover my passion for microscopy. Thank you to my collaborator in Seattle, Dr. Kimberly Alonge, who went from being an author I used to cite to a key figure behind a main chapter in my thesis.

A special acknowledgment goes out to the McGill Group for Suicide Studies (MGSS) members, especially the Mechawarians, for fostering a nurturing environment where failure is acknowledged and questions are encouraged, supporting genuine growth throughout my graduate studies. A heartfelt thank you to Maria Antonietta Davoli, for being not just a lab mentor but an emotional support system. I would also like to recognize the students I've had the privilege of mentoring, who taught me the virtues of patience and leadership and contributed significantly to my research. Special thanks to Ashley McFarquhar, Refilwe Mpai, Stéphanie Théberge, Clémentine Hosdey, Stefanie Netto Rhea Xinxo and Nikki Lumley.

I owe a debt of gratitude to Dr. Arnaud Tanti and Dr. Reza Rahimian, whose postdoctoral expertise profoundly influenced my lab experience and depth of research. Your guidance has been invaluable.

To my parents, Antonia Di Paola and Dr. Thomas Belliveau, thank you for generously providing a rent-free haven and unwavering support during moments of research-induced

frustration and big presentations. To my sisters, Dr. Janet Belliveau and Pauline Belliveau, I could not have done this without your validation and emotional support. I would also like to extend gratitude to my extended family, including my grandma, aunts, uncles, cousins and friends, for being a consistent pillar of strength when I needed it most. To my love JS Chabot, thank you for assuming the role of my caretaker these past three years, I genuinely could not have written this thesis without your support.

This thesis is a culmination of the collective encouragement and support from each of you, and I am profoundly grateful for the role you've played in this significant journey.

I reserve my utmost appreciation for the individuals whose brains I had the privilege of studying. Their contribution has not only advanced scientific knowledge but has also left a profound impact on society. I hope their families recognize the significant role they've played in shaping our collective understanding.

~

This thesis is written in memory of

Antonino Di Paola, Paolina Vaccarino, Alessio Di Rico, Donald Belliveau, Vanessa Musacchio, Connie Chabala and Susan Mears.

~

Preface to the thesis

This thesis is presented in the manuscript-based format for Doctoral Theses, as described in the Thesis Preparation Guidelines set forth by the Department of Graduate and Postdoctoral Studies at McGill University. The work described here was performed by Claudia Belliveau under the supervision of Dr. Naguib Mechawar. This thesis contains four chapters: Chapter I is a review of the current background literature relevant to this thesis; Chapter II is an empirical manuscript that was published in *Molecular Psychiatry*; Chapter III is an empirical manuscript that is in preparation to be submitted for publication; Chapter IV is an empirical manuscript that is in preparation to be submitted for publication; Chapter V is a discussion of the findings from Chapters II-IV including concluding remarks and future directions.

Original contribution to knowledge

In our first study published in *Molecular Psychiatry*, we investigated the long-lasting impacts of child abuse on PNNs in postmortem human brain. The major impact of this publication is that we discovered a child abuse associated significant increase in density and maturity of PNNs in the vmPFC of depressed suicides. We described the phenotype of neurons encapsulated by PNNs in the vmPFC, providing the first detailed account of PNNs around excitatory cells in the postmortem human brain. Moreover, we established for the first time in human brain the potential involvement of oligodendrocyte precursor cells in PNN development—a process that is also disrupted by child abuse. The significance of this research has been highlighted by the publication of a Correspondence Article in the same journal by Poggi et al. [1] and our subsequent reply [2].

Our second study, soon to be submitted for publication in an academic journal, explores PNN composition in the postmortem human and mouse brains. This marks the first cross-species

comparison across multiple brain regions that characterizes the PNN sulfation code and labeling pattern. Our findings revel that sulfation code varies similarly across the healthy human and mouse brain with the hippocampus exhibiting hypersulfation and the (v)mPFC displaying hyposulfation. Intriguingly, PNN labeling by *Wisteria Floribunda Lectin* (WFL) and anti-aggrecan (ACAN) is dissimilar between brain regions and species. Notably, we are the first to examine these PNN phenotypes in the context of child abuse and in a limited bedding and nesting paradigm from postnatal day (PD)2-9 revealing a lack of disturbance in composition but not density.

Our third study, also prepared for journal submission, investigates the pathways orchestrating microglial regulation of PNNs in postmortem human brain. For the first time, we show that microglial MMP-9, -3 and their inhibitors are downregulated in the vmPFC of depressed suicides with a history of child abuse (DS-CA) compared to psychiatrically healthy controls (CTRL). Moreover, we suggest that communication between microglia and neurons through CX3CR1 and IL33R is dampened with child abuse, contributing to the increase in PNNs we observed in the first study.

Collectively, these findings are the first to identify lasting child abuse-associated changes in PNNs in brains from individuals having experienced child abuse. We also provide evidence for an involvement of oligodendrocyte precursor cells and of microglia in this phenomenon. Moreover, our identification of a limited bedding and nesting ELS mouse model that replicates our human findings provides a valuable tool for future exploration in this field.

Contribution of authors

Chapter I

CB conducted the literature review and wrote the introductory chapter under supervision of NM.

Chapter II

AT and NM conceived the study. GT participated in the acquisition and clinical characterization of the brain samples. AT, **CB**, FD, MAD, CC, RM and AM contributed to immunohistological experiments. AT, CN, MM and KP generated and analyzed the snRNA-seq data set. AT, **CB**, FC and ST performed the in-situ hybridization experiments. AT, **CB** and NM prepared the manuscript and all authors contributed to and approved its final version.

Chapter III

CB, KA and NM conceived the study. GT participated in the acquisition and clinical characterization of the brain samples. **CB**, ST, SN, CH and MAD contributed to immunohistological experiments. RR, GF and BG conducted animal work. KA, AH and KH conducted LC-MS/MS experiments. **CB** conducted data analysis. **CB**, NM, KA prepared the manuscript and all authors contributed to and approved its final version.

Chapter IV

CB, RR and NM conceived the study. GT participated in the acquisition and clinical characterization of the brain samples. **CB**, RR, GF and MAD contributed to experiments. BG and

NM supervised the study. **CB** conducted data analysis. **CB**, RR and NM prepared the manuscript and all other authors contributed and approved of its final version.

Chapter V

The writing and synthesis of all the information included in this thesis were conducted by **CB** under the supervision of NM.

List of abbreviations outside manuscripts

PNNs: perineuronal nets

ECM: extracellular matrix

CS: chondroitin-sulfate

GAG: glycosaminoglycan

CS-d: chondroitin-sulfate disaccharides

vmPFC: human ventromedial prefrontal cortex

LC-MS/MS: liquid chromatography tandem mass spectrometry

ELS: early-life stress

MMPs: matrix metalloproteinases

FPN: filets périneuronaux

MEC: matrice extracellulaire

MGSS: McGill Group for Suicide Studies

mPFC: mouse medial prefrontal cortex

WFL: *Wisteria Floribunda Lectin*

ACAN: aggrecan

PD: postnatal day

DS-CA: depressed suicides with a history of child abuse

CTRL: controls

HPA: hypothalamic-pituitary-adrenal

MDD: Major Depressive Disorder

PV: Ca^{2+}-binding protein parvalbumin

PSA-NCAM: α-2,8-polysialic acid bound to neural cell adhesion molecule

Otx2: orthodenticle homeobox 2

BDNF: brain-derived neurotrophic factor

NARP: neuronal regulated pentraxin

GlcNAc: N-acetylglucosamine

GalNAc: N-acetylgalactosamine

GlcA: D-glucuronic acid

IdoA: L-iduronic acid

CSPGs: chondroitin-sulfate proteoglycans

TnR: Tenascin-R

HAPLN1: hyaluronan and proteoglycan link protein 1

chABC: chondroitinase ABC

SDPS: social defeat-induced persistent stress

LCM: laser capture microdissection

Chapter I: Introduction

Child abuse and suicide

The latest Canadian Economic and Social Report (2023) reveals that nearly 60% of Canadians have experienced at least one form of maltreatment or neglect before the age of 15 [3]. Child abuse encompassing sexual, physical or emotional maltreatment or neglect of a youth by a parent or caregiver causes harm to a child's development and is a pervasive issue [4]. This maltreatment's repercussions extend far beyond childhood, impacting neurodevelopment fostering social, emotional and cognitive challenges. Such challenges often manifest in risky behaviors, leading to broader issues like disability, low socio-economic status, disease and premature mortality [5, 6]. Experiencing child abuse has been linked to dysregulation of the hypothalamic-pituitary-adrenal (HPA) axis, the sympathetic nervous system and inflammation which confers a high risk of developing physical health issues such as coronary heart disease, hypertension and diabetes mellitus [7]. Moreover, individuals with a history of child abuse face an increased susceptibility to psychopathologies like posttraumatic stress disorder, substance use disorder and mood disorders [8-10].

Impact on the brain

Given the significant association between child abuse and adverse outcomes in adulthood, it is crucial to delve into the specific changes that contribute to these negative consequences. Extensive research supports the notion that child abuse profoundly shapes the trajectory of brain development [10-12]. Studies indicate precocious maturation of the HPA axis [13, 14] and the memory network [15] with lasting effects observable later in life. The impact extends beyond

functional aspects, with evidence pointing towards molecular [16, 17] and epigenetic [18] alterations in the brain's regulatory mechanisms. Research from our lab underscores this impact, revealing specific child abuse associated DNA methylation changes in oligodendrocyte genes and reduced myelin thickness within the brain of adults who died by suicide during a depressive episode [19]. Furthermore, these individuals exhibit a shift towards more mature phenotypes of oligodendrocyte lineage cells in the vmPFC white matter, highlighting the enduring consequences of early-life maltreatment [20]. Lifelong effects are further evidenced through neuroimaging studies, exposing impaired connectivity between regions that also exhibit structural changes. For example, there is a childhood maltreatment specific increase in responsiveness of the right amygdala to threatening faces. This heightened reactivity is particularly noteworthy considering the amygdala's extensive connections with regions commonly impacted by child abuse including the hippocampus, vmPFC and the dorsal anterior cingulate cortex. Intriguingly, these interconnected areas play a crucial role in the conscious perception of threat detection [21]. Volume loss and hypoactivity of the medial prefrontal cortex [22-24] and abnormalities in the fronto-limbic white matter tracts [25, 26] further underscore the far-reaching impact of child abuse on the brain into adulthood. Overall, alterations in network architecture and brain connectivity related to childhood maltreatment are present in adulthood and may be linked to developmental maladaptations carried throughout life [27, 28].

Major Depressive Disorder

Child abuse is a significant predisposing factor associated with the development of mood disorders. Globally, a staggering 300 million people suffer from Major Depressive Disorder (MDD) [29]. This psychopathology is a leading cause of disability worldwide, imposing burden

to those who suffer by interfering with everyday life and hindering role performance [29, 30]. Symptoms include but are not limited to anhedonia, appetite issues, disturbed sleep and suicidal ideation. Current treatments include pharmacotherapy, psychotherapy or a combination of both. However, the response to treatment remains moderate, achieving remission of symptoms in only a subset of patients (~50%) [31, 32]. Complicating matters further, most antidepressants exhibit a delayed onset of action (4-6 weeks) often accompanied by many negative side effects. These factors, coupled with low patient motivation, contribute to non-compliance [33]. Furthermore, depressed individuals with a history of child abuse suffer more recurrent and severe episodes and are more likely to be non-responders to treatments [6, 34]. Tragically, the much too frequent outcome of MDD is suicide, claiming over 700,000 lives annually worldwide [35]. In Canada, the suicide rate is approximately three times higher in males compared to females, with the most affected age group ranging from 50-64 years old [36]. Understanding the profound impact of child abuse and unraveling the neurobiological underpinnings of MDD is imperative for developing more precise and effective treatments that can significantly enhance the quality of life for those suffering. Additionally, investigating the effects of child abuse lasting into adulthood is especially important in the prevention of suicide, providing concrete evidence to inform policy makers and shape strategies for betterment of mental health outcomes.

Critical periods of brain plasticity

Childhood and early adolescence are marked by a critical period of neural plasticity primarily described in the cerebral cortex. During this period, neural connections are quite malleable and more susceptible to external environmental influences. Seminal research from Hubel and Wiesel (1963) illuminating the essential role of visual stimulation for proper

neurodevelopment within the visual system was pivotal in understanding the dynamics of normal critical periods [37, 38]. Their studies on cats and monkeys revealed that monocular deprivation early in life, or during a critical period of plasticity, leads to cortical expansion for the non-deprived eye. When monocular deprivation occurs after this window has closed, the shift in cortical circuit response is absent, implying reduced plasticity in more mature brain circuits [37].

This phenomenon of activity-dependent development is not exclusive to the visual system but also extends to other cortical areas, such as the rodent somatosensory (barrel) cortex [39] and auditory cortex [40]. Critical periods, characterized by synaptic pruning, axonal growth, and neural circuit modifications, necessitate the convergence of sensory stimulation and molecular events for their proper initiation. In the pre-critical period, inhibitory connections mature later than excitatory circuits and only once a balancing of excitatory/inhibitory neurotransmission is achieved can a critical period of plasticity begin [41]. Critical periods are initiated by the downregulation of molecules inhibiting plasticity and the maturation of GABAergic inhibitory interneurons. In neocortex, neuronal networks primarily consist of glutamatergic excitatory pyramidal neurons, with GABAergic inhibitory interneurons accounting for approximately 10% of neurons [42]. These interneurons modulate the information relay capacity of pyramidal neurons through strong inhibitory inputs proximal to the cell soma. GABAergic interneurons can be categorized into subclasses based on their morphology, electrophysiological properties and expression of cell markers such as Ca^{2+}-binding protein parvalbumin (PV), neuropeptide somatostatin and ionotropic serotonin receptor [43, 44]. PV interneurons, the most common and extensively studied inhibitory interneurons, play a crucial role in critical period plasticity [43, 45]. Recognized for their fast-spiking action potentials, PV interneurons directly regulate the firing of neighboring excitatory neurons [46]. They can be classified as basket or chandelier cells based on their morphology and

location of their synaptic end feet on the pyramidal cell. PV basket cells have multiple dendrites extending through multiple layers of the cortex and provide massive inhibition by wrapping around pyramidal cell soma and proximal dendrites [47]. PV basket cells are integral to feedforward and feedback inhibition, orchestrating neural circuit synchronization that gives rise to gamma oscillations crucial for normal cognition and memory consolidation [47, 48].

In early life, critical period onset is impeded by α-2,8-polysialic acid bound to neural cell adhesion molecule (PSA-NCAM) on the cell surface which prevents the internalization of non-cell autonomous maturation factors like orthodenticle homeobox 2 (Otx2) into PV interneurons. Essentially, sensory input causes up-regulation of brain-derived neurotrophic factor (BDNF) and neuronal regulated pentraxin (NARP), promoting inhibitory cell maturation and downregulation of PSA-NCAM [41], ultimately allowing for the opening of the critical period of plasticity.

Critical periods in the human brain are well illustrated by amblyopia (lazy eye) which is effectively treated before the eighth year of life by increasing sensory input to the affected eye. Treatment outside of this timeframe proves futile, leading to permanent loss of visual acuity [49]. Human neurodevelopment is defined by multiple cascading critical periods, initiating with the development of sensory areas, progressing to motor and language areas and culminating in the modification of higher cognition circuits during late adolescence / early adulthood [45].

Broadly speaking, these critical periods are primarily dampened by molecular brakes known as PNNs, as discussed below. While additional factors such as epigenetic (posttranslational) modifications and myelin-associated signaling through Nogo receptor/PirB contribute to the closure of critical periods of plasticity [41] they fall outside the scope of this thesis.

Perineuronal nets

The ECM, a structural framework composed of collagens, enzymes, and glycoproteins, forms a three-dimensional network surrounding cells, providing essential support. Present throughout the body, ECM properties and composition vary depending on its location [50]. The brain ECM is primarily composed of GAGs, unbranched polysaccharide chains made up of repeating CS-disaccharide units. These units consist of N-acetylglucosamine (GlcNAc) or N-acetylgalactosamine (GalNAc) paired with either D-glucuronic acid (GlcA) or L-iduronic acid (IdoA). These GAGs exist either in an unbound form called hyaluronan or are bound to a core protein and named proteoglycans. Brain ECM contains minimal amounts of fibrous proteins like fibronectin and collagens in comparison to connective tissue [51].

PNNs are a condensed form of ECM that form a net-like covering around certain cells in the central nervous system. These structures were first described in 1893 by Camilo Golgi as reticular structures enwrapping the largest dendrites and cell bodies of particular neurons. For twenty years, the nets were studied intently by histologists, until Ramón y Cajal described them as staining artifact and many lost interest [52]. However, renewed curiosity in the past two decades recognizes PNNs as significant contributors to the attenuation of critical periods of plasticity.

Establishment of PNNs begins as neurons mature, occurring as early as PD14 in the rodent cortex [53] and from as young as 2 months after birth in humans [54]. The number of PNNs continues to increase until PD33/40 in rodents [53, 55] and until between 8-12 years old in humans [54, 56], coinciding with the end of the critical period of plasticity. Present throughout most of the central nervous system, PNNs have been identified in amphibians, reptiles [57], songbirds [58] and mammals. Studies in rodents and humans reveal their highest densities in the motor and somatosensory cortex. Additionally, these structures are also present in the spinal cord, prefrontal

cortex, cerebellum and extend into subcortical structures such as the hippocampus and amygdala [59, 60]. Interestingly, PNNs predominantly enwrap PV interneurons, constituting around 70-80% of the covered neurons in the visual, sensory, and motor cortices, as well as the amygdala and hippocampus [54, 59]. While further research is needed to identify the entirety of the remaining 20-30% of covered cells, it has been observed that in CA2 of the hippocampus, in the amygdala and cortex, excitatory pyramidal cells can also be ensheathed by PNNs [59].

Structure and function

PNNs are predominantly composed of chondroitin-sulfate proteoglycans (CSPGs) from the lectican family, including aggrecan, brevican, neurocan and versican. While the synthesis of PNNs is not entirely understood, their components seem to be secreted by various cell types, including neurons or surrounding glial cells [57]. For example, neurocan and brevican mRNA are present in neurons, phosphocan mRNA is detected in astrocytes and versican mRNA is found in both astrocytes and oligodendrocytes [61, 62]. These CSPGs consist of varying numbers of CS-GAG side chains attached to a core protein. The complexity deepens with the number of disaccharides present in a CS-GAG side chain and their sulfation pattern offering several isoforms that facilitate the preferential binding of specific proteins or growth factors [63]. The ratio of 4-sulfation (4S) to 6-sulfation (6S) is important for the stability of the PNN structure [64-66]. An experimental increase in 6-sulfation, establishing a low 4S/6S ratio, induces increased plasticity in the brain [67]. Moreover, di-sulfation (4S6S) is responsible for the binding of Semaphorin 3A, an axonal chemorepellent molecule [68] and Otx2 protein [69, 70]. Interestingly, there is a positive feedback loop with mature PNNs capturing extracellular Otx2, facilitated by the specific binding motif 4S6S. This allows for persistent accumulation of Otx2 in PV cells throughout adulthood, believed

to be crucial for inhibitory cell function [70, 71]. CSPGs of PNNs are attached at their N-terminus through link proteins to a hyaluronan backbone secreted by hyaluronan synthase located on the cell surface. At their C-terminus, these CSPGs bind to one another through Tenascin-R (TnR), forming a highly organized mesh-like structure [72, 73].

The molecular organization of PNNs creates specific holes that may play a role in the storage of long-term memories [74]. These openings seem to stabilize incoming connections onto the enwrapped cell. Literature suggests that processes from other inhibitory interneurons, astrocytes and pyramidal cells enter the holes forming synaptic connections with the cell beneath [75]. As PNNs mature, the apertures gradually diminish, implying a tightening grasp on the processes entering them. This phenomenon has been examined with super-resolution microscopy, revealing an increase in inhibitory connections through the perforations onto the cell beneath, accompanied by a reduction in the surface area of the holes over time [76]. These findings complement the body of literature suggesting that PNN maturity can be inferred by the intensity of their immunohistochemical staining, which correlates with the activity level of the cell enwrapped introducing variability from one PNN to the next [77, 78].

Visualizing PNNs involves labeling with various lectins or a combination of different antibodies targeting the lectican family of CSPGs. WFL stands out as the most extensively published PNN marker in the literature. It is believed to bind to non-sulfated carbohydrate structures terminating in GalNAc, linked α or β to the 3 or 6 position of galactose [79, 80]. Intriguingly, WFL was initially considered pan-PNN marker expected to always co-label with anti-CSPG in immunofluorescence [81]. However, more rigorous examination across various species and brain regions reveal that different labeling methods capture distinct sub-populations of PNNs [82-85].

PNNs play a pivotal role as versatile regulators in the brain, orchestrating various essential functions. At the molecular-level, they intricately regulate synaptic plasticity by restricting the lateral mobility of AMPA receptors on the cell membrane [86]. Due to their highly negative charge, PNNs provide a protective environment for the underlying cell by acting as a cation buffer barrier [87]. Furthermore, PNNs generally enhance the excitability of fast-spiking inhibitory neurons, contributing to the amplification of network inhibition (reviewed in [88]). This phenomenon is demonstrated by the inability of PV interneurons to maintain fast-firing after local treatment with chondroitinase ABC (chABC) in the medial nucleus of the trapezoid body [89], hippocampus [90], entorhinal cortex [91] and within the prefrontal cortex [92]. It has also been shown that PV neurons with PNNs have higher levels of perisomatic excitatory and inhibitory puncta and when these nets are degraded with chABC in the mPFC, there is a reduction in gamma oscillations, suggesting network connectivity issues with the loss of PNNs [93].

Additionally, these nets play a role in mediating the toxicity of reactive-oxidative species generated by the high-frequency firing of the PV inhibitory interneurons beneath [94, 95]. Notably, the protective properties of PNNs against iron-induced oxidative stress is contingent on the presence of specific components including aggrecan, TnR and hyaluronan and proteoglycan link protein 1 (HAPLN1) [94]. Altering the structure of PNNs through enzymatic degradation of their CS-GAGs using chABC has allowed for the study of this functional property more closely. This process renders mature PV neurons and their fast rhythmic firing more susceptible to oxidative stress [95].

PNNs also regulate the closure of the critical period of plasticity. This phenomenon has been investigated through loss-of-function experiments. For instance, in the visual cortex of adult rodents, when chABC is used to degrade PNNs, a juvenile-like shift in ocular dominance is

observed [96]. This research provides insights into the understanding that the critical period of brain plasticity is not simply terminated but actively controlled by factors such as PNNs. Furthermore, literature from the same brain region suggests that chABC-induced degradation of PNNs can reinstate juvenile-like plasticity, resulting in decreased inhibition and increased gamma activity [92].

Information storage

PNNs are implicated in the storage of long-term memories by limiting feedback inhibition from PV cells onto projection neurons [97]. These nets play a crucial role in learning and memory (reviewed in [98]). In rodent research, it has been observed that the transition in fear memory resilience occurs at the conclusion of the critical period, aligning with the establishment of PNNs. Fear memories formed in adulthood, which are resistant to extinction and associated with posttraumatic stress disorder, are actively protected by PNNs in the amygdala. Notably, degradation of these nets with chABC allows for the extinguishment of subsequent fear memories in adult mice [99]. Moreover, ELS such as maternal separation, can induce a premature shift in fear memory resilience in rodent models. This suggests that juvenile rats exhibit adult-like resistance to fear memory extinction [100], aligning with the precocious maturation theory of child abuse [13, 14].

Additionally, investigations into addiction relapse, focusing on persistent drug memories during abstinence shed light on PNNs as regulators of this phenomenon [101]. Specifically, studies show that cocaine self-administration [102] and cue-induced reinstatement of cocaine seeking are decreased in mice with intracranial infusion of chABC directly into the lateral hypothalamic area [103].

Collectively, these findings suggest the potential for treatments that influence critical periods by degrading PNNs in vivo, thereby reopening critical periods of plasticity and facilitating the reformation of learning circuits. However, it is crucial to acknowledge the dual nature of this approach, as excessive plasticity may pose risks. The carefully orchestrated cascade of critical periods has evolved for specific reasons and interventions influencing plasticity in one area or circuit may lead to network dysregulation and unintended long-lasting effects [104].

Regulation

Despite the existence of PNNs being recognized since 1893 [52], there are numerous aspects that remain elusive. In the last four years, researchers have dedicated efforts to unravel the intricacies of how PNNs are regulated in health and disease. As mentioned previously, the formation of these nets appears to involve various cell types, encompassing both neurons and glia. The maintenance and remodelling of PNNs also seems to engage multiple cell types. For instance, oligodendrocytes appear to orchestrate PNN remodelling in the adult mouse median eminence under fasting and refeed conditions. This process involves the upregulation of Adamts4 (disintegrin and metalloproteinase with thrombospondin motifs 4) in the fasted state leading to a reduction in WFL+ PNNs. Conversely, in the refed state, oligodendrocytes upregulate PNN components such as TnR, resulting in a reinstatement of homeostatic levels of PNNs in this brain area implicated in energy balance [105].

More prominently, microglia emerge as potent regulators of PNNs, either through secretion of enzymes that degrade PNN components or by directly digesting the nets. Firstly, MMPs stand out on their own as important enzymes involved in the regulation of cortical plasticity [106]. Specifically, MMP-9 is expressed in the brain, secreted by both neurons and glia and plays a pivotal

role in the development and maturation of neural circuits [107]. Interestingly, microglial MMP-9 has been shown to be involved in PNN degradation in multiple studies [108-111]. Animal studies demonstrate that MMP-9 deficient mice have abnormalities in neural circuit formation and a surplus of PNNs forming around PV interneurons in the auditory cortex [110].

Multiple studies in humans have found elevated MMP-9 levels in blood plasma [112], as well as a reduction in PNNs in postmortem amygdala, entorhinal cortex [113] and layers III and V of the prefrontal cortex [56] in individuals with schizophrenia. The diminished density of nets is proposed to exemplify a failure to stabilize inhibitory circuitry leading to the development of psychosis [41]. Moreover, disturbances in the 4S/6S ratio in schizophrenia, evidenced by an increase in 4-sulfation measured by immunoblotting in postmortem human hippocampus, may contribute to abnormalities observed in PNNs in this psychopathology [114]. Recent advancements, such as the method optimized by Alonge et al. (2019), enable the detection of differentially sulfated CS-disaccharides within the ECM, particularly PNNs, using LC-MS/MS with a multiple reaction monitoring method [66]. This advanced technology promises to unveil the composition, binding properties and integrity of PNNs in various psychiatric disorders and neurodegenerative diseases. Furthermore, inconclusive results comparing MMP-9 expression in peripheral blood between depressed and psychiatrically healthy controls necessitate further research to comprehend the intricate link between MMP-9 and the regulation of PNNs in depression [115].

Two seminal studies conducted by Crapser et al. (2020 a,b) establish a direct relationship between PNNs and microglia across various conditions, including healthy mouse brain, a Huntington's disease mouse model and Alzheimer's disease in both a mouse model and human brain [116, 117]. In the Huntington's disease mouse model marked by heightened microglia

activation, a noticeable reduction in WFL+ PNN density occurs in the striatum. Intriguingly, depleting microglia in this disease model the naïve littermate results in an augmented presence of PNNs [116]. Furthermore, in the Alzheimer's disease brain, microglia are observed in proximity to damaged PNNs, with fragments of the nets discovered in the lysosomes of activated microglia in both species [117]. This phenomenon has also been observed in visual cortex of both male and female adult mice. Upon microglial depletion using CSF1R inhibitor, there are dramatic increases in PNN intensity and density and enhanced activity of both excitatory and PV inhibitory neurons [118]. While the association between microglia regulation and PNNs is evident, the precise mechanisms underlying this relationship remain to be elucidated.

Perineuronal nets in mood disorders

Recently, PNNs have emerged as significant players in the context of depression (reviewed in [119]). Specifically, a rat model of social defeat-induced persistent stress (SDPS) revealed noteworthy implications. In the dorsal hippocampus CA1, there was an observed augmentation in PNN-covered PV interneurons, coinciding with a decrease in inhibitory firing frequency of these cells. Notably, the administration of chABC to SDPS mice resulted in a reduction of perineuronal nets, subsequently restoring inhibition [120]. These discoveries propose a nuanced function for PNNs in regulating inhibition across distinct brain regions, as evidenced by contrary associations between PNNs and firing observed in the medial nucleus of the trapezoid body [89], hippocampus [90], entorhinal cortex [91] and within the prefrontal cortex [92]. Furthermore, in a rodent model of depression induced by chronic unpredictable mild stress, a decreased density of PNNs are found in the prelimbic cortex [121]. Although investigations into PNNs in MDD among humans are lacking, a decrease in PNNs in layer II of the entorhinal cortex has been reported in postmortem

human brains diagnosed with bipolar disorder [113], with no discernible difference in the prefrontal cortex [56]. These intriguing findings underscore the intricate involvement of PNNs in the neurobiology of depression and emphasize the need for further exploration in human subjects.

Antidepressants, while effective for a subpopulation of MDD patients, pose a conundrum as their mechanisms of action remain incompletely understood. Questions persist regarding their impact on neurogenesis and the enhancement of excitatory transmission. Moreover, the efficacy of antidepressants is minimized in individuals with a history of child abuse, yet the precise reasons for this phenomenon remain elusive [34]. Studies propose that monoamine reuptake inhibitors, such as Venlafaxine, reduce PNN integrity, thereby decreasing the excitability of inhibitory PV interneurons. Alaiyed et al. (2018, 2019) suggest that Venlafaxine achieves this by upregulating proteases such as MMP-9 in the hippocampus. This hypothesis has been tested both in wild type mice [108] and a stress induced depression mouse model characterized by an increased number of PNNs [109]. Additionally, Fluoxetine treatment in adult mice has been found to decrease the number of PNNs in the amygdala, CA3 of the hippocampus and the mPFC of mice. Additionally, it leads to a reduction in the expression of PV within interneurons [122]. These findings suggest that monoamine reuptake inhibitors induce juvenile-like states in mature inhibitory PV interneurons to alleviate symptoms of depression.

Gamma oscillations are modulated by PV inhibitory interneurons and are disturbed in depressed individuals with the dampening of these waves related to decreased cognition and memory deficits [123]. Achieving remission with antidepressants like ketamine or monoamine reuptake inhibitors is associated with the restoration of gamma oscillations in humans [123]. Animal models, in this context, show us that an increase in gamma power is accompanied by a decrease in number of perineuronal nets [108, 109]. Understanding these effects is particularly

significant for future treatments, especially for individuals with a history of child abuse who exhibit increased resistance to conventional treatments. It is also crucial to consider the potential influence of antidepressant medications when studying PNNs, as subjects may have been prescribed and taken antidepressants before death.

Perineuronal nets and early-life stress

The impact of child abuse on PNNs have not yet been investigated in the postmortem human brain, serving as the central focus of this thesis. Despite this gap in knowledge, recent studies have delved into the effects of ELS on WFL+ PNNs using rodent models [124]. In a 2015 study examining perinatal exposure to specific substances, fluoxetine exposure did not alter parvalbumin expression or density but resulted in a delayed formation of PNNs, leading to reduced PNNs at postnatal days 17 and 24 in the amygdala and hippocampus [125]. A 2018 study using a scarcity-adversity mouse model linked an enhanced threat response from the basolateral amygdala to a reduction in PV-mediated synaptic inhibition and decreased PNNs at weaning age [126]. Another study in the same year, employing chronic mild unpredictable stress in mice, revealed a decrease in PV cell number in the prelimbic cortex, with no effect of ELS on PNN density. In 2019, a study using a maternal separation mouse model with early weaning reported a decreased intensity of PV inhibitory interneurons along with an increased intensity of PNNs. Interestingly, no change in density was observed in the ventral CA1 of the hippocampus [127]. A 2020 study in a rat model of maternal separation revealed sex-specific, region-specific effects, including decreased density in the prelimbic and prefrontal cortex of juvenile male mice, restored in adulthood. Changes in the intensity of PNNs around PV interneurons were noted in adulthood, with no such effect observed for those surrounding other unspecified cell types. Both males and females exhibited a reduced

density of PNNs in the infralimbic cortex in adulthood, with no effect on intensity. Additionally, there was an increased number of nets in the basolateral amygdala of male adolescent rats [128]. Later in the same year, the same findings, along with increased synaptic plasticity, were replicated in an ELS model of limited bedding but only observed in the right hemisphere [129]. In 2022, ACAN+ PNNs were found to be upregulated in the anterior cingulate cortex of an early-life social stress model [130].

These studies underscore the existence of region-specific changes to PNNs resulting from diverse paradigms of ELS. Emphasizing the need to explore the effects of child abuse on PNNs in human samples. This research is crucial considering the vast differences in the human experience compared to that of rodents.

Rationale and objectives

In the above comprehensive review of relevant literature, it is evident that stressful external environments during early-life exert profound and enduring effects on brain development, supported by extensive animal studies and a limited number of human studies. Notably, different animal models yield divergent results, underscoring the necessity for research endeavors examining the model of interest, human brain. The primary objective of this thesis is to examine postmortem brains from individuals who died by suicide during a depressive episode, specifically aiming to decode the enduring impacts of child abuse on the human brain. This investigation is particularly focused on PNNs, recognizing their significance as a regulator of neuroplasticity.

The research hypothesis postulates that child abuse induces alterations in brain network connectivity through the modified recruitment and regulation of PNNs, particularly orchestrated by glia, in brain areas previously shown to be affected by child abuse. The specific aims of this research are as follows:

Aim 1: Characterize PNNs in brain samples from individuals having experienced child abuse

1.1 Identify the cell types enwrapped by WFL+ PNNs.

1.2 Examine WFL+ PNN density and intensity.

1.3 Explore PNN sulfation and labeling patterns

Aim 2: Explore microglial regulation of PNNs in brain samples from individuals having experienced child abuse

2.1 Examine bulk tissue expression levels of PNN regulators.

2.2 Investigate expression levels of PNN regulators in microglia.

Aim 3: Explore cortical PNNs in a mouse model of early-life adversity

3.1 Investigate WFL+ PNN density.

3.2 Explore PNN sulfation and labeling patterns.

Chapter II

Preface to chapter II

To fulfill the objectives of my research, we initiated a comprehensive exploration of the PNN landscape in the healthy human brain. Subsequently, we conducted a comparative analysis involving depressed suicides, considering their history of child abuse. Within this chapter, we present a detailed overview not only of the distribution of WFL+ PNNs in the vmPFC across different layers but also illuminate the specific cell types enwrapped by PNNs in the human brain. For the first time, we provide a description of the contribution of PNN components by oligodendrocyte precursor cells. Furthermore, we delve into the spatial relationship between this cell type and PV interneurons, offering fresh insights into the intricate arrangement of PNNs in the human brain. This chapter was published in *Molecular Psychiatry* in 2022 and successfully completes Aim 1.1 and 1.2 of the thesis goals.

Child abuse associates with increased recruitment of perineuronal nets in the ventromedial prefrontal cortex: a possible implication of oligodendrocyte progenitor cells

Arnaud Tanti[1,2,5], Claudia Belliveau[1,3,5], Corina Nagy[1], Malosree Maitra[1,3], Fanny Denux[1], Kelly Perlman[1,3], Frank Chen[1], Refilwe Mpai[1,3], Candice Canonne[1,3], Stéphanie Théberge[1,3], Ashley McFarquhar[1], Maria Antonietta Davoli[1], Catherine Belzung[2], Gustavo Turecki[1,3,4] and Naguib Mechawar[1,3,4]

[1]McGill Group for Suicide Studies, Douglas Mental Health University Institute, McGill University, Montreal, QC, Canada.

[2]UMR 1253, iBrain, Inserm, Université de Tours, Tours, France.

[3]Integrated Program in Neuroscience, McGill University, Montreal, QC, Canada.

[4]Department of Psychiatry, McGill University, Montréal, QC, Canada.

[5]These authors contributed equally: Arnaud Tanti, Claudia Belliveau.

Correspondence and requests for materials should be addressed to Arnaud Tanti (arnaud.tanti@inserm.fr) or Naguib Mechawar (naguib.mechawar@mcgill.ca).

Molecular Psychiatry (2022) 27:1552–1561; https://doi.org/10.1038/s41380-021-01372-y

Abstract

Child abuse (CA) is a strong predictor of psychopathologies and suicide, altering normal trajectories of brain development in areas closely linked to emotional responses such as the prefrontal cortex (PFC). Yet, the cellular underpinnings of these enduring effects are unclear. Childhood and adolescence are marked by the protracted formation of perineuronal nets (PNNs), which orchestrate the closure of developmental windows of cortical plasticity by regulating the functional integration of parvalbumin interneurons into neuronal circuits. Using well-characterized post-mortem brain samples, we show that a history of CA is specifically associated with increased densities and morphological complexity of WFL-labeled PNNs in the ventromedial PFC (BA11/12), possibly suggesting increased recruitment and maturation of PNNs. Through single-nucleus sequencing and fluorescent in situ hybridization, we found that the expression of canonical components of PNNs is enriched in oligodendrocyte progenitor cells (OPCs), and that they are upregulated in CA victims. These correlational findings suggest that early-life adversity may lead to persistent patterns of maladaptive behaviors by reducing the neuroplasticity of cortical circuits through the enhancement of developmental OPC-mediated PNN formation.

Introduction

Child abuse (CA) has enduring effects on psychological development. Severe adversity during sensitive periods, during which personality traits, attachment patterns, cognitive functions, and emotional responses are shaped by environmental experiences, has a profound effect on the structural and functional organization of the brain [1].

At the cellular level, childhood and adolescence are marked by the protracted maturation of neural circuits, characterized by windows of heightened plasticity that precede the development of

functional inhibitory connections and the balance of excitatory–inhibitory neurotransmission [2]. A major mechanism involved in this process is the recruitment of perineuronal nets (PNNs), a condensed form of extracellular matrix (ECM) forming most notably around parvalbumin-expressing (PV+) interneurons. PNNs are thought to gradually decrease heightened plasticity by stabilizing the integration and function of PV+ cells into cortical networks and hindering the remodeling of these networks [3,4]. This has been notably linked to the persistence of long-term associations, including fear memories [5–7].

Evidence in rodents suggests that early-life stress associates with precocious functional maturation of PV+ neurons and the early emergence of adult-like characteristics of fear and extinction learning [8], in addition to discrete changes in the immunoreactivity of inhibitory neuron markers and PNNs [9]. Taken together, these observations suggest that CA may alter the formation of PNNs.

We addressed this question using well-characterized post-mortem samples from adult depressed suicides, who died during an episode of major depression with (DS-CA) or without (DS) a history of severe CA and from matched psychiatrically healthy individuals (CTRL). Standardized psychological autopsies were conducted to provide comprehensive post-mortem diagnosis and retrieve various dimensions of childhood experience, including history and severity of CA. We focused on the ventromedial prefrontal cortex (vmPFC), encompassing Brodmann areas 11 and12 in our study, a brain area closely linked to emotional learning, and which is structurally and functionally altered in individuals with a history of CA [1,10–13].

Materials and methods

Human post-mortem brain samples

Brain samples were obtained from the Douglas-Bell Canada Brain Bank (Montreal, Canada). Phenotypic information was retrieved through standardized psychological autopsies, in collaboration with the Quebec Coroner's Office and with informed consent from the next of kin. Presence of any or suspected neurological/neurodegenerative disorder signaled in clinical files constituted an exclusion criterion. Cases and controls are defined with the support of medical charts and Coroner records. Proxy-based interviews with one or more informants best acquainted with the deceased are supplemented with information from archival material obtained from hospitals, Coroner's office, and social services. Clinical vignettes are then produced and assessed by a panel of clinicians to generate Diagnostic and Statistical Manual of Mental Disorders (DSM-IV) diagnostic criteria, providing sociodemographic characteristics, social developmental history, DSM-IV axis I diagnostic information, and behavioral traits—information that is obtained through different adapted questionnaires. Toxicological assessments and medication prescription are also obtained. As described previously [14], characterization of early-life histories was based on adapted Childhood Experience of Care and Abuse interviews assessing experiences of sexual and physical abuse, as well as neglect [15], and for which scores from siblings are highly concordant [16]. We considered as severe early-life adversity (ELA) reports of non-random major physical and/or sexual abuse during childhood (up to 15 years). Only cases with the maximum severity ratings of 1 and 2 were included. This information was then complemented with medical charts and Coroner records. Because of this narrow selection criterion, it was not possible to stratify different types of abuse within the sample.

Group characteristics are described in Table 1. Correlations between covariates (age, post-mortem interval (PMI), pH, substance dependence, and medication) and the variables measured in our study are presented in Supplementary Table 1.

Tissue dissections

Dissections were performed by expert brain bank staff on fresh-frozen 0.5cm-thick coronal sections with the guidance of a human brain atlas [17]. vmPFC samples were dissected in sections equivalent to plate 3 (approximately−48 mm from the center of the anterior commissure) of this atlas, corresponding to Brodmann areas 11 and 12. Samples were either kept frozen or fixed overnight in 10% formalin until processed for in situ hybridization or immunofluorescence, respectively. Samples used for PV immunohistochemistry were stored long term in 10% formalin until processed.

Immunostaining

Frozen tissue blocks were fixed in 10% neutral buffered formalin overnight at 4 °C, rinsed in phosphate-buffered saline (PBS), and kept in 20% sucrose/PBS solution until serially sectioned at 40µm on a cryostat. Free-floating sections were rinsed in PBS and then incubated overnight at 4 °C under constant agitation with the antibody (mouse anti-NeuN (Millipore, 1:500, MAB377), goat anti-Versican (R&D, 1:100, AF3054)), or lectin (biotinylated Wisteria Floribunda Lectin (WFL), Vector Laboratories, 1:2500, B-1355) of interest diluted in a blocking solution of PBS/0.2% Triton-X/2% normal donkey serum. Sections were then rinsed and incubated for 2 h at room temperature with the appropriate fluorophore-conjugated secondary antibody (Alexa-488 anti-Mouse (Jackson ImmunoResearch, 1:500) for NeuN, Dylight-594 anti-goat (Jackson

ImmunoResearch, 1:500) for VCAN, or Cy3-conjugated Streptavidin (Jackson ImmunoResearch, 016-160-084;1:500) for the detection of PNNs, and diluted in the same blocking solution as the primary incubation. Next, sections were rinsed and endogenous autofluorescence from lipofuscin and cellular debris was quenched with Trueblack (Biotium), omitted for tissues used for intensity measurements. Sections were mounted on Superfrost charged slides and coverslipped with Vectashield mounting medium (Vector Laboratories, H-1800).

Whole vmPFC sections were scanned on a Zeiss Axio Imager M2 microscope equipped with a motorized stage and Axiocam MRm camera at ×20. The ImageJ [18] software (NIH) Cell Counter plugin was used by a blinded researcher to manually count PNNs. An average of four sections per subject was used. Cortical layers were delineated based on NeuN+ cell distribution and morphology, and the number of PNNs and the area of each layer were measured, allowing to generate PNN density values (n/mm^2). Densities were obtained by averaging by subject the density of PNNs per layer and section, and then averaging subjects' densities to yield group means.

For PV immunohistochemistry, tissue blocks stored in 10% formalin were first transferred to 30% sucrose/PBS. Once sunk, blocks were flash frozen in isopentane and kept at -80 °C until embedded and serially sectioned on a sliding microtome (40µm). Prior to immunohistochemical staining, tissues underwent antigen retrieval by incubating for 15 min in hot 10 mM sodium citrate buffer pH 6.0 (Sigma catalog number S-4641). Sections were rinsed in PBS and incubated in 3% H_2O_2/PBS for 15 min. After being rinsed, sections were incubated overnight at 4 °C under constant agitation with a mouse anti-Parvalbumin antibody (Swant, 1:500, PV235) diluted in a blocking solution of PBS/0.2% Triton-X/2% normal horse serum. Sections were then rinsed and incubated for 2 h at room temperature in biotinylated horse anti-mouse antibody (1:500, Vector Laboratories, Inc., BA-2001, Burlington, ON, Canada). Then, sections were incubated in the avidin–biotin

complex (ABC Kit, Vectastain Elite, Vector Laboratories, Inc., Burlington, ON, Canada) for 30 min at room temperature. Labeling was revealed with the diaminobenzidine (DAB) kit (Vector Laboratories, Inc., Burlington, ON, Canada), then sections were rinsed and mounted on Superfrost charged glass slides, dehydrated, and coverslipped with Permount (Fisher Scientific, Inc., Pittsburgh, PA, USA). Immunohistological controls were performed by omitting primary antibodies. After a first round of imaging, the coverslips were removed and samples were counterstained with cresyl violet to differentiate cortical layers and imaged a second time. Image acquisition was performed on an Olympus VS120 Slide Scanner at ×10. Image analysis was performed in QuPath [19] (v 0.1.2). Automatic cell detection was used to detect PV+ cells. DAB images were overlaid on the cresyl-counterstained image using the function Interactive Image Alignment—which allowed a blinded researcher to delineate the cortical layers based on cresyl violet-stained cells. Densities were calculated by cortical layer.

Fluorescent in situ hybridization

Frozen vmPFC blocks were cut serially with a cryostat and 10 µm-thick sections were collected on Superfrost charged slides. In situ hybridization was performed using Advanced Cell Diagnostics RNAscope® probes and reagents following the manufacturer's instructions. Sections were first fixed in cold 10% neutral buffered formalin for 15 min, dehydrated by increasing gradient of ethanol baths, and air dried for 5 min. Endogenous peroxidase activity was quenched with hydrogen peroxide for 10 min followed by protease digestion for 30 min at room temperature (omitted for samples undergoing subsequent WFL staining). The following probes were then hybridized for 2 h at 40 °C in a humidity-controlled oven: Hs-PVALB (catalog number 422181), Hs-VCAN (catalog number 430071-C2), Hs-PDGFRA (catalog number 604481-C3), Hs-TNR

(catalog number 525811), Hs-PTPRZ1 (catalog number 584781-C2), Hs-SLC17A7 (catalog number 415611), and Hs-GAD1 (catalog number 573061-C3). Amplifiers were added using the proprietary AMP reagents and the signal visualized through probe-specific HRP-based detection by tyramide signal amplification (TSA) with Opal dyes (Opal 520, Opal 570, or Opal 690; Perkin Elmer) diluted 1:700. Slides were then coverslipped with Vectashield mounting medium with 4′,6-diami-dino-2-phenylindole (DAPI) for nuclear staining (Vector Laboratories) and kept at 4 °C until imaging. Both positive and negative controls provided by the supplier (ACDbio) were used on separate sections to confirm signal specificity. For immunohistochemical staining of PNNs following PVALB, GAD1 (glutamate decarboxylase 1), or SLC17A7 (vesicular glutamate transporter 1) in situ hybridization, slides were rinsed in PBS, incubated for 30 min at room temperature with biotinylated WFL, followed by 488-conjugated Streptavidin for 30 min prior to coverslipping. To better define the cellular identity of neuronal populations surrounded by WLF-labeled PNNs, TrueBlack was used to remove endogenous autofluorescence from lipofuscin and cellular debris.

Cellular identity and ratios of each cell type surrounded by WFL-labeled PNNs

Image analysis was performed in QuPath (v 0.2.3). Each subject had two sections stained with various cellular markers: DAPI, PVALB, SLC17A7, GAD1, and WFL. To identify the population of cells covered by PNNs and calculate the percentage of each cell type that is covered by a net; a blinded researcher manually identified PNNs and categorized each nucleus within a region of interest (spanning layers III–VI) dependent on the presence of canonical cellular markers. A total of 3145 PNNs were classified and a total of 18,600 SLC17A7+, 2209 GAD1+/PVALB+ and 8659 GAD1+/PVALB− cells were classified.

A replication experiment was conducted for the proportions of PVALB+ cells enwrapped by WFL-labeled PNNs, which were determined in a single section with an average of 55 PVALB+ cells per subject imaged under a ×20 objective through vmPFC layers IV–V.

Imaging and analysis of in situ RNA expression in OPCs

Image acquisitions was performed on a FV1200 laser scanning confocal microscope (FV1200) equipped with a motorized stage. For each experiment and subject, six to ten stack images were taken to capture at least 20 oligodendrocyte progenitor cells (OPCs) (PDGFRA+) per subject. Images were taken using a ×60 objective (NA=1.42) with an XY pixel width of ~0.25 μm and Z-spacing of 0.5 μm. Laser power and detection parameters were kept consistent between subjects for each set of experiment. As TSA amplification with Opal dyes yields a high signal-to-noise ratio, parameters were optimized so that autofluorescence from lipofuscin and cellular debris was filtered out. OPCs were defined by bright clustered puncta-like PDGFRA signal present within the nucleus of the cells. Using ImageJ, stacks were first converted to Z-projections, and for each image the nuclei of OPCs were manually contoured based on DAPI expression. Expression of versican (VCAN), tenascin-R (TNR), or phosphacan (PTPRZ1) in OPCs was quantified using the area fraction, whereby for each probe the signal was first manually thresholded by a blinded researcher and then the fraction of the contoured nucleus area covered by signal was measured for each OPC. Area fraction was the preferred measure to reflect RNA expression, as punctate labeling generated by fluorescence in situ hybridization (FISH) often aggregates into clusters that cannot readily be dissociated into single dots or molecules.

Intensity, area, and distance measurements

For each subject, ~15 z-stacks (0.26 µm Z-spacing) spanning all layers of the vmPFC were acquired at ×40 magnification on an Olympus FV1200 laser scanning confocal microscope. Images for intensity measurement were all acquired at the same laser strength and voltage to avoid imaging differences in intensity or over-exposure. PNNs were traced manually with ImageJ by a blinded researcher using maximum intensity projections generated from each stack. All the PNNs that were observed were traced as long as their whole morphology was in the field of view. For each PNN, the mean pixel value of adjacent background was subtracted to the mean pixel value of the contoured soma of the PNN, yielding the mean corrected fluorescence intensity (arbitrary units). To infer on their morphological complexity, we measured the area covered by each contoured PNN, including soma and ramifications extending over proximal dendrites.

To quantify closest distance between OPCs and PV+ cells, low magnification (×10) images of PDGFRA and PVALB FISH sections were taken by a blinded researcher along layers IV and V of the vmPFC, using the granular layer IV as a visual reference. For each PDGFRA+ cell in the field of view, the distance to the nearest PVALB+ cell was measured using the measure tool in ImageJ. An average of 90 OPCs per group were quantified.

OPC density measurements

Image acquisition was performed on an Olympus VS120 Slide Scanner at ×20. Image analysis was performed in QuPath (v 0.2.3) by a blinded researcher. Automatic cell detection was used to detect DAPI nuclei. Then, an object classifier was trained on five training images from five different subjects. Cells were deemed PDGFRA+ based on the mean intensity of PDGFRA

staining compared to the mean staining of a background channel. In total, 21 subjects were included (CTRL=6, DS=7, and DS-CA=8) in this analysis.

Cell-type-specific expression of PNN canonical components using single-nucleus sequencing

Cell-type-specific expression of canonical components of PNNs was explored using a single-nucleus RNA sequencing (snRNA-seq) data set from the human dorsolateral PFC (BA9) previously generated by our group [20], for which methodology is extensively described in this published resource. Average expression for each PNN component in each cell type was calculated by weighting the expression values (normalized transcript counts) of each cluster by the size (number of nuclei) of the cluster. Weighted average expression values are displayed in a heatmap, scaled by row (i.e., gene). The color bar therefore represents the expression values as z-scores, with darker colors indicating higher expression.

Statistical analyses

Independently of PMI, pH, and approach used, the quality of post-mortem samples is notoriously variable and is influenced by tissue degradation, quality of fixation, and other artefacts. Only samples that showed reliable labeling were included in the different experiments without prior knowledge about group affiliation. Analyses were performed on Statistica version 12 (StatSoft) and Prism version 6 (GraphPad Software). Distribution and homogeneity of variances were assessed with Shapiro–Wilk and Levene's tests, respectively. PNN densities were analyzed using a mixed-effects model, using layer and group as fixed factors, followed by Tukey's honestly significant difference test for corrected post hoc comparisons. For all other variables (WFL intensity, WFL area per PNN, PNN+/PVALB ratios, RNA expression in OPCs and distance of

OPCs from PVALB+ cells) group effects were detected using one-way ANOVAs or Kruskal–Wallis test followed by Tukey's honestly significant difference or Dunn's test, respectively. Linear regressions and Spearman's correlation were used to address the relationship between dependent variables and covariates (age, PMI and pH, medication, and substance dependence) (Supplementary Table 1). Statistical tests were two-sided. Significance threshold was set at 0.05 and all data presented represent mean ± SEM.

Results

PNN densities, visualized by WFL labeling and NeuN immunostaining (Fig. 1A), were markedly higher through layers III–VI of vmPFC (BA11/12) samples from individuals with a history of CA compared to controls and depressed suicides with no history of CA (Fig. 1B). Although the recruitment of PNNs is developmentally regulated, we did not find any correlation between age and densities of PNNs (Supplementary Table 1), perhaps suggesting that PNN recruitment may already have reached a plateau in our cohort [21]. Likewise, controlling for age did not affect our results (analysis of covariance (ANCOVA) with group as fixed factor and age as covariate; group effect: $F(2,35)=11.230$, $P < 0.001$). To investigate whether CA also associates with maturational or morphological changes of PNNs, we compared the intensity of WFL staining between groups (Fig. 1C) as an indication of their maturity, as well as the area covered by individual PNNs as an indicator of their morphological complexity (Fig. 1D). CA was both associated with higher intensity of WFL staining per PNN (Fig. 1C) and cells were more extensively covered by PNNs (Fig. 1D), suggesting overall that CA may precipitate the maturation and the recruitment of PNNs.

PNNs have been most extensively described around PV+ cells, but are also found around other neuronal types [22]. We first wanted to specify the identity of cells covered by PNNs in the human vmPFC. We measured the ratios of PNNs surrounding either PV+ cells, glutamatergic neurons, and other interneurons in a subset of control, psychiatrically healthy subjects (Fig. 1E, F). As PV antigenicity is particularly susceptible to freezing and lost altogether in samples snap frozen prior to fixation, we developed an approach to combine FISH and immunofluorescence to visualize PVALB-expressing cells and WFL+ PNNs in frozen samples. Similarly, glutamatergic neurons and other subtypes of interneurons were visualized with FISH using probes against SLC17A7 and GAD1, respectively (Fig. 1E). The majority of cells covered by WFL staining were PVALB+ (~74%), followed by GAD1+/PVALB− cells (~23%), indicating that a small fraction of PNNs is likely surrounding other subtypes of interneurons (Fig. 1F). As previously reported [23,24], some PNNs stained with WFL were also found to surround glutamatergic neurons (SLC17A7+), although only a very small fraction of them (~3%, Fig. 1F).

To clarify the cellular specificity of the observed increase in PNNs recruitment, we next quantified the ratios of PVALB+, SLC17A7+, andGAD1+/PVALB− cells surrounded by WFL+ PNNs. Here, ~65% of PVALB+ cells were surrounded by PNNs (Fig. 1G), in line with previous observations [25], whereas only a small proportion of GAD1+/PVALB− and SLC17A7+ cells were covered by PNNs (Fig. 1G). Interestingly, ratios of cells covered by WFL-labeled PNNs showed a positive correlation with age (Supplementary Table 1), suggesting an increased recruitment of PNNs with age regardless of cell type. Importantly, samples from DS-CA individuals displayed a robust increase in the percentage of PVALB+ cells surrounded by PNNs compared to DS and CTRL samples (Fig. 1G), whereas no change in the proportion of other cell types covered by PNNs was found between group. Controlling for age as a covariate did not change

the outcome of these group comparisons (%PVALB+/PNN+ cells: $F(2,15) = 4.08$, $P = 0.047$; %GAD1+/PVALB−/PNN+ cells: $F(2,15) = 0.237$, $P = 0.793$; %SLC17A7+/PNN+ cells: $F(2,15) = 1.430$, $P = 0.281$).

Finally, we addressed whether the increased densities of PNNs and higher ratios of PV+ cells surrounded by PNNs observed in DS-CA subjects could be linked to changes in the number of PV+ cells in the vmPFC and found no evidence of altered PV+ cell densities between groups (Fig. 1H). Of note, PV+ cell densities were inversely correlated with age (Supplementary Fig. 1), but controlling for this factor did not change the outcome of group comparisons (ANCOVA with group as fixed factor and age as covariate: group effect, $P = 0.251$; age effect, $P = 0.007$).

Altogether, these results suggest that a history of CA in depressed suicides is associated with increased recruitment and maturation/morphological complexity of PNNs around PV+ neurons, rather than changes in cell populations.

We then sought to indirectly explore the molecular underpinnings of this phenomenon and reasoned that increased recruitment of PNNs associated with CA should translate or be induced by changes in the molecular programs controlling PNN assembly. Our understanding of these transcriptional programs is scarce, hindered by the fact that several known molecules participating in PNN recruitment are released non-locally and by different cell types, implying a complex cellular crosstalk orchestrating PNN assembly. To gain insight into how, in humans, different cell types contribute to the synthesis of canonical components of PNNs, we explored a single-nucleus sequencing data set previously generated by our group in the human dorsolateral PFC [20] (Brodmann area 9) and screened their expression across eight major cell types. The main canonical components of PNNs, namely aggrecan (ACAN), neurocan (NCAN), versican (VCAN), phosphacan (PTPRZ1), brevican (BCAN), and tenascin-R (TNR), were highly enriched in OPCs,

in particular VCAN, PTPRZ1, BCAN, and TNR (fold change of 140, 37, 7.9, and 22.9, respectively, between gene expression in OPCs vs. PV+ cells) (Fig. 2A and Supplementary Fig. 1). As this data set originates from the dlPFC and region-specific patterns of ECM-related gene expression could exist, this was further validated using FISH (Fig. 2B, C) in the vmPFC for VCAN and PTPRZ1, as they showed the strongest expression in OPCs and are two major signature genes in late OPCs [26]. We found that in the vmPFC, cells expressing these genes are almost all PDGFRA+ OPCs (97.9% of VCAN-expressing cells were co-expressing PDGFRA, and 92% of PTPRZ1-expressing cells were co-expressing PDGFRA) (Fig. 2D). Interestingly, despite that VCAN gene expression was restricted to OPCs, immunolabeling of the versican protein showed a characteristic pattern of PNNs and an overlap with WFL-labeled PNNs (Fig. 2E), suggesting overall that OPCs could be potent regulators of PNN formation.

In support of a possible involvement of OPCs in mediating CA-related changes in PNNs, the expression of VCAN, PTPRZ1, and TNR was upregulated in OPCs of CA victims (Fig. 2F–H), and both the expression of PTPRZ1 and TNR in OPCs correlated with WFL-labeled PNNs densities regardless of group (Fig. 2I, J).OPCs were on occasion directly juxtaposed to PVALB+ cells (Fig. 2B), as previously reported in rodents [27]. Interestingly, OPC proximity to PVALB+ cells modestly correlated with PNN density (Fig. 2L, $R^2 = 0.36$, $P = 0.024$) and was increased in individuals with a history of CA (Fig. 2M), further suggesting an interplay between these two cell types. To clarify whether these changes could be linked or associated with changes in cell numbers, we compared the density of OPCs between groups. Interestingly OPC densities showed a marked decrease with age (Supplementary Table 1), but no difference between groups were found (Fig. 2N), even after controlling for this factor (ANCOVA, with group as fixed factor and age as covariate: group effect, $P = 0.13$; age affect, $P = 0.001$).

Discussion

Overall, our results suggest that a history of CA may associate with increased recruitment and maturation of PNNs, as well as an upregulation of their canonical components by OPCs, a cell type that likely plays a key role in the cellular crosstalk that orchestrates PNN formation. Although, to our knowledge, this is the first evidence in humans that ELA affects the recruitment of PNNs, recent studies in animals have approached this question. Guadagno et al. [28] found that in the limited bedding paradigm, adolescent pups have increased densities of PNNs in the amygdala. Murthy et al. [9] showed that in the ventral dentate gyrus, maternal separation combined with early-weaning, another model of early-life stress mimicking some aspects of adversity, led to an increase in PNN intensity around parvalbumin-positive interneurons with no change in PNN density. Importantly, these effects were present in adults, suggesting a long-lasting impact of ELA on PV+ cell function and PNN remodeling. Gildawie et al. [29] also recently reported that in the prelimbic cortex, maternal separation in rats increased the intensity of PNNs surrounding PV+ neurons, an effect only observed in adulthood. This suggests that changes in PNN integrity and maturation following ELA could possibly be protracted and develop over time. Although we cannot address this question with our post-mortem design, our results show at the very least that changes in PNN integrity in victims of CA are observable at an adult age. Few studies have so far been conducted on this topic, however, with one of them showing a decrease in the intensity of WFL fluorescent labeling in both the PFC and hippocampal CA1 following an early-life sub-chronic variable stress paradigm [30]. Clearly, more work is needed to better characterize the effects of ELA on PNNs integrity, particularly in light of the multiple paradigms used in animal studies.

Despite the fact that much of the literature has focused on the influence of PNNs on PV+ cell physiology, it is important to note that PNNs are not exclusively present around PV+ neurons [22,23,31]. Although our data indicate that in the vmPFC PV-surrounding PNNs are the majority, a portion of them were identified around other GABAergic neurons, as well as around a small fraction of excitatory neurons. Our data suggest that CA associates with a selective increase in the recruitment of PNNs around PV+ neurons, considering that the higher percentage of cells surrounded by WFL-labeled PNNs was only found for PV+ cells, but not for other cell types. However, we cannot exclude that given the smaller pool of non-PV cells surrounded by WFL-labeled PNNs, we were unable to detect such effects in our design. It is also likely that the sole use of WFL immunostaining to detect PNNs may be a limitation to fully understand their distribution. It is becoming increasingly clear that PNNs vary in molecular composition, and perhaps function, and that WFL-labeled PNNs may be biased towards specific neuronal types [32,33]. The use of additional markers should help decipher how ELA affects the remodeling of the ECM more broadly. It is also noteworthy that this analysis, by focusing on cortical layers IV–V, did not allow to clarify the possible layer specificity of PNN cellular distribution. Given the molecular, cellular, and connectivity heterogeneity in different cortical layers, it is possible that PNNs differentially interact with these different cell types, and that ELA may affect these interactions in a layer-specific manner.

One particularly noteworthy aspect of our results is the specific association between changes in PNNs and a history of CA. When comparing DS and controls for the expression of all PNN-related genes reported in our study (Fig. 2A), based on the snRNA-seq data generated by Nagy et al. [20] (Supplementary Tables 30 and 31), none showed differential expression between groups in OPCs. The fact that our FISH experiments did not show significantly enhanced expression of

these markers in DS samples is therefore consistent both with results obtained by Nagy et al. [20] and with our own findings, indicating that PNNs are more abundant and mature specifically in samples from DS with a history of CA. Overall, this suggests that although transcriptomic changes in OPCs may be a strong feature of depressed suicides [20], PNN-related changes are more specific to a history of CA. As such changes are absent in depressed suicides without a history of CA, our findings suggest possible vulnerability windows during which PV+ cell function and PNN maturation are more susceptible to experience-dependent remodeling and adversity. If these changes may mediate some of the negative mental health outcomes or cognitive and emotional traits associated with CA in adulthood, they likely do not represent a hallmark of depression, in accordance with a recent post-mortem study finding no change in the density of PNNs in the PFC of depressed patients [34].

The search for possible mechanisms involved in the effects of ELA on PNN development is an unexplored field. PNN recruitment is likely orchestrated by a complex interplay between activity-dependent autonomous pathways in parvalbumin neurons, with signals originating from different cell types involved in their assembly. As parvalbumin neurons have been shown to be particularly sensitive to stress and glucocorticoids, in particular early-life stress [35–39], we can speculate that elevated glucocorticoids in CA victims [40] can impact PV+ neuron function early-on. This could translate into increased GABA release following glucocorticoid receptor activation [38] and indirect increase in the recruitment of PNNs, which has been directly linked to PV+ neuron activity [41,42] and GABA levels [43]. A myriad of factors could however indirectly affect PV+ cells during this period of protracted maturation associated with childhood and adolescence, such as increased pro-inflammatory cytokine expression associated with ELA [36,44] or changes in neurotrophic factor expression [45–47].

An interesting molecular candidate is the transcription factor OTX2, released non-locally by cells in the choroid plexus and acting as a major initiator of PNN development [48]. Recent evidence suggests a role of OTX2 in mediating vulnerability to early-life stress [49] and Murthy et al. [9] reported elevated expression of OTX2 in the choroid plexus following maternal separation and around PV+/PNNs+ cells in the ventral dentate gyrus. Although the precise mechanisms involved in the effects of ELA on the release of OTX2 are not known, it is noteworthy that DNA methylation of the OTX2 gene in children has been shown to correlate with increased risk for depression as well as increased functional connectivity between the vmPFC and bilateral regions of the medial frontal cortex [50]. This highlights that beyond discrete changes in PV+ cell function, ELA could affect the release of distal cues by non-neuronal cells and contribute to extracellular matrix remodeling, thus affecting brain function and vulnerability to psychopathology.

As mentioned previously, although PNN development has been strongly linked to neuronal activity [3,41,51], PNN integrity and assembly are likely orchestrated by the complex integration by PV+ neurons of cues originating from multiple cell types [52,53]. Accordingly, we found that the expression of genes encoding for the major canonical components of PNNs were strongly enriched in oligodendrocyte-lineage cells, in particular in OPCs, whereas PV+ neurons barely expressed any of those components. Although our single-cell expression data originates from the dorsolateral PFC, this was validated in the vmPFC, thus decreasing the possibility that this pattern of enrichment is region-specific. This is also in accordance with previous literature in rats, albeit in the cerebellum, similarly showing that VCAN, PTPRZ1, and TNR are almost exclusively expressed in oligodendrocyte-lineage cells [54]. This is also consistent with more recent single-cell RNA-seq studies showing an enrichment of extracellular components, including VCAN and PTPRZ1, in OPCs [55–57].

The interplay between oligodendrocyte-lineage cells and PV+ neurons, in particular during developmental windows of plasticity, are being increasingly documented [58]. Interestingly, OPCs have been shown to be ontogenetically related to PV+ neurons [59]. OPCs also receive functional synaptic inputs from GABAergic interneurons, a connectivity that reaches its peak during early postnatal development along with the maturation of PNNs [60–62]. It is therefore particularly tempting to speculate that OPC-PV neuron communication during critical windows of development may play a fundamental role in modeling cortical plasticity and the maturation of PNNs. This has never been addressed and we therefore approached this question by investigating how CA associates with changes in the expression of PNN canonical components specifically in OPCs, and how this correlates with the changes in PNN integrity observed in victims of CA. First, we found that OPC proximity to PV+ neurons positively correlated with PNN densities, and that in victims of CA, OPCs tended to be more proximal to PV+ neurons. As a proportion of OPCs are in direct physical contact with neuronal populations, and preferentially around GABAergic neurons [27,63], we could speculate that CA associates with increased recruitment of OPCs around PV+ cells, thereby promoting the formation of PNNs around these cells. Caution is however needed in interpreting these correlational results that functionally relate the distance between OPCs and PV+ cells to the recruitment of PNNs. The high percentage of PV+ cells enwrapped by PNNs in our data (~65%) and low percentage of PV+ cells paired with an OPC (~3% based on [27], albeit in rodents) rather indicates that is unlikely that direct pairing of OPCs is necessary for the formation of PNNs. This question should therefore be further addressed with appropriate functional tools in cellular or animal models. Of important note, we did not address whether OPCs proximity with other cell types was changed, and how it could relate to changes in various cell populations. In addition, although we did not observe any change in overall OPCs densities

between groups, a more refined layer-specific analysis of OPCs densities would be informative to rule out the influence of cell numbers on the physical proximity of these two cell types.

Second, we also found that the expression of canonical components of PNNs in OPCs was positively correlated with PNN densities and upregulated in victims of CA. This strongly suggests that CA has a durable impact on OPC molecular programs that may contribute to PNN development. Although we focused on VCAN, PTPRZ1, and TNR based on their high enrichment in OPCs, it would be important to describe more broadly how CA affects the transcriptional signature of PNNs. In particular, some of these components, although present in PNNs, are also found in other ECM compartments, such as the perinodal ECM and around excitatory cells, contributing to synaptic function [3]. Although we did not address this question, the impact of CA on OPC function may therefore more broadly affect ECM physiology and remodeling. It is also becoming increasingly clear that multiple populations with distinct functional or transcriptomic features are encompassed in OPCs [64,65]. While we can speculate that these subtypes may have distinct role in the remodeling of the ECM, we did not address this important question.

Our results, nonetheless, further strengthen previous reports by our group [66,67] that CA has profound effects on oligodendrocyte-lineage cells, which may extend well beyond affecting myelination by contributing to the reprogramming of various aspects of brain plasticity.

How precisely OPC-PV communication contributes to the development of PNNs and impacts PV+ neuron functional integration and circuit dynamics certainly deserves further investigation using functional approaches. Inherent to our post-mortem design, a major limitation of this study lies in our inability to infer on the precise timing of these changes and whether dynamic remodeling of the ECM occurs in a protracted way. Given the correlational nature of our results, we cannot elaborate on the possible influence of recent and emotionally salient events on

PNN remodeling, or possible state-dependent factors at the time of death. Several rodent studies have indeed reported that behavioral manipulations in adulthood, in particular learning and memory paradigms in which plasticity events are recruited, can affect PNN dynamics [68–71].

Although it is also tempting to infer that CA selectively affects PNN remodeling around PV+ neurons, caution is needed in this interpretation. As previously mentioned, WFL immunostaining may only label a specific fraction of PNNs [32,33], and the continuum between PNN components and other ECM compartments imply more refined approaches are necessary to fully understand how CA impacts ECM remodeling and the role of OPCs in this form of plasticity.

Another limitation is that our study only included very few female samples, given the much higher prevalence of suicide in males. Sex is known to moderate both the biological and the psychopathological effects of CA [72], and increasing evidence points towards a sexual dimorphism in the effects of stress, in particular early-life stress, on PV+ neuron function and perhaps PNN development [8,39,73]. Future studies should therefore explore this aspect to further understand how ELA modifies trajectories of brain development.

Other limitations are inherent to post-mortem studies of psychiatric cohorts, such as the presence of medication in some subjects. Although this was the case for both depressed suicides groups, and that the observed changes seem specific to a history of CA, we cannot exclude interactive effects of medical treatments and life trajectories on our variables. Similarly, relatively long PMIs in our cohorts, although not statistically linked to changes in our variables, could potentially confound our results.

To conclude, our findings suggest that CA may lead to persistent patterns of maladaptive behaviors by reducing the neuroplasticity of cortical circuits through the enhancement of developmental OPC-mediated PNN formation. Future preclinical models should help determine

whether changes in OPCs are causal in the increased recruitment of PNNs following CA or an indirect response following altered PNN dynamics. Likewise, the consequences of these molecular changes should be examined at the network level to determine their functional impact on intra-and inter-regional communication.

Author contributions

AT and NM conceived the study. GT participated in the acquisition and clinical characterization of the brain samples. AT, CB, FD, MAD, CC, RM, and AM contributed to immunohistological experiments. AT, CN, MM, and KP generated and analyzed the snRNA-seq data set. AT, CB, FC, and ST performed the in situ hybridization experiments. AT, CB, and NM prepared the manuscript, and all authors contributed to and approved its final version.

Funding

This work was funded by a CIHR Project grant (PJT-173287) to NM. AT was supported by fellowships from the FRQ-S and Toronto Dominion, and an American Foundation for Suicide Prevention (AFSP) Young Investigator Innovation Grant (YIG-0-146-17). C. Belliveau holds an FRQ-S doctoral scholarship. The Molecular and Cellular Microscopy Platform and the Douglas-Bell Canada Brain Bank (DBCBB) are partly funded by Healthy Brains for Healthy Lives (CFREF) and Brain Canada platform grants to GT and NM. The DBCBB is also funded by the Réseau Québécois sur le suicide, le troubles de l'humeur et les troubles associés (FRQ-S).

Competing interests

The authors declare no competing interest.

Figures and Figure Legends

Fig.1: Increased density, morphological complexity and recruitment of PNNs around parvalbumin neurons in the vmPFC of depressed suicides with a history of child abuse.

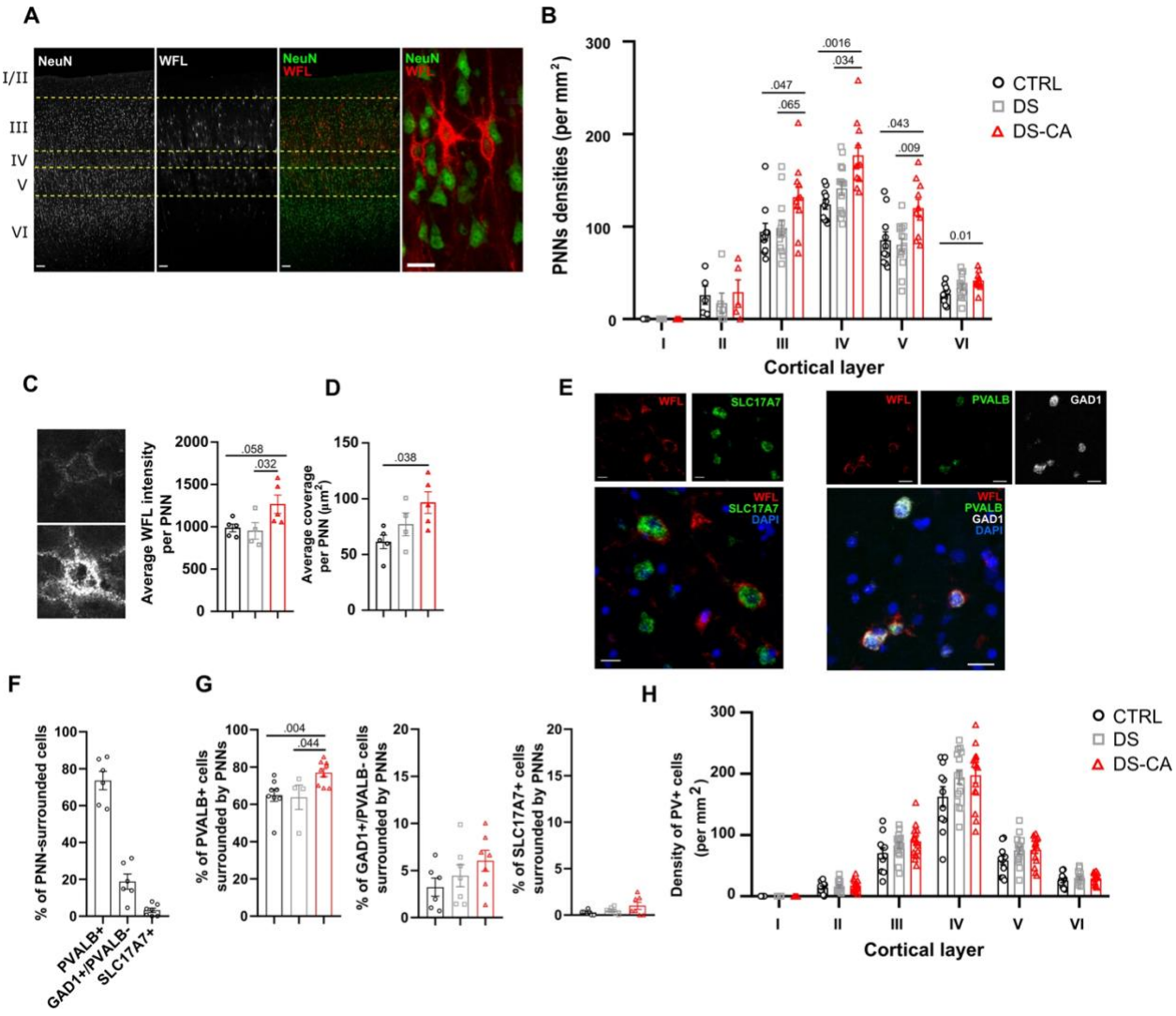

A Representative images of PNNs labeled with WFL and their distribution throughout human vmPFC cortical layers. Scale bars = 100 and 20 µm (high-magnification panel). **B** Depressed suicides with a history of child abuse (DS-CA, N = 11) have significantly higher PNN densities compared to controls (CTRL, N = 10) and depressed suicides without history of child abuse (DS, N = 14) (group effect: $F(2, 32) = 7.029$, $P = 0.0029$; layer effect: $F(3.395, 78.09) = 194.2$, $P < 0.0001$; layer × group: $F(10, 115) = 2.07$, $P = 0.0029$, followed by Tukey's multiple comparison test). **C** Representative images of a low (top) and high (bottom) intensity PNN in the vmPFC. PNNs from DS-CA subjects (N = 5) showed higher average WFL intensity (arbitrary units) compared to CTRLs (N = 5) or DS (N = 4) (Kruskal–Wallis ANOVA: $H(2, 14) = 5.57$, $P = 0.049$, followed by Dunn's test). **D** PNNs from DS-CA subjects (N = 5) showed higher complexity (area covered by PNNs) compared to CTRLs (N = 5) or DS (N = 4) (Kruskal–Wallis ANOVA: $H(2, 14) = 6.223$, $P = 0.034$, followed by Dunn's test). **E** Left: representative images of in situ hybridization for SLC17A7 (green) followed by WFL labeling (red). Nuclei were stained with DAPI (blue); right: representative images of in situ hybridization for PVALB (green) and GAD1 (white) followed by WFL labeling (red). Nuclei were stained with DAPI (blue). Scale bars = 20 µm. **F** Proportions of WFL-labeled PNNs expressing PVALB (PV+ neurons), GAD1 but not PVALB (other inhibitory neurons), and SLC17A7 (excitatory neurons). **G** DS-CA (N = 9) subjects have higher ratios of PVALB+ cells surrounded by PNNs compared to CTRLs (N = 8) and DS subjects (N = 4) (Kruskal–Wallis ANOVA $H(2,21) = 9.45$, $P = 0.0037$, followed by Dunn's test), but not of GAD1+/PVALB− cells (Krukal–Wallis ANOVA $H(2,20) = 3.28$, $P = 0.2$) nor SLC17A7+ cells (Kruskal–Wallis ANOVA, $H(2,21) = 2.58$, $P = 0.29$). **G** Densities of PV+ cells assessed by immunohistology. No change between groups was observed (group effect: $P = 0.132$; layer effect: $P < 0.0001$; group × layer: $P = 0.083$).

Fig. 2: Gene expression of canonical PNN components is enriched in OPCs and upregulated in depressed suicides with a history of child abuse.

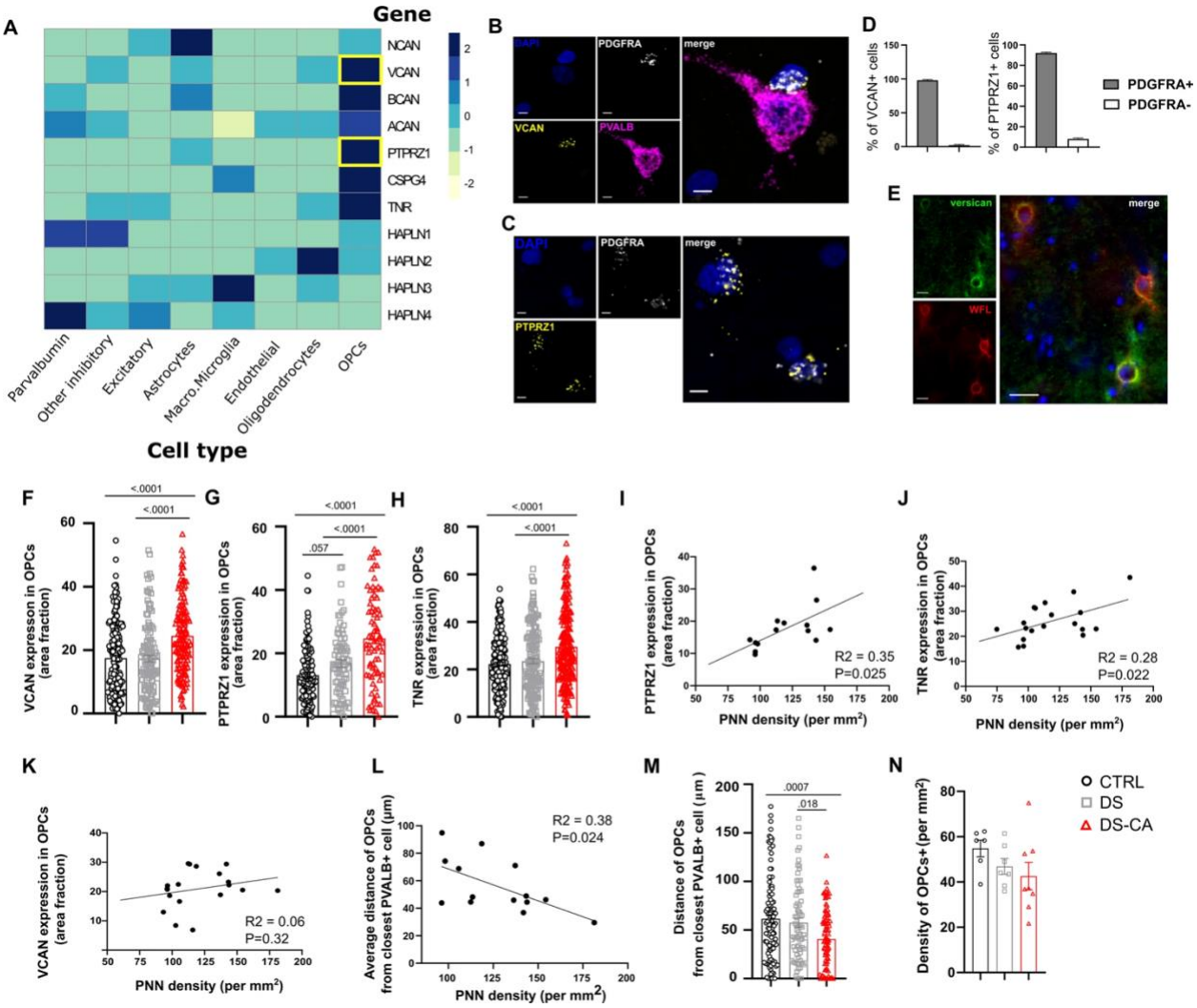

A Expression of canonical components of PNNs according to cell type, derived from single-nucleus RNA sequencing of 34 human dlPFC (BA9) samples [20]. OPCs consistently express higher levels of most of these components compared to other cell types. **B** Representative images of FISH validation of VCAN (Versican, yellow) expression in OPCs (PDGFRA+ cells, white). Note the VCAN-expressing OPC juxtaposed to a PVALB+ (magenta) cell. Nuclei were counterstained with DAPI (blue). Scale bar = 5 µm. **C** Representative images of FISH validation of PTPRZ1 (Phosphacan, yellow) expression in OPCs (PDGFRA+ cells, white). Nuclei were counterstained with DAPI (blue). Scale bar = 5 µm. **D** Both VCAN (left) and PTPRZ1 (right) expression is highly enriched in OPCs, with 97.8% of VCAN+ cells (N = 225) co-expressing PDGFRA and 91.8% of PTPRZ1+ cells (N = 281) co-expressing PDGFRA. **E** Representative image of versican (green) immunolabeling. Despite enrichment of VCAN gene in OPCs, the versican protein shows a characteristic PNN staining pattern and colocalized with WFL (red). Nuclei were counterstained with DAPI (blue). Scale bar = 25 µm. **F** The average expression of VCAN in OPCs was significantly higher in DS-CA subjects (N = 139 cells, 7 subjects) compared to CTRLs (N = 160 cells, 8 subjects) and DS (N = 119 cells, 6 subjects) (one-way ANOVA $F(2, 415) = 17.25$, $P < 0.0001$, followed by Tukey's multiple comparison test). **G** The average expression of PTPRZ1 in OPCs was significantly higher in DS-CA subjects (N = 63 cells, 4 subjects) compared to CTRLs (N = 117 cells, 6 subjects) and DS (N = 81 cells, 5 subjects) (one-way ANOVA $F(2, 258) = 31.65$, $P < 0.0001$, followed by Tukey's multiple comparison test). **H** The average expression of TNR in OPCs was significantly higher in DS-CA subjects (N = 200 cells, 8 subjects) compared to CTRLs (N = 207 cells, 7 subjects) and DS (N = 160 cells, 5 subjects) (one-way ANOVA, $F(2, 564) = 18.69$, $P < 0.0001$, followed by Tukey's multiple comparison test). Both PTPRZ1 (**I**) and TNR (**J**), but not VCAN (**K**) average expression in OPCs modestly correlated

with PNNs densities ($R2 = 0.35$, $P = 0.025$ and $R2 = 0.28$, $P = 0.022$, respectively). **L** A negative correlation was found between average distance of OPCs from closest PVALB+ cell and PNNs density ($R2 = 0.36$, $P = 0.024$), suggesting that OPCs proximity with PVALB+ cells could be associated with changes in PNN density. **M** Proximity of OPCs with PVALB+ cells was increased in DS-CA subjects ($N = 90$ OPCs, 5 subjects) compared to CTRLs ($N = 106$ OPCs, 6 subjects) and DS ($N = 73$ OPCs, 4 subjects) (one-way ANOVA: $F(2, 266) = 7.963$, $P = 0.0004$, followed by Tukey's multiple comparison test). **N** Average densities of PDGFRA+ OPCs were not changed between DS-CA ($N = 8$), DS ($N = 7$), and CTRL ($N = 6$) groups (Kruskal–Wallis ANOVA, $H(2,21) = 4.67$, $P = 0.095$).

Tables

Table 1: Group characteristics

	CTRL	DS	DS-CA
N	11	16	12
Axis 1 diagnosis	0	MDD (14); DD-NOS (2)	MDD (11); DD-NOS (1)
Age (years) ($P = 0.38$)	43.18 ± 7.11	46.63 ± 3.48	37.75 ± 3.10
Sex (M/F)	9/2	14/2	9/3
PMI (h) ($P = 0.74$)	35.95 ± 7.15	45.95 ± 8.06	40.92 ± 6.68
Tissue pH ($P = 0.42$)	6.40 ± 0.09	6.52 ± 0.07	6.56 ± 0.08
Substance dependence	0	6	5
Medication	0	SSRI (4); SNRI (1); TCA (1); Benzodiazepines (3); Antipsychotics (2); Antimanic (1)	SSRI (2); Benzodiazepines (2); Antipsychotics (1); Antimanic (1)

Data represent mean ± SEM. P-values generated with one-way ANOVAs.

DD-NOS depressive disorder not otherwise specified, MDD major depressive disorder, PMI post-mortem interval, SNRI selective norepinephrine reuptake inhibitor, SSRI selective serotonin reuptake inhibitor, TCA tricyclic antidepressant.

Supplementary information

Supplementary Figure 1

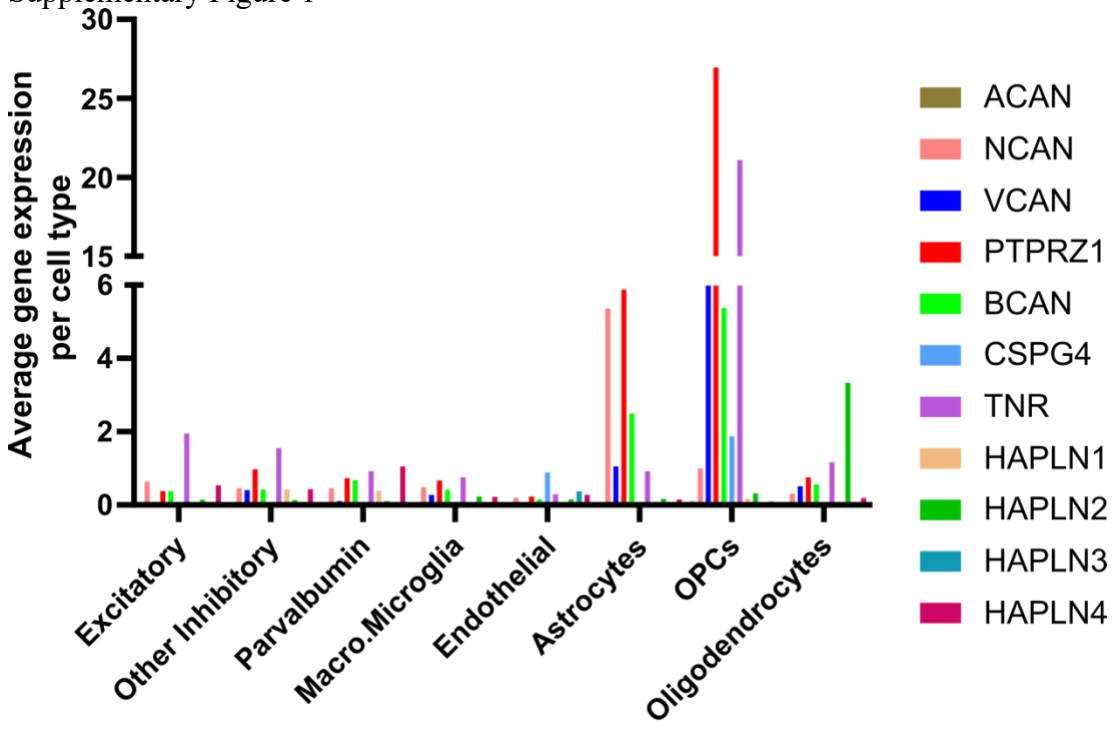

Average normalized expression of PNN-related genes (See Figure 2) in major cell types of the human prefrontal cortex. Data derives from a previous snRNA-seq study published by our group20 (see Supplementary Tables 30-31 of this study). A strong enrichment of some of these genes is observed in OPCs, in particular VCAN (versican), PTPRZ1 (phosphacan) and TNR (tenascin-R).

Supplementary Table 1

Correlation coefficients and P values for Spearman's rho non-parametric measure of association between co-variates and dependent variables

Spearman's rho		PNNs densities	WFL intensity per PNN	coverage per PNN	PV+ cells densities	%PVALB+ cells covered by PNNs	%SLC17A7+ cells covered by PNNs	%GAD1+/PVALB- cells covered by PNNs	PTPRZ1 expression in OPCs	VCAN expression in OPCs	TNR expression in OPCs	PDGFRA+ (OPCs) cells densities
Age	Coef	.042	.156	.015	-.411**	.433*	.472*	.586**	.258	-.078	-.131	-.669**
	Sig.	.810	.594	.958	.007	.050	.035	.007	.354	.737	.582	.001
PMI	Coef	-.008	-.349	.165	.241	.231	.006	-.147	-.306	.263	-.094	-.351
	Sig.	.964	.221	.573	.124	.313	.980	.535	.268	.250	.693	.119
pH	Coef	.115	.033	-.145	.038	.220	.113	-.021	.018	-.153	-.185	-.387
	Sig.	.511	.911	.620	.811	.337	.635	.930	.949	.507	.434	.083
Substance dependence	Coef	-.101	-.194	-.324	.100	.280	.272	.070	.091	.280	.369	.045
	Sig.	.564	.506	.259	.527	.218	.245	.769	.748	.218	.110	.847
Medication	Coef	.058	-.075	.447	-.114	.140	.130	.338	.194	-.393	.392	-.196
	Sig.	.774	.828	.168	.535	.620	.658	.259	.568	.148	.165	.483

References

1. Teicher MH, Samson JA, Anderson CM, Ohashi K. The effects of childhood mal- treatment on brain structure, function and connectivity. Nat Rev Neurosci. 2016;17:652–66.
2. Ferguson BR, Gao W-J. PV interneurons: critical regulators of E/I balance for prefrontal cortex-dependent behavior and psychiatric disorders. Front Neural Circuits. 2018;12:37.
3. Fawcett JW, Oohashi T, Pizzorusso T. The roles of perineuronal nets and the perinodal extracellular matrix in neuronal function. Nat. Rev. Neurosci. 2019. https://doi.org/10.1038/s41583-019-0196-3.
4. Sorg BA, Berretta S, Blacktop JM, Fawcett JW, Kitagawa H, Kwok JCF et al. Casting a wide net: role of perineuronal nets in neural plasticity. J Neurosci. 2016;36:11459–68.
5. Gogolla N, Caroni P, Lüthi A, Herry C. Perineuronal nets protect fear memories from erasure. Science. 2009;325:1258–61.
6. Thompson EH, Lensjø KK, Wigestrand MB, Malthe-Sørenssen A, Hafting T, Fyhn M. Removal of perineuronal nets disrupts recall of a remote fear memory. Proc Natl Acad Sci USA. 2018;115:607–12.
7. Shi W, Wei X, Wang X, Du S, Liu W, Song J et al. Perineuronal nets protect long- term memory by limiting activity-dependent inhibition from parvalbumin inter- neurons. Proc Natl Acad Sci USA. 2019. https://doi.org/10.1073/pnas.1902680116.
8. Bath K, Manzano-Nieves G, Goodwill H. Early life stress accelerates behavioral and neural maturation of the hippocampus in male mice. Horm Behav. 2016;82:64–71.
9. Murthy S, Kane GA, Katchur NJ, Lara Mejia PS, Obiofuma G, Buschman TJ, et al. Perineuronal nets, inhibitory interneurons, and anxiety-related ventral hippo- campal neuronal oscillations are altered by early life adversity. Biol Psychiatry. 2019;85:1011–20.

10. Tanti A, Kim JJ, Wakid M, Davoli M-A, Turecki G, Mechawar N. Child abuse associates with an imbalance of oligodendrocyte-lineage cells in ventromedial prefrontal white matter. Mol Psychiatry. 2018;23:2018–28.
11. Colich N, Rosen M, Williams E, McLaughlin K. Biological aging in childhood and adolescence following experiences of threat and deprivation: a systematic review and meta-analysis. Psychol Bull. 2020;146:721–64.
12. Hiser J, Koenigs M. The multifaceted role of the ventromedial prefrontal cortex in emotion, decision making, social cognition, and psychopathology. Biol Psy- chiatry. 2018;83:638–47.
13. Teicher M, Samson J. Annual research review: enduring neurobiological effects of childhood abuse and neglect. J Child Psychol Psychiatry. 2016;57:241–66.
14. Lutz P-E, Tanti A, Gasecka A, Barnett-Burns S, Kim JJ, Zhou Y et al. Association of a history of child abuse with impaired myelination in the anterior cingulate cortex: convergent epigenetic, transcriptional, and morphological evidence. Am J Psy- chiatry. 2017: appi.ajp.2017.1.
15. Bifulco A, Brown GW, Harris TO. Childhood experience of care and abuse (CECA): a retrospective interview measure. J Child Psychol Psychiatry. 1994;35:1419–35.
16. Bifulco A, Brown GW, Lillie A, Jarvis J. Memories of childhood neglect and abuse: corroboration in a series of sisters. J Child Psychol Psychiatry. 1997;38:365–74.
17. Mai JK, Paxinos G, Voss T. Atlas of the human brain. Elsevier Acad. Press; 2008.
18. Schindelin J, Arganda-Carreras I, Frise E, Kaynig V, Longair M, Pietzsch T, et al. Fiji: an open-source platform for biological-image analysis. Nat Methods. 2012;9:676–82.
19. Bankhead P, Loughrey MB, Fernández JA, Dombrowski Y, McArt DG, Dunne PD, et al. QuPath: open source software for digital pathology image analysis. Sci Rep. 2017;7:1–7.

20. Nagy C, Maitra M, Tanti A, Suderman M, Théroux JF, Davoli MA, et al. Single-nucleus transcriptomics of the prefrontal cortex in major depressive disorder implicates oligodendrocyte precursor cells and excitatory neurons. Nat Neurosci. 2020;23:771–81.
21. Mauney S, Athanas K, Pantazopoulos H, Shaskan N, Passeri E, Berretta S, et al. Developmental pattern of perineuronal nets in the human prefrontal cortex and their deficit in schizophrenia. Biol Psychiatry. 2013;74:427–35.
22. Pantazopoulos H, Lange N, Hassinger L, Berretta S. Subpopulations of neurons expressing parvalbumin in the human amygdala. J Comp Neurol. 2006;496:706–22.
23. Morikawa S, Ikegaya Y, Narita M, Tamura H. Activation of perineuronal net- expressing excitatory neurons during associative memory encoding and retrieval. Sci Rep. 2017;7. https://doi.org/10.1038/SREP46024.
24. Carstens K, Phillips M, Pozzo-Miller L, Weinberg R, Dudek S. Perineuronal nets suppress plasticity of excitatory synapses on CA2 pyramidal neurons. J Neurosci. 2016;36:6312–20.
25. Enwright JF, Sanapala S, Foglio A, Berry R, Fish KN, Lewis DA. Reduced labeling of parvalbumin neurons and perineuronal nets in the dorsolateral prefrontal cortex of subjects with schizophrenia. Neuropsychopharmacology. 2016;41:2206–14.
26. Perlman K, Couturier CP, Yaqubi M, Tanti A, Cui Q, Pernin F, et al. Developmental trajectory of oligodendrocyte progenitor cells in the human brain revealed by single cell RNA sequencing. Glia. 2020;68:1291–303.
27. Boulanger JJ, Messier C. Oligodendrocyte progenitor cells are paired with GABA neurons in the mouse dorsal cortex: unbiased stereological analysis. Neu- roscience. 2017;362:127–40.

28. Guadagno A, Verlezza S, Long H, Wong TP, Walker CD. It is all in the right amygdala: increased synaptic plasticity and perineuronal nets in male, but not female, juvenile rat pups after exposure to early-life stress. J Neurosci. 2020;40:8276–91.
29. Gildawie KR, Honeycutt JA, Brenhouse HC. Region-specific effects of maternal separation on perineuronal net and parvalbumin-expressing interneuron for- mation in male and female rats. Neuroscience. 2019. https://doi.org/10.1016/j. neuroscience.2019.12.010.
30. Ueno H, Suemitsu S, Murakami S, Kitamura N, Wani K, Matsumoto Y, et al. Juvenile stress induces behavioral change and affects perineuronal net formation in juvenile mice. BMC Neurosci. 2018;19:1–21.
31. Lensjø K, Christensen A, Tennøe S, Fyhn M, Hafting T. Differential expression and cell-type specificity of perineuronal nets in hippocampus, medial entorhinal cortex, and visual cortex examined in the rat and mouse. eNeuro. 2017;4. https:// doi.org/10.1523/ENEURO.0379-16.2017.
32. Matthews R, Kelly G, Zerillo C, Gray G, Tiemeyer M, Hockfield S. Aggrecan gly- coforms contribute to the molecular heterogeneity of perineuronal nets. J Neu- rosci. 2002;22:7536–47.
33. Galtrey CM, Kwok JCF, Carulli D, Rhodes KE, Fawcett JW. Distribution and synthesis of extracellular matrix proteoglycans, hyaluronan, link proteins and tenascin-R in the rat spinal cord. Eur J Neurosci. 2008;27:1373–90.
34. Alcaide J, Guirado R, Crespo C, Blasco-Ibáñez JM, Varea E, Sanjuan J, et al. Alterations of perineuronal nets in the dorsolateral prefrontal cortex of neu- ropsychiatric patients. Int J Bipolar Disord. 2019;7:24.

35. Helmeke C, Ovtscharoff W, Poeggel G, Braun K. Imbalance of immunohisto- chemically characterized interneuron populations in the adolescent and adult rodent medial prefrontal cortex after repeated exposure to neonatal separation stress. Neuroscience. 2008;152:18–28.
36. Grassi-Oliveira R, Honeycutt JA, Holland FH, Ganguly P, Brenhouse HC. Cognitive impairment effects of early life stress in adolescents can be predicted with early biomarkers: Impacts of sex, experience, and cytokines. Psychoneuroendocrinol- ogy. 2016;71:19–30.
37. Uchida T, Furukawa T, Iwata S, Yanagawa Y, Fukuda A. Selective loss of parvalbumin-positive GABAergic interneurons in the cerebral cortex of maternally stressed Gad1-heterozygous mouse offspring. Transl Psychiatry. 2014;4:e371.
38. Hu W, Zhang M, Czéh B, Flügge G, Zhang W. Stress impairs GABAergic network function in the hippocampus by activating nongenomic glucocorticoid receptors and affecting the integrity of the parvalbumin-expressing neuronal network. Neuropsychopharmacology. 2010. https://doi.org/10.1038/npp.2010.31.
39. Holland FH, Ganguly P, Potter DN, Chartoff EH, Brenhouse HC. Early life stress disrupts social behavior and prefrontal cortex parvalbumin interneurons at an earlier time-point in females than in males. Neurosci Lett. 2014;566:131–6.
40. Heim C, Mletzko T, Purselle D, Musselman DL, Nemeroff CB. The dexamethasone/ corticotropin-releasing factor test in men with major depression: role of child- hood trauma. Biol Psychiatry. 2008;63:398–405.
41. Devienne G, Picaud S, Cohen I, Piquet J, Tricoire L, Testa D et al. Regulation of perineuronal nets in the adult cortex by the electrical activity of parvalbumin interneurons. J Neurosci. 2019;41:5779–90. https://doi.org/10.1101/671719.

42. Cisneros-Franco JM, De Villers-Sidani É. Reactivation of critical period plasticity in adult auditory cortex through chemogenetic silencing of parvalbumin-positive inter- neurons. Proc Natl Acad Sci USA. 2019. https://doi.org/10.1073/pnas.1913227117.

43. Deidda G, Allegra M, Cerri C, Naskar S, Bony G, Zunino G et al. Early depolarizing GABA controls critical-period plasticity in the rat visual cortex. Nat Neurosci. 2015. https://doi.org/10.1038/nn.3890.

44. Heim C, Newport DJ, Mletzko T, Miller AH, Nemeroff CB. The link between childhood trauma and depression: Insights from HPA axis studies in humans. Psychoneuroendocrinology. 2008;33:693–710.

45. Huang ZJ, Kirkwood A, Pizzorusso T, Porciatti V, Morales B, Bear MF et al. BDNF regulates the maturation of inhibition and the critical period of plasticity in mouse visual cortex. Cell. 1999. https://doi.org/10.1016/S0092-8674(00)81509-3.

46. Cirulli F, Francia N, Berry A, Aloe L, Alleva E, Suomi SJ. Early life stress as a risk factor for mental health: Role of neurotrophins from rodents to non-human primates. Neurosci. Biobehav. Rev. 2009. https://doi.org/10.1016/j.neubiorev.2008.09.001

47. Begum MR, Sng JCG. Molecular mechanisms of experience-dependent matura- tion in cortical GABAergic inhibition. J. Neurochem. 2017. https://doi.org/10.1111/ jnc.14103.

48. Beurdeley M, Spatazza J, Lee HHC, Sugiyama S, Bernard C, Di Nardo AA, et al. Otx2 binding to perineuronal nets persistently regulates plasticity in the mature visual cortex. J Neurosci. 2012;32:9429–37.

49. Peña CJ, Kronman HG, Walker DM, Cates HM, Bagot RC, Purushothaman I et al. Early life stress confers lifelong stress susceptibility in mice via ventral tegmental area OTX2. Science. 2017. https://doi.org/10.1126/science.aan4491.

50. Kaufman J, Wymbs NF, Montalvo-Ortiz JL, Orr C, Albaugh MD, Althoff R et al. Methylation in OTX2 and related genes, maltreatment, and depression in children. Neuropsychopharmacology. 2018. https://doi.org/10.1038/s41386-018-0157-y.

51. Dityatev A, Brückner G, Dityateva G, Grosche J, Kleene R, Schachner M. Activity- dependent formation and functions of chondroitin sulfate-rich extracellular matrix of perineuronal nets. Dev Neurobiol. 2007;67:570–88.

52. Simard S, Coppola G, Rudyk CA, Hayley S, McQuaid RJ, Salmaso N. Profiling changes in cortical astroglial cells following chronic stress. Neuropsycho- pharmacology. 2018. https://doi.org/10.1038/s41386-018-0105-x.

53. Song I, Dityatev A. Crosstalk between glia, extracellular matrix and neurons. Brain Res. Bull. 2018. https://doi.org/10.1016/j.brainresbull.2017.03.003.

54. Carulli D, Rhodes KE, Brown DJ, Bonnert TP, Pollack SJ, Oliver K, et al. Composition of perineuronal nets in the adult rat cerebellum and the cellular origin of their components. J Comp Neurol. 2006;494:559–77.

55. Velmeshev D, Schirmer L, Jung D, Haeussler M, Perez Y, Mayer S, et al. Single-cell genomics identifies cell type–specific molecular changes in autism. Science. 2019;364:685–9.

56. Kumar MP, Du J, Lagoudas G, Jiao Y, Sawyer A, Drummond DC, et al. Analysis of single-cell RNA-seq identifies cell-cell communication associated with tumor characteristics. Cell Rep. 2018;25:1458–.e4.

57. Habib N, Avraham-Davidi I, Basu A, Burks T, Shekhar K, Hofree M, et al. Massively parallel single-nucleus RNA-seq with DroNc-seq. Nat Methods. 2017. https://doi.org/10.1038/nmeth.4407

58. Yang SM, Michel K, Jokhi V, Nedivi E, Arlotta P. Neuron class–specific responses govern adaptive myelin remodeling in the neocortex. Science. 2020;370. https://doi.org/10.1126/SCIENCE.ABD2109.

59. Orduz D, Benamer N, Ortolani D, Coppola E, Vigier L, Pierani A, et al. Develop- mental cell death regulates lineage-related interneuron-oligodendroglia func- tional clusters and oligodendrocyte homeostasis. Nat Commun. 2019;10:4249.

60. Orduz D, Maldonado PP, Balia M, Vélez-Fort M, de Sars V, Yanagawa Y, et al. Interneurons and oligodendrocyte progenitors form a structured synaptic net- work in the developing neocortex. Elife. 2015;2015:1–53.

61. Lin SC, Bergles DE. Synaptic signaling between GABAergic interneurons and oligodendrocyte precursor cells in the hippocampus. Nat Neurosci. 2004. https://doi.org/10.1038/nn1162.

62. Vélez-Fort M, Maldonado PP, Butt AM, Audinat E, Angulo MC. Postnatal switch from synaptic to extrasynaptic transmission between interneurons and NG2 cells. J Neurosci. 2010. https://doi.org/10.1523/JNEUROSCI.0238-10.2010.

63. Butt AM, Hamilton N, Hubbard P, Pugh M, Ibrahim M. Synantocytes: the fifth element. J Anat. 2005;207:695–706.

64. Bribián A, Medina-Rodríguez EM, Josa-Prado F, García-Álvarez I, Machín-Díaz I, Esteban PF, et al. Functional heterogeneity of mouse and human brain OPCs: relevance for preclinical studies in multiple sclerosis. J Clin Med. 2020;9:1681.

65. Spitzer SO, Sitnikov S, Kamen Y, Evans KA, Kronenberg-Versteeg D, Dietmann S, et al. Oligodendrocyte progenitor cells become regionally diverse and hetero- geneous with age. Neuron. 2019;101:459–.e5.

66. Lutz P-E, Tanti A, Gasecka A, Barnett-Burns S, Kim JJ, Zhou Y et al. Association of a history of child abuse with impaired myelination in the anterior cingulate cortex: convergent epigenetic, transcriptional, and morphological evidence. Am J Psy- chiatry. 2017:appiajp201716111286.

67. Tanti A, Kim JJ, Wakid M, Davoli M-A, Turecki G, Mechawar N. Child abuse associates with an imbalance of oligodendrocyte-lineage cells in ventromedial prefrontal white matter. Mol Psychiatry. 2018;23:2018–28.

68. Slaker M, Jorgensen E, Hegarty D, Liu X, Kong Y, Zhang F et al. Cocaine exposure modulates perineuronal nets and synaptic excitability of fast-spiking inter- neurons in the medial prefrontal cortex. eNeuro. 2018;5. https://doi.org/10.1523/ ENEURO.0221-18.2018.

69. Banerjee SB, Gutzeit VA, Baman J, Aoued HS, Doshi NK, Liu RC, et al. Perineuronal nets in the adult sensory cortex are necessary for fear learning. Neuron. 2017;95:169–.e3.

70. Pintér A, Hevesi Z, Zahola P, Alpár A, Hanics J. Chondroitin sulfate proteoglycan-5 forms perisynaptic matrix assemblies in the adult rat cortex. Cell Signal. 2020;74. https://doi.org/10.1016/J.CELLSIG.2020.109710.

71. Pantazopoulos H, Gisabella B, Rexrode L, Benefield D, Yildiz E, Seltzer P, et al. Circadian rhythms of perineuronal net composition. eNeuro. 2020;7:1–21.

72. Wellman CL, Bangasser DA, Bollinger JL, Coutellier L, Logrip ML, Moench KM, et al. Sex differences in risk and resilience: stress effects on the neural substrates of emotion and motivation. J Neurosci. 2018;38:9423–32.

73. Gildawie KR, Honeycutt JA, Brenhouse HC. Region-specific effects of maternal separation on perineuronal net and parvalbumin-expressing interneuron formation in male and female rats. Neuroscience. 2020. https://doi.org/10.1016/j. neuroscience.2019.12.010.

Chapter III

Preface to chapter III

Chapter II shed light on the enduring effects of child abuse on WFL+ PNNs in the human vmPFC. While not covered in this thesis, our examination revealed no significant alterations in WFL+ PNN densities in the hippocampus or entorhinal cortex. This implies that the impact of child abuse on density is specific to the vmPFC. This brain area is highly vulnerable to the effects of childhood maltreatment [21] and patients with damaged vmPFC have impaired emotional responses and moral judgement calls [131]. Moreover, individuals with suicide attempts exhibit abnormal communication between the vmPFC and frontoparietal regions that are associated to value-based decision making issues [132]. As we navigate these intricate neural landscapes, it becomes apparent that the targeted impact of child abuse on the vmPFC holds profound implications for emotional regulation and moral reasoning. Understanding these dynamics not only expands our comprehension of the nuanced effects of ELS but also lays the groundwork for future investigations and interventions aimed at mitigating the consequences of abuse.

Soon after the publishing of our work in Chapter II, a brief research report was published highlighting that WFL might not serve as a comprehensive pan-PNN marker [83]. The lack of characterization of PNN labeling with various markers in the same tissue (anti-ACAN and WFL) for both human and mouse brains, prompted our interest. Additionally, an ongoing international collaboration with Dr. Kimberly Alonge and her team aimed to characterize the sulfation pattern of CS-disaccharides within the human brain, with the hope of gaining a better understanding of PNN composition and function in our postmortem tissue.

These developments laid the foundation for Chapter III, where we, for the first time, characterize PNN labeling across the healthy vmPFC, entorhinal cortex and hippocampus in

human and mouse samples. The inclusion of the entorhinal cortex and hippocampus in our study is motivated by the understanding that the absence of density differences within these regions post-child abuse does not eliminate the possibility of other potential impacts. In simpler terms, our goal is to uncover diverse effects, recognizing that different brain regions may respond differently to challenges. Additionally, we used a limited bedding and nesting ELS paradigm to see if ELS had a similar impact on the mPFC of mice. Comparisons of sulfation and labeling patterns between groups were conducted to explore potential differences in PNN composition associated with child abuse. This chapter achieves aim 1.3, contributing to the overarching goal of characterizing PNNs in postmortem human brain in both psychiatrically healthy and child-abused subjects. Furthermore, it fulfills aim 3 (3.1 and 3.2) by delving into PNNs in a mouse model of ELS.

Chondroitin-sulfate disaccharide sulfation patterns influence the labeling of perineuronal nets in post-mortem human and mouse brain

Claudia Belliveau[1,2], Stéphanie Théberge[1,2], Stefanie Netto[1], Reza Rahimian[1], Gohar Fakhfouri[3], Clémentine Hosdey[1,2], Maria Antonietta Davoli[1], Aarun Hendrickson[4], Kathryn Hao[5], Bruno Giros[3], Gustavo Turecki, Kimberly Alonge[4,*] & Naguib Mechawar[1,2,3,*]

Affiliations

[1]McGill Group for Suicide Studies, Douglas Mental Health University Institute, McGill University, Montreal, Qc, Canada

[2]Integrated Program in Neuroscience, McGill University, Montreal, Qc, Canada

[3]Department of Psychiatry, McGill University, Montreal, Qc, Canada

[4]Department of Medicinal Chemistry, University of Washington, Seattle, USA

[5]Health and Human Sciences, University of Southern California, Los Angeles, USA

(*) denotes shared authorship

Corresponding Authors

Naguib Mechawar, PhD

Douglas Mental Health University Institute

Department of Psychiatry

McGill University

naguib.mechawar@mcgill.ca

Kimberly Alonge, PhD

Department of Medicinal Chemistry

University of Washington

kalonge@uw.edu

Abstract

Perineuronal nets (PNNs) are a condensed form of extracellular matrix that form a net-like covering around certain neurons in the brain. PNNs are primarily composed of chondroitin-sulfate (CS) proteoglycans from the lectican family that consist of CS glycosaminoglycan side chains attached to a core protein. CS disaccharides (CS-d) can exist in various isoforms with different sulfation patterns. Literature suggests that CS-d sulfation patterns can influence the function of PNNs as well as their labeling. This study was conducted to characterize such patterns in different regions of the adult human (N = 81) and mouse (N = 19) brains and then investigate how early-life stress (ELS) impacts these PNN features. Liquid chromatography tandem mass spectrometry was used to quantify five different CS-d sulfation patterns. Immunolabeling for Wisteria Floribunda Lectin (WFL) and anti-aggrecan were performed to identify PNNs and determine if they were single- or double-labeled. In healthy brains, significant regional and species-specific differences in CS-d sulfation and labeling pattern were identified. Although ELS increases WFL+ PNN density, sulfation code and labeling pattern are conserved in all brain areas of both species. These results underscore PNN complexity, emphasizing the need to consider their heterogeneity in future experiments.

Introduction

Perineuronal nets (PNNs), first described by Camillo Golgi in 1893, are a condensed and specialized form of extracellular matrix (ECM) that surround the soma and proximal dendrites of various neurons in the central nervous system [1]. PNNs form preferentially around parvalbumin (PV) expressing inhibitory interneurons and, to a lesser extent, excitatory neurons [2]. Comprising mainly chondroitin sulfate proteoglycans (CSPGs) from the lectican family (aggrecan, brevican,

neurocan, versican), PNNs are synthesized by both the surrounding glia and neurons themselves and exhibit a highly organized mesh-like structure (**Figure 1A**) [2-5]. The CSPGs are attached at their N-terminus through link proteins to a hyaluronan backbone that is secreted by hyaluronan synthase located on the cell surface [6] (**Figure 1B**). The CSPGs then bind to one another through Tenascin-R at their C-terminus forming the characteristic PNN net-like structure [7].

PNN CSPGs consist of varying numbers of attached chondroitin sulfate-glycosaminoglycan (CS-GAG) side chains [4]. An additional layer of complexity is added by the CS-GAG length as well as the sulfate modifications (**Figure 1C**). Sulfate addition can occur on the C-4 and C-6 of the *N*-acetylgalactosamine (GalNAc), and C-2 of D-glucuronic acid (GlcA) that make up the CS disaccharide unit [8]. CS-disaccharides exist in five differentially sulfated isomers including non-sulfated (CS-O (0S)), mono-sulfated (CS-A (4S), -C (6S)) and di-sulfated (CS-D (2S6S), -E (4S6S)) variations. The relative abundances of these isomers incorporated into the PNNs constitute a sulfation code [9] that relates PNN composition to function (reviewed in [8]). For example, the ratio of 4-sulfation to 6-sulfation is important for brain development and aging. In the developing visual cortex, 6-sulfation is highly expressed and permissive to neurocircuit plasticity and reorganization necessary for neurodevelopment. At the end of the critical period, the 6-sulfation is replaced by 4-sulfation that stabilizes and matures the PNN matrices, thus limiting plasticity of the underlying neurons [10]. Extracellular growth factors and proteins, including orthodenticle homeobox protein 2 (Otx2) [11, 12], interact with PNN CS-GAG chains and play a crucial role in the proper maturation of PV interneurons and the timing of the critical period of plasticity [11]. For example, PNNs capture Otx2 through protein-glycan binding to the CS-E and CS-D variants, which allows maturation of the enmeshed neurons [13]. Notably, overexpression of chondroitin 6-sulfotransferase-1 (C6ST-1) in PV interneurons restricts the formation of stable PNNs and prevents

binding of Otx2, resulting in aberrant maturation of PV interneurons and persistent cortical plasticity [10].

PNNs are also associated with the storage of long-term memories by limiting feedback inhibition from PV cells onto projection neurons [14]. It is theorized that these nets preserve spatial information about synapses through the patterning of their holes [15]. Fear memories that persist into adulthood are actively preserved by PNNs in the amygdala, as illustrated by a reopening of the critical period and extinction of fear memory in adult mice in which local PNN CS-GAGs are enzymatically degraded using chondroitinase ABC (chABC) [16]. Due to their protracted development and role in dampening the critical period of brain plasticity in humans and rodents, PNNs have attracted increasing attention in the fields of neurodevelopment [17], neurodegeneration [18] and psychopathology [19-21].

Early-life stress (ELS) coinciding with the critical period can alter PNN development in the rodent brain [22-25] and the effects seem to be paradigm-specific, PNN detection method-specific and region-specific. We previously reported that PNN density is significantly increased in the ventromedial prefrontal cortex (vmPFC) of individuals who experienced child abuse compared to controls [2]. Building upon this, we hypothesize that not only are PNNs increased after child abuse, but their PNN CS-GAG sulfation patterning, and consequently their function, are also affected. This study aimed to characterize PNN sulfation code and labeling pattern across three brain regions: the human vmPFC, entorhinal cortex (EC) and hippocampus (HPC), as well as their corresponding mouse equivalents (mPFC, EC, vHPC). Then, we explored the impact of ELS on these PNN characteristics in both species, recognizing the susceptibility of these brain regions to such influences [26, 27].

Materials and Methods

Human post-mortem brain samples

Brain samples from a total of 81 individuals were obtained from the Douglas-Bell Canada Brain Bank (DBCBB; Montreal, Canada). In collaboration with Quebec's Coroner and the McGill Group for Suicide Studies, informed consent was obtained from the next of kin. Standardized psychological autopsies, medical records and Coroner reports were used to define cases and controls. Any presence of suspected neurodevelopmental, neurodegenerative, or neurological disorders in clinical files were basis for exclusion. In addition, proxy-based interviews with one or more informants that were closely acquainted with the deceased were used to create clinical vignettes with detailed medical and personal histories. Characterization of early-life histories were based on adapted Childhood Experience of Care and Abuse (CECA) interviews addressing the experiences of sexual and physical abuse as well as neglect [28, 29]. Reports of non-random major physical and/or sexual abuse during the first 15 years of life with a score of 1 or 2 on the CECA were considered as severe child abuse. A panel of clinicians reviewed and assessed all clinical vignettes to generate Diagnostic and Statistical Manual of Mental Disorders (DSM-IV) diagnostic criteria and classify the deceased as a case or control. Toxicology reports and medication prescriptions were also obtained. Three groups were compared in this study consisting of healthy individuals having died suddenly (CTRL; n=19), and depressed suicides with (DS-CA; n=33) or without (DS; n=30) a history of severe child abuse (characteristics detailed in **Table 1**).

Human tissue dissections and preparation

Expert staff at the DBCBB dissected 0.5cm-thick coronal sections from isopentane snap-frozen brain samples with the guidance of the human brain atlas [30]. vmPFC samples were

dissected from coronal sections equivalent to plate 3 (approximately -48mm from the center of the anterior commissure) of this atlas. Anterior HPC samples were obtained from sections equivalent to plate 37 of the atlas, by dissecting around hippocampal CA1-CA3, then between the EC and the parahippocampal gyrus. Samples were then fixed in 10% formalin for 24 h, followed by storage in 30% sucrose at 4°C until they sank. Tissue blocks were snap-frozen in isopentane at -35°C before being stored at -80°C until they were sectioned on a cryostat. 40µm-thick free-floating serial sections were stored in cryoprotectant at -20°C until use.

Early-life stress mouse model

Animal housing and experiments followed the Canadian Council on Animal Care (CCAC) guidelines, procedures were approved by the Animal Care Committee of the Douglas Research Center (Protocol number 5570), and all experiments were conducted in accordance with ARRIVE guidelines [31]. 8-week-old male and female C57BL/6J mice were purchased from Charles Rivers. Mice were kept at the Douglas animal facility for at least a week before being bred by housing a single female with one male for one week. Females were monitored daily for the birth of pups. ELS was induced using the limited bedding and nesting paradigm, which causes fragmented maternal care from postnatal day (P)2 to P9, resulting in chronic stress in pups [32, 33]. Briefly, at P2, in the ELS group, mother and litters were moved to cages with a small amount of corn husk bedding at the bottom and half of the standard amount of nesting material (2.5 x 5 cm piece of cotton nesting material) on top of a stainless-steel mesh which was placed 1 cm above the cage floor. Animals were left undisturbed until P9, when they were moved back to cages with regular housing conditions. CTRL cages were equipped with standard amounts of bedding and nesting material (5 x 5cm). Mice had access to standard chow and water *ad libitum* and were kept under a

12:12 h light-dark cycle. Animals were weaned at P21 and sacrificed at P70. Both male (CTRL = 5, ELS = 9) and female (CTRL = 5, ELS =5) mice were used in this study and no sex differences were observed.

Mouse brain preparation

At P70, mice were deeply anesthetized with an intraperitoneal injection of ketamine/xylazine (100/10 mg/kg, Sigma-Aldrich) and perfused transcardially with phosphate buffered saline (PBS) followed by 4% paraformaldehyde (PFA, pH 7.4, dissolved in PBS). Brains were then extracted and post-fixed overnight in 4% PFA at 4 ºC and subsequently cryoprotected in 30% sucrose dissolved in PBS for 48 h at 4 ºC. Sunken brains were snap-frozen in isopentane at -35°C. Lastly, 35µm-thick serial coronal brain sections were collected free-floating and stored in cryoprotectant at -20°C until use.

Liquid chromatography tandem mass spectrometry

Six to ten serial sections from human vmPFC (CTRL = 14, DS = 16, DS-CA = 12), EC (CTRL = 7, DS = 21, DS-CA = 22), HPC (CTRL = 10, DS = 19, DS-CA = 20) or mouse (CTRL = 10, ELS = 9) mPFC, EC, vHPC samples were processed for liquid chromatography tandem mass spectrometry (LC-MS/MS) as previously described [34, 35]. Briefly, samples were shipped from Montreal to Seattle in PBS + 0.02% sodium azide at 4°C. After manual dissections of the brain regions of interest (ROI), sections were washed thrice in Optima LC/MS-grade water and once in 50mM ammonium bicarbonate (pH 7.6) at room temperature (RT). Tissues were incubated with 50mU/mL of chABC (Sigma-Aldrich, C3667, Burlington, Massachusetts, USA) for 24 h at 37°C.

The supernatant was filtered and lyophilized, then reconstituted in LC/MS-grade water for LC-MS/MS analysis.

LC-MS/MS + MRM quantification of isolated chondroitin sulfate disaccharides

Human and mouse CS isomers were subjected to quantification using a triple quadrupole (TQ) mass spectrometer equipped with an electrospray ion (ESI) source (Waters Xevo TQ-S) and operated in negative mode ionization as previously described [9, 34, 35]. Briefly, CS-disaccharides were resolved on porous graphite column (Hypercarb column; 2.1 × 50 mm, 3 µm; Thermo Fisher Scientific) and LC-MS/MS + MRM were performed using a Waters Acquity I-class ultra-performance liquid chromatographic system (UPLC) using the following MRM channels: CS-A (4S), *m/z* 458 > 300; CS-C (6S), *m/z* 458 > 282; CS-D (2S6S) and CS-E (4S6S), *m/z* 268 > 282; CS-O (0S), *m/z* 378 > 175. MassLynx software version 4.1 (Waters) was used to acquire and quantify all data using a modified peak area normalization function [34]. Each CS-disaccharide is shown as the relative percentage of all CS isomers within the sample. CS sulfation was computed using the weighed mean formula for the average number of sulfates (Avg#S) per CS-disaccharide (ΔCS):

$$Avg\#S/\Delta CS = \sum_{(i=1)}^{n} (x_i + w_i) \,/\, \sum_{(i=1)}^{n} w_i x_i = \#Sulfates(0-2)$$

$$w_i = percent\Delta CS$$

Immunolabelings, WFL staining, and image analysis

Free-floating sections of human or mouse brain were labeled for two PNN markers, the PNN CSPG aggrecan (anti-ACAN) and the PNN CS-GAGs (WFL), and co-localized with a neuronal

marker (anti-NeuN) marker (**Table 2**). First, sections were rinsed thrice in PBS and then incubated overnight at 4°C under constant agitation with the appropriate antibody or lectin diluted in a blocking solution of PBS containing 0.2% Triton-X and 2% normal goat serum. Mouse tissues had an additional 1 h of blocking with 10% normal goat serum in PBS with 0.2% Triton-X before primary labeling. After overnight primary incubation, sections were rinsed thrice in PBS and incubated for 2h at RT with the appropriate fluorophore-conjugated secondary antibody or streptavidin (**Table 2**) diluted in the blocking solution. Next, tissues were rinsed and incubated with TrueBlack® (Biotium, #23007, Fremont, California, USA) for 80 seconds to remove endogenous autofluorescence from lipofuscin and other cellular debris. Sections were then mounted on Superfrost charged slides and coverslipped with Vectashield mounting medium with DAPI (Vector Laboratories, H-1800, Newark, California, USA) and stored at 4°C until imaged on an Evident Scientific VS120 Slide Scanner at 20X magnification.

Image analysis was conducted with QuPath [36] version 0.3.2. Two to four ROIs spanning all cortical or subcortical layers were counted per human sample in the vmPFC (CTRL = 11, DS = 9, DS-CA = 9), EC (CTRL = 8, DS = 16, DS-CA = 14), HPC (CTRL = 8, DS = 15, DS-CA = 16) or mouse sample in the mPFC, EC, vHPC (CTRL = 10, ELS = 9). ROIs were manually investigated by a blinded researcher who manually classified PNNs as double positive (WFL+/ ACAN+) or solely labeled by WFL+ or ACAN+. A total of 30982 PNNs were classified in the human brain (14644 in vmPFC, 6920 in EC, 9418 in HPC) and 5902 in the mouse brain (1419 in mPFC, 2233 in EC, 2250 vHPC). PNN counts were normalized to 100 allowing for comparison between groups using percentage of total PNNs classified.

Statistical analyses

Analysis of variance (ANOVA) were performed on Prism version 10 (GraphPad Software, Boston, Massachusetts, USA) and SPSS version 29.0 (IBM Corp, Armonk, New York, USA). Distribution and homogeneity of variances were assessed with Shapiro-Wilk and Levene's tests, respectively. Each statistical test used is specified within the text when comparing sulfation code or labeling pattern between experimental group and brain region. Statistical tests were all two-sided with a significance threshold of 0.05. All data are represented as mean ± standard error mean, unless otherwise indicated.

Results

PNN sulfation code across the healthy brain

Human

To address confounding factors which may contribute to varied findings across brain regions in ELS research, we first characterized CS-GAG sulfation code in healthy postmortem human brain using LC-MS/MS across three regions involved in emotion regulation and the threat response: the vmPFC, EC and HPC [26]. In psychiatrically healthy controls, mono-sulfated CS-A was the most abundant isomer in adult vmPFC (77.6%), EC (76.2%) and HPC (81.2%) compared to CS-C in the vmPFC (5.6%), EC (8.4%), and HPC (9.5%) (**Figure 2A**). This finding is consistent with developmental literature suggesting that CS-A replaces CS-C after the closure of the critical window of developmental neuroplasticity [8, 10, 37]. Meanwhile, di-sulfated CS-D (between 2.0-3.1% of total CS isomers) and CS-E (1.1-1.2% of total CS isomers) were the least abundant in all three brain regions.

When testing for differences in sulfation patterning between human brain regions, we found significant variations between cortical and deep brain structures. The HPC (0.99 Avg#S/ΔCS) exhibited an increase in hypersulfation compared to the EC (0.92 Avg#S/ΔCS) and vmPFC (0.90 Avg#S/ΔCS) (**Figure 2B**). This effect is driven by both the high abundance of mono- and di-sulfated isomers (CS-A, -C, -D), and decreased abundance of non-sulfated isomer (CS-O) specific to this brain region (**Figure 2C**). Meanwhile, the vmPFC contained the least amount of sulfated CS-C and CS-D and greatest abundance non-sulfated CS-O, which contributes to its CS-GAG hyposulfation (**Figure 2C**). The EC presented an intermediate Avg#S/ΔCS and abundance of non-sulfated, mono-sulfated and di-sulfated isomers in all three brain regions (**Figure 2B-C**).

Mouse

To determine whether these region-specific differences in PNN CS-GAG sulfation profiling is conserved across species, we determined the relative abundance of CS isomers by LC-MS/MS in fixed wild type mouse brain. In control animals, CS-A was the most abundant isomer in the mPFC (70%), EC (73.9%), and vHPC (79.6%) (**Figure 3A**), which is consistent with previous research showing decreased CS-A in the somatosensory cortex compared to dorsal hippocampus [9]. Di-sulfated CS-E was the least abundant with 1.4% in the mPFC, 0.9% in the EC and 0.7% in the vHPC.

Similar to human samples (**Figure 2**), major differences in CS-GAG sulfation patterning were observed between mouse brain regions with vHPC hypersulfation (0.94 Avg#S/ΔCS) compared to mPFC (0.85 Avg#S/ΔCS) and EC (0.85 Avg#S/ΔCS) (**Figure 3B**). vHPC hypersulfation appeared to be driven by the high abundance of mono-sulfated isomers CS-A and CS-C and low abundance of non-sulfated CS-O (**Figure 3C**). Unlike the human samples, the

mPFC (17.6% of CS isomers) and EC (16.8% of CS isomers) exhibited similar CS-O sulfation levels.

Labeling patterns of PNNs across the healthy brain

Human

To characterize the labeling pattern of PNNs in relation to sulfation changes, tissues were co-labeled with both ACAN (PNN core protein) and WFL (PNN CS-GAGs). Matching previous reports, healthy human brain showed strong PNN heterogeneity including nets that were WFL-/ACAN+, WFL+/ACAN- and WFL+/ACAN+ [9, 38-41] (**Figure 4A**). ACAN immunoreactivity was found to be associated with PNNs but also within the cytoplasm of some cells (**Figure 4A cyan arrow**), as previously reported in neurons [42] as well as glia [43]. Therefore, only ACAN labeling appearing as PNNs was included (**Figure 4A yellow arrow**). PNN heterogeneity varied between brain regions, with the vmPFC exhibiting the greatest amount of double labeled PNNs (48.3% WFL+/ACAN+) compared to the HPC (20.1%) and EC (12.7%) (**Figure 4B**). Meanwhile, the EC presented the most WFL+/ACAN- labeling (66.8% of total PNNs) compared to HPC (25.7%) and vmPFC (28.3%), suggesting additional PNN core proteins may prevail in this region. Finally, the HPC exhibited the greatest amount of deglycosylated ACAN+ PNNs (54.2% WFL-/ACAN+) compared to the EC (20.5%) and vmPFC (23.4%).

We hypothesized that differences in PNN heterogeneity may be related to differences in PNN CS-GAG sulfation patterning unique to each brain region. When examining the total labeling of a marker (for example: total ACAN labeling includes both the WFL-/ACAN+ labeled PNNs and the double positive WFL+/ACAN+ category) great differences in total labeling were found between brain regions (**Figure 4C**). The vmPFC showed no difference in total ACAN (71.7%) vs total WFL

(76.6%) labeled PNNs, whereas the EC exhibited a significantly higher total amount of WFL (79.4%) labeled PNNs compared to ACAN (33.2%) labeled PNNs. In contrast, the HPC exhibited a significantly higher amount of ACAN (74.3%) labeled PNNs compared to WFL (45.8%) labeled PNNs (**Figure 3G**).

Mouse

To investigate whether labeling pattern of PNNs is conserved across species, healthy mouse brain was also co-labeled with WFL and ACAN (**Figure 5A**). Surprisingly, the labeling pattern of PNNs is highly dissimilar between species. In the mouse mPFC and EC, 94.7% and 92.3% respectively, of all PNNs were labeled solely by WFL+ (**Figure 5B**). Nearly all other PNNs in these brain areas were found to be double positive for WFL+/ACAN+ (5.5-7.1%). While very few PNNs in the mPFC and EC labeled solely for ACAN+ (0-0.6% respectively, **Figure 5C**), the specificity of the ACAN antibody was demonstrated by intracellular ACAN immunoreactivity (as observed in human samples and not considered for analysis) as well as by the abundance of ACAN+ PNNs in the adjacent brain regions within the same coronal sections (**Figure 5C**). The vHPC displayed more heterogeneity in PNN labeling with all three populations being present: 12.5% WFL-/ACAN+, 39.5% WFL+/ACAN- and 47.9% WFL+/ACAN+ (**Figure 5B**). Once again, the mPFC and EC display much higher levels of glycosylation than the vHPC, as seen in humans.

When comparing the total labeling of ACAN or WFL between regions, we observed a similar labeling pattern of WFL across the brain in mice and humans, but ACAN was dispersed differently (**Figure 5D**). In the mPFC and EC, 99.4-100% of PNNs were labeled with WFL, while in the

vHPC only 87.5% of PNNs were labeled. In contrast, the vHPC exhibited 60.5% of PNNs labeled with ACAN while the mPFC and EC only had 5.4-7.7% of PNNs stained with ACAN respectively.

ELS influences PNN abundance but not sulfation code

Human

Although we previously reported an increase in density of WFL+ PNNs in the vmPFC of DS-CA [2], there was no significant difference in the relative abundance of CS isomers associated with abuse in any of the three regions analysed (**Figure 6A-C**). Additionally, the labeling pattern landscape did also not vary with abuse throughout the brain (**Figure 6D-F**).

Mouse

Initially, to validate our mouse model of ELS, we examined the density of WFL+ PNNs in the mPFC. Replicating our previously published human data [2] we found that there are significantly more WFL+ PNNs in the mPFC of ELS mice (N = 9) compared to CTRL mice (N = 10) (**Figure 6G**). ELS did not influence sulfation code (**Figure 6H-J**) or labeling pattern (**Figure 6K-M**) in any of the mouse brain regions investigated, suggesting that ELS only has a long-lasting effect on PNN abundance and not composition, a finding conserved between species.

Discussion

We observed and characterized for the first time vastly different relative abundances of CS-disaccharide isomers and PNN labeling patterns between brain regions and species, shedding light on the intricate foundations of PNN composition, which remain poorly understood. Although there was no significant correlation between labeling pattern and sulfation score (data not shown)

hyposulfated brain areas had the highest levels of glycosylation. In both healthy human and mouse brain, the (v)mPFC and EC had the most glycosylation (total WFL labeling) and the most CS-O; while the (v)HPC had the least glycosylation and least CS-O. Interestingly, the hippocampus is also the brain region with the highest amount of CS-A which has been shown to be useful for creating a healthy niche for neural stem cells through its ability to bind basic fibroblast growth factor [8].

This study highlights the importance of using multiple markers in order to accurately represent the degree of regional PNN diversity. Intriguingly, most studies investigating changes in PNN abundance are conducted using WFL as a PNN marker, a widely accepted histochemical visualization method. WFL is thought to bind to carbohydrate structures terminating in GalNAc linked α or β to the 3 or 6 position of galactose [44] which aggregate in PNNs. Thus, it was previously thought that PNNs would double label when combining WFL staining and immunohistochemistry with anti-CSPG antibodies [45]. However, more recent evidence suggests that, depending on the brain region, WFL binds favourably to non-sulfated CS-disaccharides (CS-O) [46] and does not always co-label PNNs detected with anti-CSPG antibodies [9, 38-41] such as anti-aggrecan (ACAN). We expected there would be a higher amount of double labeled PNNs in all brain regions across species as there is evidence suggesting that ACAN is necessary for PNN formation in vitro [47] and in vivo [48]. However, rodent literature shows that different antibodies bind to different portions of the large proteoglycan such that three different antibodies for ACAN (Cat-301, Cat-315 and Cat-316) bind selectively to this antigen. Nevertheless, their labeling pattern is completely different depending on the brain region and glycosylation pattern of the CSPG [38]. The adult human cortex, specifically Brodmann area 6, expresses all forms of ACAN isoforms [49] to different extent throughout the layers and on different cell types. In our study, Cat-301,

which labels the core protein itself, was the anti-ACAN antibody used to label human brain samples. Cat-316 binds selectively to non-sulfated CS-GAG on ACAN, more similarly to WFL [38], so the use of that antibody would have presented a different landscape of PNN labeling. The antibody used in the mouse brain for this study also binds to the core protein itself, as apparent by the molecular weight reported by the manufacturer (**Table 2**). This highlights the limitation of not having a pan-PNN marker as was once thought for WFL. The unique composition of PNNs in different brain regions, as seen here and by others [38, 50], suggests region-specific roles in regulating plasticity and memory processes. Literature indicates that PNN formation is dependent on neuronal activity [48, 51-53] suggesting that regions with more staining are highly active compared to regions with less staining. Interestingly, this phenomenon has been observed using both WFL and ACAN to visualize the nets, however, relative abundance of each labeling have not been compared in the context of cellular activity. Given PNN heterogeneity, future studies should explore their composition at the single-cell level, as this should shed light on the functional consequences of varied sulfation patterns on different neuronal subtypes, in different brain regions.

The present study also investigated the long-lasting impact of early-life adversity on PNNs in the (v)mPFC, EC and (v)HPC of adult human and mouse brain. Using an ELS mouse model of limited bedding and nesting from P2-9 [33], we found that WFL+ PNNs are increased in the mPFC of P70 male and female mice compared to controls. Moreover, our findings elucidate that PNN sulfation code and labeling pattern are undisturbed in adult human and mouse brains that have experienced early-life adversity. We cannot exclude, however, that this code was altered earlier in life and restored thereafter. Biochemical composition changes of PNNs are not solely restricted to the critical period of plasticity early in life. For example, glia are becoming increasingly involved in the production, maintenance and degradation of cerebral PNNs [54] in adult mice [55] and

humans [56] in health and disease. Glia are also known to produce and secrete chondroitin 4-sulfotransferase-1 [57] and C6ST-1 [58], main regulators of CS-GAG sulfation. Moreover, noteworthy CS-GAG dynamics influenced by circadian rhythms may serve as a plausible explanation for the observed resilience of the sulfation code to early-life adversity [59]. It will be important to further investigate how cerebral PNNs are affected by early-life adversity, given the rich body of research highlighting the long-lasting impact of ELS on WFL+ PNNs across various paradigms and brain regions in different species [2, 22-25].

This study is not without limitations. Firstly, we examined bulk tissue for LC-MS/MS and not individual PNNs which means that we were not only looking at CS-disaccharides from PNNs as the interstitial diffuse ECM is also comprised of CS. However, interstitial ECM has 9X more hyaluronan sulfate than CS, and CS are highly condensed into PNNs [60], so we are confident in the readout of the sulfation code. A more detailed longitudinal study in an animal model should be conducted to further investigate temporal changes in sulfation code and resultant labeling.

Author contributions

CB, KA and NM conceived the study. GT participated in the acquisition and clinical characterization of the brain samples. CB, ST, SN, CH and MAD contributed to immunohistological experiments. RR, GF and BG conducted animal work. KA, AH and KH conducted LC-MS/MS experiments. CB conducted data analysis. CB, NM, KA prepared the manuscript and all authors contributed to and approved its final version.

Acknowledgments

We express our profound gratitude to the families of the deceased who graciously agreed to donate the brains of their loved ones.

Funding

This work was funded by a CIHR Project Grant (PJT-173287) to NM. CB received a doctoral scholarship from FRQ-S. The Douglas-Bell Canada Brain Bank is funded by platform support grants to GT and NM from the RQSHA (FRQ-S), HBHL and Brain Canada. The present study used the services of the Molecular and Cellular Microscopy Platform at the Douglas Hospital Research Centre. This work was also supported by the National Institutes of Health (NIH) grants P30 AG066509 (KA), R21 AG074152 (KA), and DP2 AI171150 (KA). Mass spectrometry work was supported by University of Washington School of Pharmacy's Mass Spectrometry Center (MSC).

Conflict of interest

The authors declare no competing interests.

Figures and figure legends

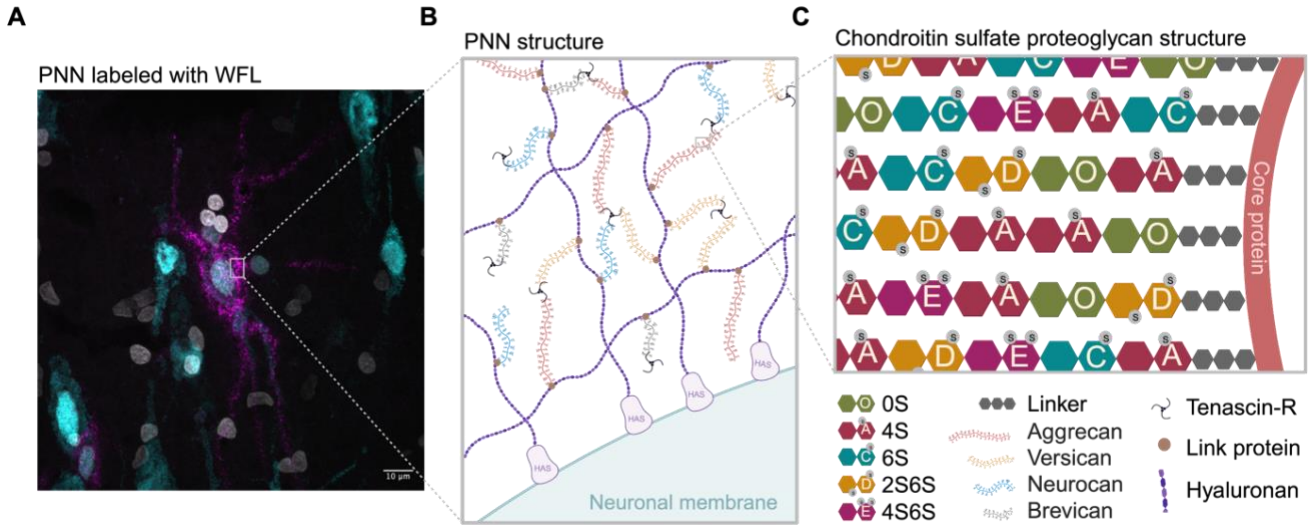

Figure 1: Perineuronal net composition and structure **A** Representative micrograph of a WFL+ PNN surrounding the soma and proximal dendrites of a neuron in the postmortem human entorhinal cortex. Imaged at 60X on Evident Scientific FV1200 Confocal, scale bar 10μm **B** PNNs are primarily composed of CSPGs from the lectican family (aggrecan, versican, neurocan and brevican) intricately linked to a hyaluronan backbone synthesized on the cell surface through link proteins. CSPGs are attached to each other through Tenascin-R, resulting in a distinctive net-like structure known as the PNN. **C** CSPGs have varying number of CS-GAG side chains made up of CS-disaccharides that exist in different isomers based on sulfate groups added to either C-4 or C-6 of the GalNAc or C-2 of GlcA including non-sulfated CS-O (0S), mono-sulfated CS-A (4S), -C (6S) and di-sulfated CS-D (2S6S), -E (4S6S). WFL: Wisteria Floribunda Lectin, PNN: perineuronal net, CSPGs: chondroitin sulfate proteoglycans, CS-GAG: chondroitin sulfate glycosaminoglycan, GalNAc: N-acetylgalactosamine, GlcA: D-glucuronic acid

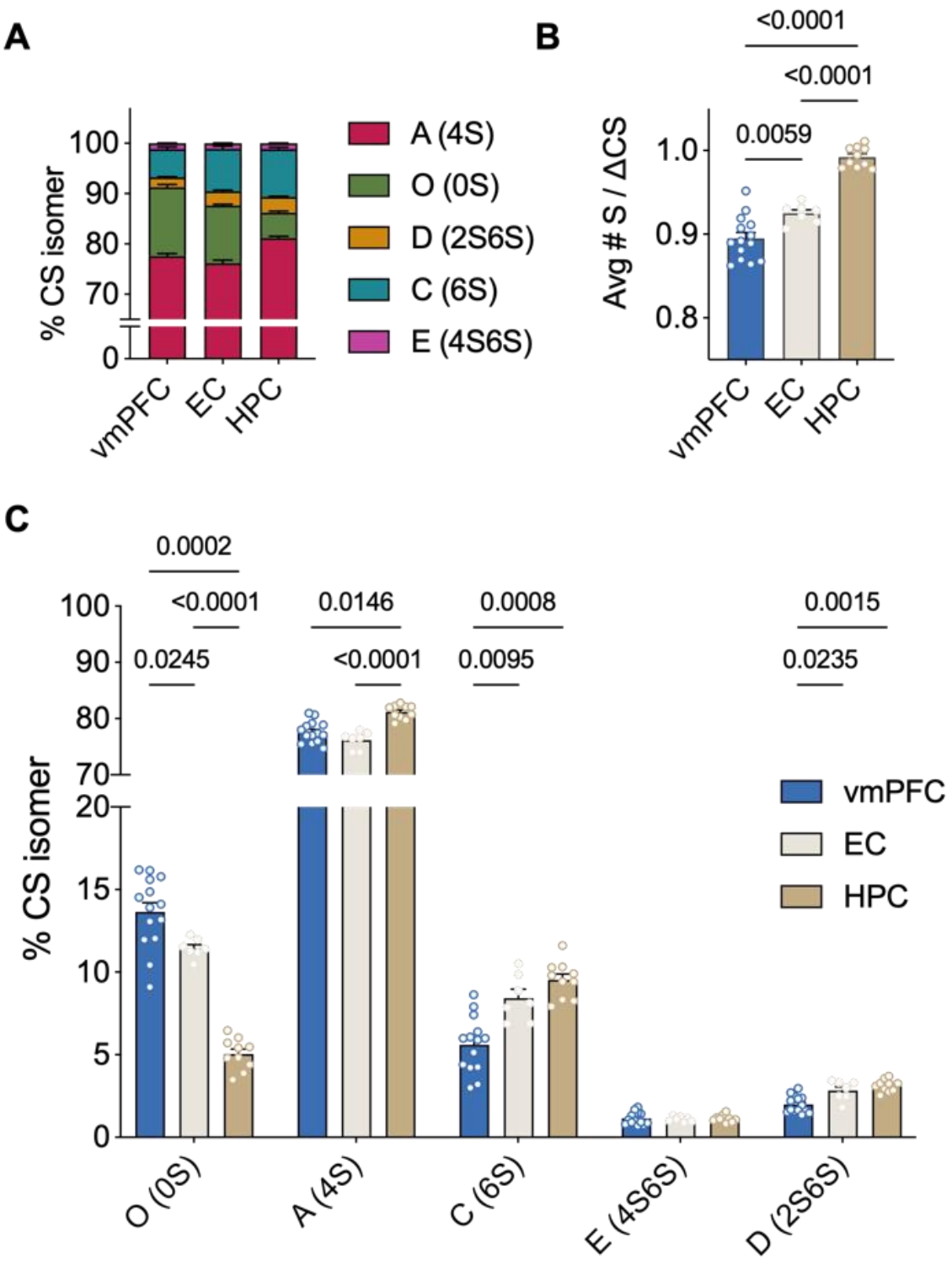
A
% CS isomer
100
90
80
70
0
A (4S)
O (0S)
D (2S6S)
C (6S)
E (4S6S)
vmPFC
EC
HPC
B
<0.0001
<0.0001
0.0059
Avg # S / ΔCS
1.0
0.9
0.8
vmPFC
EC
HPC
C
0.0002
<0.0001
0.0146
0.0008
0.0015
0.0245
<0.0001
0.0095
0.0235
% CS isomer
100
90
80
70
20
15
10
5
0
vmPFC
EC
HPC
O (0S)
A (4S)
C (6S)
E (4S6S)
D (2S6S)

Figure 2: CS-GAG sulfation code varies significantly between brain regions in healthy postmortem human brain **A** Comparison of the relative abundance of each CS isomer in the control vmPFC (N = 14), EC (N = 7) and HPC (N = 10) measured by LC-MS/MS **B** The HPC is the most hypersulfated region on average while the vmPFC is the most hyposulfated region (Welch's ANOVA: $W(2,18) = 101$, $P < 0.0001$, followed by Dunnett's test) **C** Hypersulfation in the HPC is driven by mono-sulfated CS-A, -C and di-sulfated CS-D, while hyposulfation is driven by high abundance of CS-O in the vmPFC. Each isomer is expressed differently in each brain region except for isomer CS-E (4S6S) (isomer effect: $F(2,61) = 20074$, $P < 0.0001$; region effect: $F(0.1, 10) = 5.478e\text{-}20$, $P > 0.9999$; isomer x region: $F(2,43) = 54.23$, $P < 0.0001$, followed by Tukey's test). Avg#S/ΔCS: average number of sulfates per chondroitin sulfate disaccharide, CS-GAG: chondroitin sulfate glycosaminoglycan, vmPFC: ventromedial prefrontal cortex, EC: entorhinal cortex, HPC: hippocampus, LC-MS/MS: liquid chromatography tandem mass spectrometry.

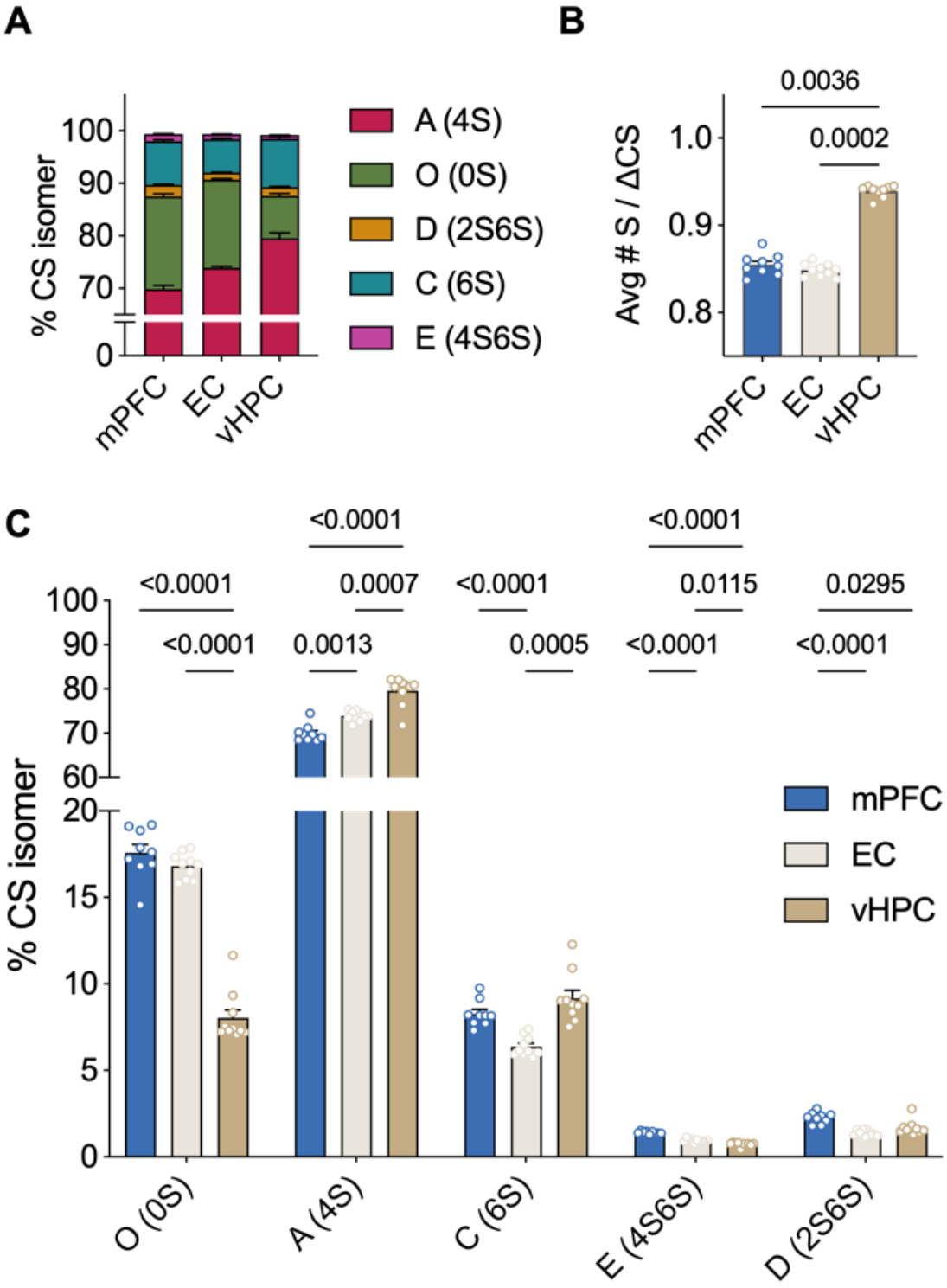
A
% CS isomer
100
90
80
70
0
mPFC
EC
vHPC
A (4S)
O (0S)
D (2S6S)
C (6S)
E (4S6S)
B
Avg # S / ΔCS
1.0
0.9
0.8
0.0036
0.0002
mPFC
EC
vHPC
C
% CS isomer
100
90
80
70
60
20
15
10
5
0
<0.0001
0.0007
<0.0001
<0.0001
0.0115
0.0295
<0.0001
0.0013
0.0005
<0.0001
<0.0001
mPFC
EC
vHPC
O (0S)
A (4S)
C (6S)
E (4S6S)
D (2S6S)

Figure 3: CS-GAG sulfation code is generally conserved between species in the healthy brain **A** Comparison of the relative abundance of each CS isomer in the control mPFC, EC and vHPC of mouse (N = 10) brain measured by LC-MS/MS **B** Like human brain, the mouse vHPC is hypersulfated compared to both the EC and mPFC, however, in this species the mPFC and EC do not differ in average sulfation (Kruskal-Wallis test: $P = 0.0001$, followed by Dunn's test) **C** All CS-isomers are expressed in significantly different abundances across the healthy mouse brain (isomer effect: $F(1,11) = 13984$, $P < 0.0001$; region effect: $F(1, 12) = 0.01896$, $P = 0.940$; isomer x region : $F(2, 16) = 97.49$, $P < 0.0001$, followed by Tukey's test). Avg#S/ΔCS: average number of sulfates per chondroitin sulfate disaccharide, CS-GAG: chondroitin sulfate glycosaminoglycan, LC-MS/MS: liquid chromatography tandem mass spectrometry, mPFC: medial prefrontal cortex, EC: entorhinal cortex, vHPC: ventral hippocampus.

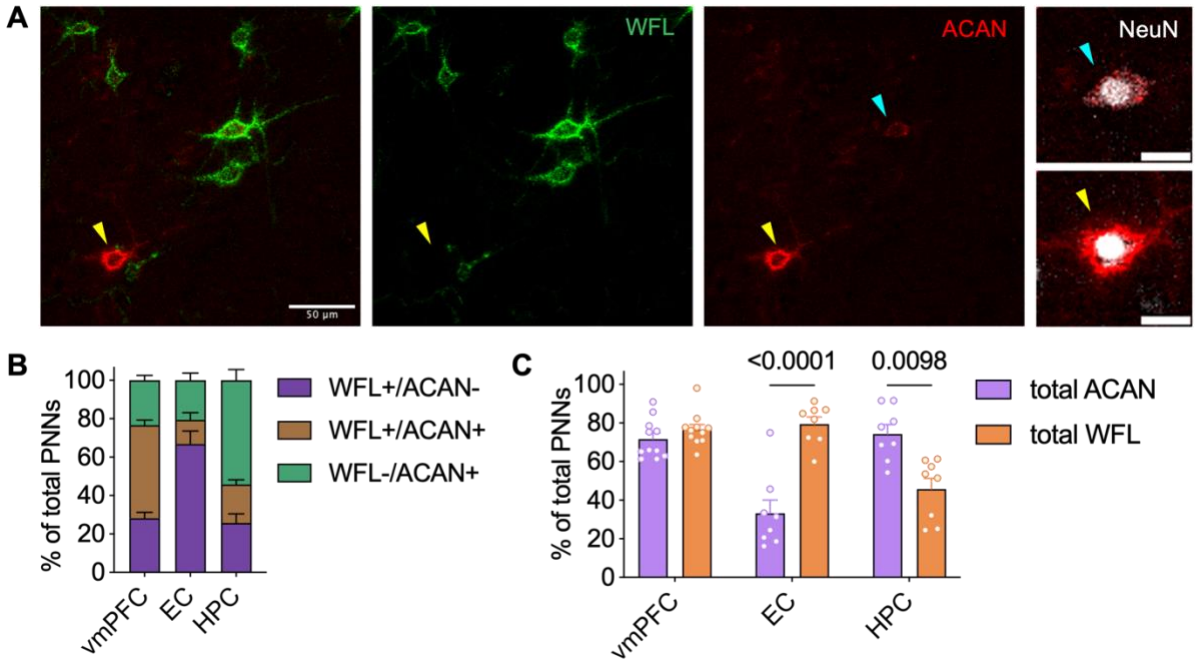
A
WFL
ACAN
NeuN
50 µm
B
% of total PNNs
100
80
60
40
20
0
WFL+/ACAN-
WFL+/ACAN+
WFL-/ACAN+
vmPFC
EC
HPC
C
<0.0001
0.0098
% of total PNNs
total ACAN
total WFL
vmPFC
EC
HPC

Figure 4: Immunohistochemical staining of healthy human brain reveals heterogeneity in perineuronal net labeling that differs between brain regions **A** PNN populations in the vmPFC (N = 11), EC (N = 8) and HPC (N = 8) display either single (WFL+/ACAN- or WFL-/ACAN+) or double (WFL+/ACAN-) labeling. ACAN staining can be found intracellularly (cyan arrow) or in the distinctive pattern of an extracellular PNN (yellow arrow), only the latter was counted in this study. Imaged at 20X on Evident Scientific FV1200 Confocal, scale bar 50µm and 20µm (right) **B** Comparison of the labeling patterning between the different brain regions investigated. **C** Total ACAN (WFL+/ACAN+ and WFL-/ACAN+) and total WFL (WFL+/ACAN- and WFL+/ACAN+) labeling can be found in different amounts depending on the brain region. Within the vmPFC the two markers label similarly, while WFL prevails in the EC and ACAN predominates in the HPC. WFL: Wisteria Floribunda Lectin, ACAN: anti-aggrecan core protein, NeuN: anti-neuronal nuclei, vmPFC: ventromedial prefrontal cortex, EC: entorhinal cortex, HPC: hippocampus.

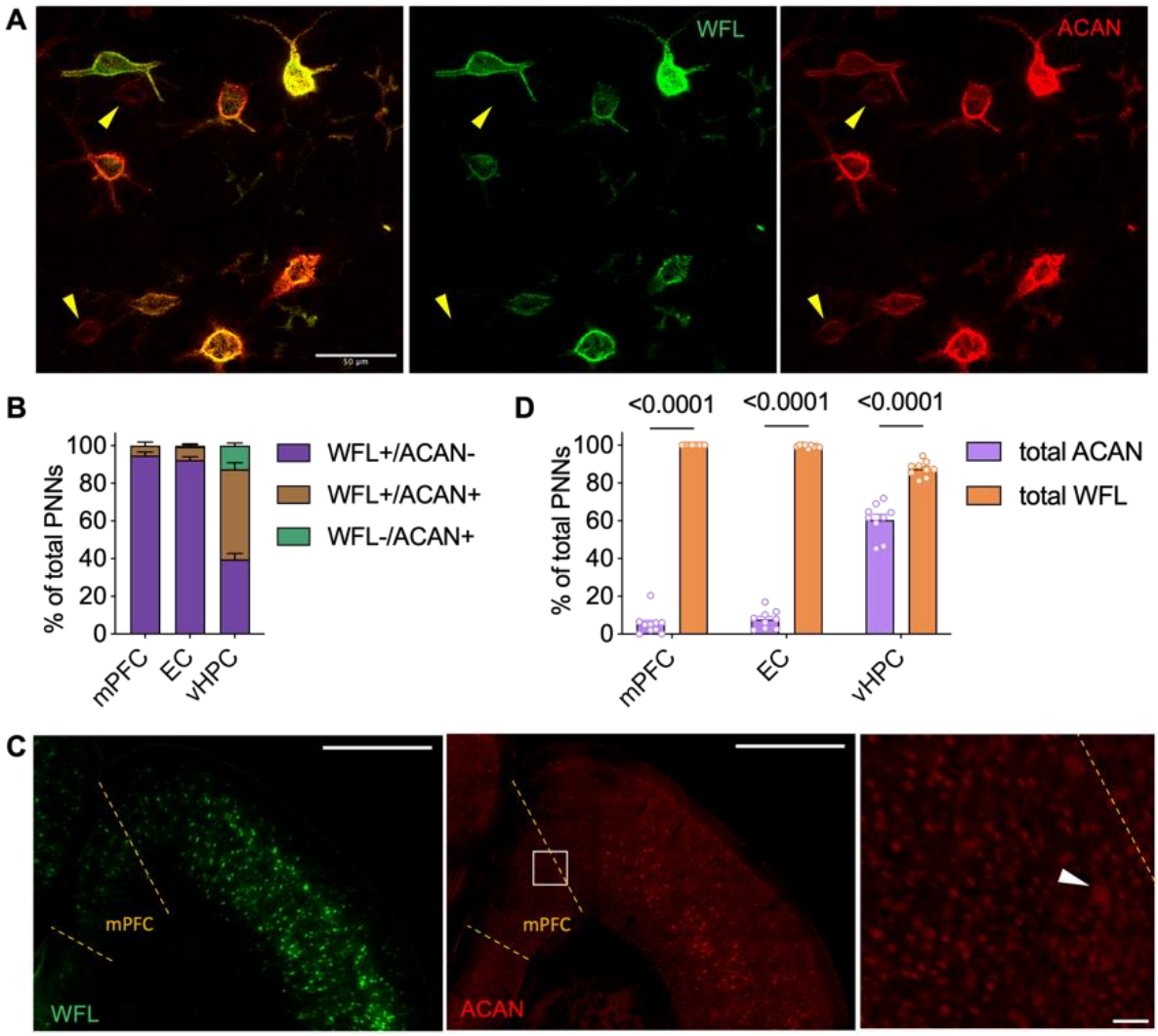
A
WFL
ACAN
B
% of total PNNs
100
80
60
40
20
0
mPFC
EC
vHPC
WFL+/ACAN-
WFL+/ACAN+
WFL-/ACAN+
D
<0.0001
<0.0001
<0.0001
% of total PNNs
mPFC
EC
vHPC
total ACAN
total WFL
C
mPFC
WFL
mPFC
ACAN

Figure 5: Perineuronal net labeling is highly dissimilar between species **A** Immunohistochemical labeling of PNNs in the vHPC displays WFL+/ACAN+ nets, WFL-/ACAN+ (yellow arrow) and WFL+/ACAN- (not displayed) populations. Imaged at 20X on Evident Scientific FV1200 Confocal, scale bar 50µm **B** Unlike the human samples, barely any PNNs were labeled solely by WFL-/ACAN+ in control mouse mPFC and EC (N=10), while the vHPC expressed all three categories of labeling **C** Representative image of a coronal section of mouse brain with the mPFC delineated. Although there is barely any PNN labeling by ACAN in the mPFC (white arrow), ACAN can be seen intracellularly, as in humans. Imaged at 20x on Evident Scientific VS120 Slide Scanner, scale bar 1 mm and 50µm (right). **D** Examination of total WFL or ACAN labeling within brain regions reveals that WFL labels significantly more PNNs in all brain regions examined. WFL: Wisteria Floribunda Lectin, ACAN: anti-aggrecan core protein, mPFC: medial prefrontal cortex, EC: entorhinal cortex, vHPC: ventral hippocampus.

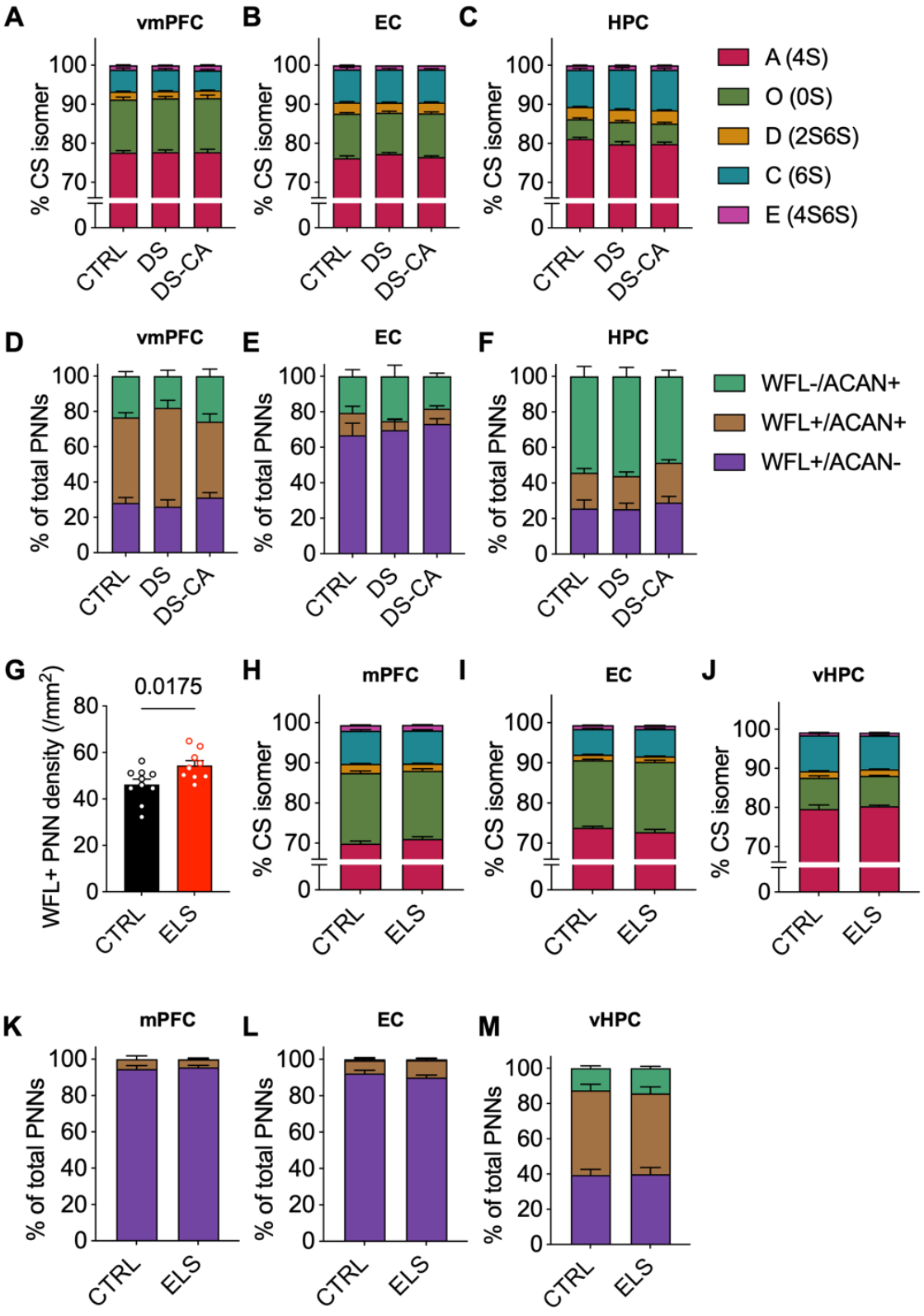
A
vmPFC
B
EC
C
HPC
% CS isomer
100
90
80
70
0
CTRL
DS
DS-CA
A (4S)
O (0S)
D (2S6S)
C (6S)
E (4S6S)
D
vmPFC
E
EC
F
HPC
% of total PNNs
100
80
60
40
20
0
CTRL
DS
DS-CA
WFL-/ACAN+
WFL+/ACAN+
WFL+/ACAN-
G
WFL+ PNN density (/mm2)
0.0175
80
60
40
20
0
CTRL
ELS
H
mPFC
I
EC
J
vHPC
% CS isomer
100
90
80
70
0
CTRL
ELS
K
mPFC
L
EC
M
vHPC
% of total PNNs
100
80
60
40
20
0
CTRL
ELS

Figure 6: Perineuronal net sulfation code and labeling pattern are preserved after the experience of early-life stress in both human and mouse brain **A-C** Within each human brain region CS-GAG sulfation code is unaffected by depression, suicide (DS) and child abuse (DS-CA) when compared to controls (CTRL) (vmPFC group x isomer: $F(3,67) = 0.132$, $P = 0.929$; EC group x isomer: $F(3,13) = 1.448$, $P = 0.275$; HPC group x isomer: $F(2,6) = 1.210$, $P = 0.372$) **D-F** Although we previously reported a significant increase in WFL+ PNNs in the vmPFC, overall labeling pattern is conserved between groups in all brain regions examined (vmPFC group x labeling: $F(4,52) = 1.774$, $P = 0.148$; EC group x labeling: $F(4,70) = 0.632$, $P = 0.642$; HPC group x labeling: $F(4,72) = 0.676$, $P = 0.611$) **G** Limited bedding and nesting from P2-9 is associated with a significant increase in WFL+ PNNS in the mPFC of adult mice ($N = 9$) compared to control ($N = 10$) (Welch's t-test: $P = 0.0175$) **H-J** Within each mouse brain region CS-GAG sulfation code is unaffected by early-life stress (mPFC group x isomer: $F(1,21) = 1.761$, $P = 0.200$; EC group x isomer: $F(1,9) = 5.029$, $P = 0.464$ although does not pass Bonferroni's multiple comparisons test; vHPC group x isomer: $F(1,22) = 0.683$, $P = 0.424$) **K-M** Although we report an increase in WFL+ PNNs in the mPFC of mice, the overall landscape of PNN labeling by WFL and ACAN is resilient to ELS (mPFC group x labeling: $F(2,34) = 0.248$, $P = 0.782$; EC group x labeling: $F(2,32) = 1.33$, $P = 0.279$; vHPC group x labeling: $F(2, 32) = 0.140$, $P = 0.870$). CTRL: psychiatrically healthy control, DS: depressed suicide, DS-CA: depressed suicide with a history of child abuse, CS-GAG: chondroitin sulfate glycosaminoglycan, WFL: Wisteria Floribunda Lectin, ACAN: anti-aggrecan core protein, vmPFC: ventromedial prefrontal cortex, EC: entorhinal cortex, HPC: hippocampus, mPFC: medial prefrontal cortex, EC: entorhinal cortex, vHPC: ventral hippocampus.

Tables

Table 1: Group characteristics			
	CTRL	**DS**	**DS-CA**
N = 81	18	30	33
Axis 1 diagnosis	0	MDD (25); DD-NOS (5)	MDD (26); DD-NOS (7)
Age (years) (P = 0.06)	48.1 ± 20.2	50.4 ± 12.5	41.5 ± 14.6
Sex (M/F)	13/5	25/5	22/11
PMI (h) (P = 0.14)	41.1 ± 25.0	54.0 ± 29.0	56.9 ± 27.7
Tissue pH (P = 0.99)	6.5 ± 0.3	6.5 ± 0.4	6.5 ± 0.4
Substance dependence	0	8	8
3 months medication	Sedative hypnotics (1)	Classic antidepressants (4); Benzodiazepines (9); SNRI (4); SSRI (6); Antipsychotic (3); TCA (2); Antimanic (1); Opioid (1)	Classic antidepressants (2); Benzodiazepines (6); SNRI (3); SSRI (7); Antipsychotic (3); TCA (1); Antimanic (1); Opioid (2); NASSA (2); SARI (1); Anticonvulsant (2); GABA analog (1)

Table 2: Specific labeling					
Abbreviation	**Primary**	**Labels**	**Target species**	**Product**	**Fluorophore conjugated-secondary**
Human samples					
WFL	Biotinylated Wisteria Floribunda Lectin	Perineuronal nets	Human	Vector Laboratories, B-1355, 1:2500	Alexa 488-Streptavidin, Jackson ImmunoResearch, 016-540-084, 1:500
NeuN	Anti-neuronal nuclei	Neurons	Human	Abcam, ab104225, 1:1000	DyLight-594 anti-rabbit, Jackson ImmunoResearch, 111-515-144, 1:500
ACAN	Anti-chondroitin sulfate proteoglycan brain core protein (Cat-301)	Perineuronal nets	Human	Millipore, MAB5284, 1:500	Alexa-647 anti-mouse, Jackson ImmunoResearch, 115-605-146, 1:500
Mouse samples					
WFA	Biotinylated Wisteria Floribunda Agglutin	Perineuronal nets	Mouse	Vector Laboratories, B-1355, 1:1500	Cy3-Streptavidin, Jackson ImmunoResearch, 016-160-084, 1:500
NeuN	Anti-neuronal nuclei	Neurons	Mouse	Millipore, MAB377, 1:500	Alexa-647 anti-mouse, Jackson ImmunoResearch, 115-605-146, 1:500
ACAN	Anti-aggrecan	Perineuronal nets	Mouse	Millipore, AB1031, 1:100	Alexa-488 anti-rabbit. Jackson ImmunoResearch, 111-485-144, 1:500

References

1. Novak, U. and A.H. Kaye, *Extracellular matrix and the brain: components and function.* J Clin Neurosci, 2000. **7**(4): p. 280-90.

2. Tanti, A., et al., *Child abuse associates with increased recruitment of perineuronal nets in the ventromedial prefrontal cortex: a possible implication of oligodendrocyte progenitor cells.* Molecular Psychiatry, 2022. **27**(3): p. 1552-1561.

3. Celio, M.R., et al., *Perineuronal nets: past and present.* Trends Neurosci, 1998. **21**(12): p. 510-5.

4. Schwartz, N.B. and M.S. Domowicz, *Proteoglycans in brain development and pathogenesis.* FEBS Lett, 2018. **592**(23): p. 3791-3805.

5. Carulli, D., et al., *Composition of perineuronal nets in the adult rat cerebellum and the cellular origin of their components.* J Comp Neurol, 2006. **494**(4): p. 559-77.

6. Kwok, J.C., et al., *Extracellular matrix and perineuronal nets in CNS repair.* Dev Neurobiol, 2011. **71**(11): p. 1073-89.

7. Lundell, A., et al., *Structural basis for interactions between tenascins and lectican C-type lectin domains: evidence for a crosslinking role for tenascins.* Structure, 2004. **12**(8): p. 1495-506.

8. Djerbal, L., H. Lortat-Jacob, and J. Kwok, *Chondroitin sulfates and their binding molecules in the central nervous system.* Glycoconj J, 2017. **34**(3): p. 363-376.

9. Scarlett, J.M., S.J. Hu, and K.M. Alonge, *The "Loss" of Perineuronal Nets in Alzheimer's Disease: Missing or Hiding in Plain Sight?* Front Integr Neurosci, 2022. **16**: p. 896400.

10. Miyata, S., et al., *Persistent cortical plasticity by upregulation of chondroitin 6-sulfation.* Nat Neurosci, 2012. **15**(3): p. 414-22, s1-2.

11. Bernard, C. and A. Prochiantz, *Otx2-PNN Interaction to Regulate Cortical Plasticity.* Neural Plast, 2016. **2016**: p. 7931693.

12. Van't Spijker, H.M., et al., *Neuronal Pentraxin 2 Binds PNNs and Enhances PNN Formation.* Neural Plast, 2019. **2019**: p. 6804575.

13. Beurdeley, M., et al., *Otx2 binding to perineuronal nets persistently regulates plasticity in the mature visual cortex.* J Neurosci, 2012. **32**(27): p. 9429-37.

14. Shi, W., et al., *Perineuronal nets protect long-term memory by limiting activity-dependent inhibition from parvalbumin interneurons.* Proc Natl Acad Sci U S A, 2019. **116**(52): p. 27063-27073.

15. Tsien, R.Y., *Very long-term memories may be stored in the pattern of holes in the perineuronal net.* Proc Natl Acad Sci U S A, 2013. **110**(30): p. 12456-61.

16. Gogolla, N., et al., *Perineuronal nets protect fear memories from erasure.* Science, 2009. **325**(5945): p. 1258-61.

17. Wen, T.H., et al., *The Perineuronal 'Safety' Net? Perineuronal Net Abnormalities in Neurological Disorders.* Front Mol Neurosci, 2018. **11**: p. 270.

18. Lemarchant, S., S. Wojciechowski, and J. Koistinaho, *Perineuronal nets in neurodegeneration.* Oncotarget, 2016. **7**(48): p. 78224-78225.

19. Pantazopoulos, H. and S. Berretta, *In Sickness and in Health: Perineuronal Nets and Synaptic Plasticity in Psychiatric Disorders.* Neural Plast, 2016. **2016**: p. 9847696.

20. Carceller, H., et al., *Perineuronal Nets: Subtle Structures with Large Implications.* Neuroscientist, 2023. **29**(5): p. 569-590.

21. Browne, C.A., et al., *Editorial: Perineuronal Nets as Therapeutic Targets for the Treatment of Neuropsychiatric Disorders.* Front Synaptic Neurosci, 2022. **14**: p. 889800.

22. Gildawie, K.R., J.A. Honeycutt, and H.C. Brenhouse, *Region-specific Effects of Maternal Separation on Perineuronal Net and Parvalbumin-expressing Interneuron Formation in Male and Female Rats.* Neuroscience, 2020. **428**: p. 23-37.

23. Santiago, A.N., et al., *Early life trauma increases threat response of peri-weaning rats, reduction of axo-somatic synapses formed by parvalbumin cells and perineuronal net in the basolateral nucleus of amygdala.* J Comp Neurol, 2018. **526**(16): p. 2647-2664.

24. Guadagno, A., et al., *Effects of Early Life Stress on the Developing Basolateral Amygdala-Prefrontal Cortex Circuit: The Emerging Role of Local Inhibition and Perineuronal Nets.* Front Hum Neurosci, 2021. **15**: p. 669120.

25. Murthy, S., et al., *Perineuronal Nets, Inhibitory Interneurons, and Anxiety-Related Ventral Hippocampal Neuronal Oscillations Are Altered by Early Life Adversity.* Biol Psychiatry, 2019. **85**(12): p. 1011-1020.

26. Teicher, M.H., et al., *The effects of childhood maltreatment on brain structure, function and connectivity.* Nat Rev Neurosci, 2016. **17**(10): p. 652-66.

27. Murthy, S. and E. Gould, *How Early Life Adversity Influences Defensive Circuitry.* Trends Neurosci, 2020. **43**(4): p. 200-212.

28. Lutz, P.E., et al., *Association of a History of Child Abuse With Impaired Myelination in the Anterior Cingulate Cortex: Convergent Epigenetic, Transcriptional, and Morphological Evidence.* Am J Psychiatry, 2017. **174**(12): p. 1185-1194.

29. Bifulco, A., G.W. Brown, and T.O. Harris, *Childhood Experience of Care and Abuse (CECA): a retrospective interview measure.* J Child Psychol Psychiatry, 1994. **35**(8): p. 1419-35.

30. Juergen Mai, M.M., George Paxinos, *Atlas of the Human Brain. 4th Ed*. 2016: Elseiver.

31. Percie du Sert, N., et al., *The ARRIVE guidelines 2.0: Updated guidelines for reporting animal research.* PLOS Biology, 2020. **18**(7): p. e3000410.

32. Rice, C.J., et al., *A novel mouse model for acute and long-lasting consequences of early life stress.* Endocrinology, 2008. **149**(10): p. 4892-900.

33. Reemst, K., et al., *Early-life stress lastingly impacts microglial transcriptome and function under basal and immune-challenged conditions.* Translational Psychiatry, 2022. **12**(1): p. 507.

34. Alonge, K.M., et al., *Quantitative analysis of chondroitin sulfate disaccharides from human and rodent fixed brain tissue by electrospray ionization-tandem mass spectrometry.* Glycobiology, 2019. **29**(12): p. 847-860.

35. Logsdon, A.F., et al., *Decoding perineuronal net glycan sulfation patterns in the Alzheimer's disease brain.* Alzheimers Dement, 2022. **18**(5): p. 942-954.

36. Bankhead, P., et al., *QuPath: Open source software for digital pathology image analysis.* Sci Rep, 2017. **7**(1): p. 16878.

37. Kitagawa, H., et al., *Developmental regulation of the sulfation profile of chondroitin sulfate chains in the chicken embryo brain.* J Biol Chem, 1997. **272**(50): p. 31377-81.

38. Matthews, R.T., et al., *Aggrecan glycoforms contribute to the molecular heterogeneity of perineuronal nets.* J Neurosci, 2002. **22**(17): p. 7536-47.

39. Härtig, W., et al., *Update on Perineuronal Net Staining With Wisteria floribunda Agglutinin (WFA).* Front Integr Neurosci, 2022. **16**: p. 851988.

40. Ueno, H., et al., *Expression of aggrecan components in perineuronal nets in the mouse cerebral cortex.* IBRO Rep, 2018. **4**: p. 22-37.

41. Miyata, S., et al., *Structural Variation of Chondroitin Sulfate Chains Contributes to the Molecular Heterogeneity of Perineuronal Nets.* Front Integr Neurosci, 2018. **12**: p. 3.

42. Domowicz, M., D. Mangoura, and N.B. Schwartz, *Cell specific-chondroitin sulfate proteoglycan expression during CNS morphogenesis in the chick embryo.* Int J Dev Neurosci, 2000. **18**(7): p. 629-41.

43. Asher, R.A., et al., *On the existence of a cartilage-like proteoglycan and link proteins in the central nervous system.* Glia, 1995. **13**(4): p. 294-308.

44. Laboratories, V., *Wisteria Floribunda Lectin (WFA, WFL) Biotinylated Data Sheet.* 2023.

45. Härtig, W., et al., *Chondroitin sulfate proteoglycan-immunoreactivity of lectin-labeled perineuronal nets around parvalbumin-containing neurons.* Brain Res, 1994. **635**(1-2): p. 307-11.

46. Nadanaka, S., et al., *Reconsideration of the Semaphorin-3A Binding Motif Found in Chondroitin Sulfate Using Galnac4s-6st-Knockout Mice.* Biomolecules, 2020. **10**(11).

47. Giamanco, K.A., M. Morawski, and R.T. Matthews, *Perineuronal net formation and structure in aggrecan knockout mice.* Neuroscience, 2010. **170**(4): p. 1314-27.

48. Rowlands, D., et al., *Aggrecan Directs Extracellular Matrix-Mediated Neuronal Plasticity.* J Neurosci, 2018. **38**(47): p. 10102-10113.

49. Virgintino, D., et al., *Differential distribution of aggrecan isoforms in perineuronal nets of the human cerebral cortex.* J Cell Mol Med, 2009. **13**(9b): p. 3151-73.

50. Lensjø, K.K., et al., *Differential Expression and Cell-Type Specificity of Perineuronal Nets in Hippocampus, Medial Entorhinal Cortex, and Visual Cortex Examined in the Rat and Mouse.* eNeuro, 2017. **4**(3).

51. Kind, P.C., et al., *The Development and Activity-Dependent Expression of Aggrecan in the Cat Visual Cortex.* Cerebral Cortex, 2012. **23**(2): p. 349-360.

52. McRae, P.A., et al., *Aggrecan expression, a component of the inhibitory interneuron perineuronal net, is altered following an early-life seizure.* Neurobiology of Disease, 2010. **39**(3): p. 439-448.

53. Devienne, G., et al., *Regulation of perineuronal nets in the adult cortex by the activity of the cortical network.* J Neurosci, 2021. **41**(27): p. 5779-90.

54. Crapser, J.D., et al., *Microglia as hackers of the matrix: sculpting synapses and the extracellular space.* Cell Mol Immunol, 2021. **18**(11): p. 2472-2488.

55. Venturino, A., et al., *Microglia enable mature perineuronal nets disassembly upon anesthetic ketamine exposure or 60-Hz light entrainment in the healthy brain.* Cell Rep, 2021. **36**(1): p. 109313.

56. Crapser, J.D., et al., *Microglia facilitate loss of perineuronal nets in the Alzheimer's disease brain.* EBioMedicine, 2020. **58**: p. 102919.

57. Bhattacharyya, S., et al., *Decline in arylsulfatase B and Increase in chondroitin 4-sulfotransferase combine to increase chondroitin 4-sulfate in traumatic brain injury.* J Neurochem, 2015. **134**(4): p. 728-39.

58. Properzi, F., et al., *Chondroitin 6-sulphate synthesis is up-regulated in injured CNS, induced by injury-related cytokines and enhanced in axon-growth inhibitory glia.* Eur J Neurosci, 2005. **21**(2): p. 378-90.

59. Pantazopoulos, H., et al., *Circadian Rhythms of Perineuronal Net Composition.* eNeuro, 2020. **7**(4).

60. Deepa, S.S., et al., *Composition of perineuronal net extracellular matrix in rat brain: a different disaccharide composition for the net-associated proteoglycans.* J Biol Chem, 2006. **281**(26): p. 17789-800.

Chapter IV

Preface to Chapter IV

To gain deeper insights into the observations outlined in Chapter II & III, particularly regarding the persistent increase in PNNs, we sought to unravel the factors contributing to this increased recruitment. We identified that oligodendrocyte precursor cells are producing more PNN components in DS-CA, aligning with the observed increase in nets. However, this finding does not entirely elucidate why PNNs are not brought back down to homeostatic levels at some point after the abuse and before death. In Chapters II and III, we made a significant observation that depressed suicides with no history of child abuse exhibited no alterations in any of the examined brain regions or experiments when compared to controls. As a result, for Chapter IV, we opted to exclude this group and concentrate exclusively on the comparison between controls and DS-CA. Furthermore, upon studying the hippocampus and entorhinal cortex in these subjects, we found no density, composition or labeling changes between groups. Consequently, we chose to narrow our focus exclusively to the vmPFC, the brain area where differences were observed.

In 2020, a ground-breaking paper directly implicated microglia in the degradation of PNNs [116]. Extending this insight to the human brain, we conducted molecular analyses of factors previously associated to PNN regulation by microglia studied in rodent brains. While the field acknowledges the direct involvement of microglia in PNN pruning, the precise mechanisms of action remain elusive. This study represents the inaugural exploration of the landscape of MMPs and their inhibitors within the context of child abuse. Additionally, we refined a protocol for isolating microglia from postmortem human brain tissue, establishing a robust platform to scrutinize the specific role of microglia in PNN degradation. Furthermore, our findings suggest a compromised communication between neurons and glia in the context of child abuse, offering

insights into why PNNs may not be effectively degraded in such conditions. Chapter IV successfully fulfills aim 2, encompassing both 2.1 and 2.2 of this thesis.

Postmortem evidence of a microglial involvement in the child abuse-associated increase of perineuronal nets in the ventromedial prefrontal cortex

Claudia Belliveau[1,2,*], Reza Rahimian[1,*], Gohar Fakhfouri[3], Maria Antonietta Davoli[1], Bruno Giros[2,3], Gustavo Turecki[1,2,3], Naguib Mechawar[1,2,3]

[1]McGill Group for Suicide Studies, Douglas Mental Health University Institute, McGill University, Montreal, Qc, Canada

[2] Integrated Program in Neuroscience, McGill University, Montreal, Qc, Canada

[3] Department of Psychiatry, McGill University, Montreal, Qc, Canada.

(*) shared first authorship

Corresponding Author

Naguib Mechawar, PhD

Douglas Mental Health University Institute

Department of Psychiatry, McGill University

naguib.mechawar@mcgill.ca

Abstract

Microglia, versatile in their functions within the central nervous system, have recently been recognized for their capacity to degrade extracellular matrix. Perineuronal nets (PNNs), a specialized form of this matrix, are crucial for stabilizing neuronal connections and constraining plasticity. Our group recently reported increased PNN densities in the ventromedial prefrontal cortex (vmPFC) of adult depressed suicides with a history of child abuse, compared to matched controls. To explore the underlying mechanisms, we used here a comprehensive approach in similar postmortem vmPFC samples, combining a human matrix metalloproteinase array, isolation of CD11b-positive microglia, and enzyme-linked immunosorbent assays. Our results indicate a significant downregulation of matrix metalloproteinase (MMP)-9, MMP-3, and (tissue inhibitors of metalloproteinases (TIMP)-1, -2, -4 in both whole vmPFC grey matter and isolated microglia. Furthermore, our experiments revealed that a history of child abuse was associated with a dampening of intercellular communication between microglia and neurons through CX3CR1 and IL33R. Taken together, these findings suggest that microglial function is lastingly disrupted in the vmPFC of adults having experienced sever adversity during childhood, thus providing a potential mechanism for the previously reported child abuse-associated PNN alterations.

Introduction

Microglia, the brain's resident immune cells, play a fundamental role in the induction of neuroinflammation through their ability to transform into reactive states in response to inflammatory insults [1, 2]. A large body of evidence has established that neuroinflammation may play an instrumental role in major depressive disorder (MDD) [3-6], at least in certain patients, through the chronic priming of microglia in limbic regions [7]. Furthermore, microglia respond to

environmental signals such as stress by releasing various molecules (cytokines, chemokines and growth factors) and by regulating phagocytosis and synaptic pruning, which are crucial for proper brain development and function [8]. Microglia have also recently gained attention for their role in early-life stress (ELS) [9-11] and regulating brain plasticity through modulation of the extracellular matrix (ECM) (reviewed in [12, 13]). One specialized form of condensed ECM, perineuronal nets (PNNs), function to inhibit axon growth and spine formation [14, 15] while acting as a scaffolding for neuronal circuitry [16, 17]. Emerging evidence implicates microglia as key players in PNN degradation [12, 18-23]. The mechanisms underlying this phenomenon, however, remain incompletely understood. Instances of direct PNN regulation through microglial phagocytosis have been recognized, as evidenced by PNN staining (*Wisteria Floribunda Lectin* (WFL) or anti-aggrecan) visible in CD68+ lysosomes of microglia in healthy brain [18, 19, 23] and spinal cord [24], Alzheimer's Disease [20], Huntington's Disease [22] and adult-onset leukoencephalopathy with axonal spheroids and pigmented glia [21]. The existing body of literature underscores the significance of intercellular communication between neurons and microglia in the intricate regulation of PNNs. However, it remains uncertain whether these communication pathways are fully responsible for initiating microglial phagocytosis of PNN components or if they just represent one mechanism. The interaction between neuronal IL33 and microglial IL33-receptor (IL33R) is a good example. This interaction has been shown to trigger microglial phagocytosis of PNN component aggrecan; an effect abolished in knockout mice of either the ligand or receptor [23]. PNN phagocytosis similarly occurs with neuronal CX3CL1 binding to microglial CX3CR1, as demonstrated by reduced PNN density in parallel to WFL accumulation in CD68+ microglial lysosomes. Knocking out either CX3CL1 or CX3CR1 also prevents this from occurring [24].

Matrix metalloproteinases (MMPs) are enzymes that catalyze glycoproteins in the ECM. Their activity is tightly controlled in the healthy brain by endogenous tissue inhibitors (TIMP-1, -2, -3, -4) that bind to their catalytic site [25]. MMPs can be classified, based on their affinity to various substrates, into different subgroups: gelatinases (MMP-2, -9), stromelysins (MMP-3, -10 and -11) and collagenases (MMP-1, -8, -13, -18) among others [25]. Importantly, all classes of MMPs have already been implicated in ECM regulation. Specifically, they have all been found to target aggrecan core protein, tenascins and link proteins which are all fundamental components of PNNs [25, 26]. Different types of MMPs, especially MMP-2 and MMP-9, are expressed by microglia and their roles have been established in neuroinflammatory cascades [26]. The most studied MMP, MMP-9, plays a fundamental role in neurodevelopment (myelination and synaptic pruning) and homeostasis in adulthood [27]. Studies show that MMP-9, released by glia and neurons, is directly responsible for pruning PNNs, as shown by increased densities of PNNs following genetic deletion of the MMP-9 gene [28]. Interestingly, antidepressant efficacy in stressed mice has been linked to PNN degradation by MMP-9 [29].

In a recent postmortem study, we identified in depressed suicides a child abuse-associated increase in WFL+ PNNs in the lower layers of the ventromedial prefrontal cortex (vmPFC) [30] a cortical region critically involved in decision-making, impulsivity and suicidal tendencies [31, 32]. The current study sought to explore the impact of child abuse on the regulation of PNNs by microglia in the same brain region. An unbiased MMP antibody array was used to quantify the relative expression of different MMPs in vmPFC using both grey matter lysate and in CD11b-positive ($CD11b^{+}$) isolated microglia. Additionally, canonical microglial markers implicated in ECM modulation such as CD68, CX3CR1, TREM2, IL33R and Cathepsin-S were quantified using enzyme-linked immunosorbent assay (ELISA). This multifaceted approach aimed at assessing

comprehensively the intricate molecular mechanisms underlying the influence of early-life adversity on PNNs in the vmPFC.

Materials and Methods

Human brain samples

The postmortem human brain samples used in this study were provided by the Douglas-Bell Canada Brain Bank (DBCBB) (Montreal, Canada). Brains, donated by familial consent, were acquired by the DBCBB thanks to a collaboration between the McGill Group for Suicide Studies and the Quebec Coroner's Office. A panel of psychiatrists created clinical vignettes for each individual by compiling all available information obtained from medical records, the coroner's report, toxicological analyses, and other sources of information, as described previously [33]. Samples used in this study were from psychiatrically healthy controls (CTRL) and depressed suicides with a history of severe child abuse (DS-CA). Non-random childhood abuse (sexual, physical and neglect) was assessed through a standardized psychological autopsy with next of kin, using a modified version of the Childhood Experience of Care and Abuse (CECA) [34]. Only the most severe cases (score of 1-2) occurring before the age of 15 were included in the DS-CA group. Any indication of neurodevelopmental, neurological, or other co-morbid mental illnesses were cause for exclusion. Group characteristics are listed in **Table 1**.

Brains were cut into 0.5cm-thick coronal sections upon arrival at the DBCBB and then flash-frozen in isopentane at -35°C and stored at -80°C until use. Expert staff at the DBCBB dissected vmPFC (Brodmann area 11/12) at the equivalent of plate 3 (approximately -48 mm from the center of the anterior commissure) of the Mai and Paxinos Atlas of the Human Brain [35].

Human MMP Antibody Array

Grey matter was dissected from vmPFC samples and lysed using RIPA buffer (Sigma, St. Louis, MO, USA). Total protein concentration for each sample was measured using a BCA Protein Assay kit (cat # 23225, Thermo Fisher Scientific, Saint-Laurent, Quebec, Canada) with a microplate reader (TECAN) at 562nm. A human MMP antibody array (RayBiotech® C-Series, Human MMP Array C1, Norcross, GA, USA) was used to compare the relative abundance of 10 MMPs and their inhibitors (TIMPs) between CTRL and DS-CA samples according to the manufacturer's protocol. This array allows for the semi-quantitative analysis of MMP-1, -2, -3, -8, -9, -10 and -13 as well as of TIMP-1, -2 and -4. Unfortunately, MMP-10 was removed from the analyses because quantities were too low and outside of the quantifiable range. An antibody array membrane was used per subject, each processed in separate wells of the provided incubation tray, printed side up. Membranes were incubated under constant agitation for 30 mins at room temperature (RT) with 2 ml of blocking buffer. Next, 1 ml of diluted sample containing 150µg of protein was added to each well and incubated overnight at 4°C under constant agitation. Membranes were washed for 5 minutes at RT thrice with Wash Buffer 1 and twice with Wash Buffer 2. Membranes were then incubated with 1 ml of the prepared Biotinylated Antibody Cocktail and incubated overnight at 4°C under constant agitation. Wash Buffer 1 + 2 were used as described above. Membranes were incubated for 2h at RT with 1X HRP-Streptavidin followed by Wash Buffer 1 + 2. Lastly, chemiluminescence detection was completed using the Detection Buffers provided. 2-D densitometry was conducted using ImageJ to detect the spot signal densities. Relative expression was calculated by subtracting background from each spot and normalizing to a reference positive control spot.

$CD11b^+$ microglia isolation

To measure the relative expression of different MMPs in vmPFC microglia, Miltenyi Biotec CD11b MicroBeads (cat # 130-093-634, Gaithersburg, MD, USA) were first utilized to isolate microglia. These beads were developed for the isolation or depletion of human and mouse cells based on their CD11b expression. In humans, CD11b is strongly expressed on myeloid cells such as cerebral microglia, and weakly expressed on NK cells and some activated lymphocytes. Using a 1 cm^3 block of fresh-non-frozen vmPFC, grey matter was dissected and $CD11b^+$ microglia were isolated using a combination of enzymatic and mechanical dissociations following Miltenyi Biotec instructions. The Neural Tissue Dissociation Kit (Papain, cat # 130-092-628, Gaithersburg, MD, USA) and the gentleMACS™ Dissociator (cat # 130-093-235, Gaithersburg, MD, USA) are effective in generating single-cell suspensions from neural tissues prior to subsequent applications, such as MACS® Cell Separation. These steps were followed by application of Debris Removal Solution, which is a ready-to-use density gradient reagent (cat # 130-109-398, Gaithersburg, MD, USA), allowing for a fast and effective removal of cell debris from viable cells after dissociation of various tissue types, while applying full acceleration and full brake during centrifugation. Prior to the positive selection of $CD11b^+$ cells, Myelin Removal Beads were employed for the specific removal of myelin debris from single-cell suspensions (cat # 130-096-433, Gaithersburg, MD, USA). Then, the $CD11b^+$ cells were magnetically labeled with CD11b MicroBeads and the cell suspension was loaded onto a MACS® Column, which was placed in the magnetic field of a MACS Separator. The magnetically labeled $CD11b^+$ cells were retained on the column, while the unlabeled cell fraction, which was depleted of $CD11b^+$ cells ran through the column. The magnetically retained $CD11b^+$ cells were finally eluted following removal of the column from the

magnetic field. Lastly, the $CD11b^+$ cells were processed for Human MMP antibody array as described above.

ELISA

ELISA was employed for quantitative measurement of human CD68 (cluster of differentiation 68), CX3CR1 (CX3C motif chemokine receptor 1), Cathepsin-S (Cat-S), TREM2 (triggering receptor expressed on myeloid cells 2), and IL33R (interleukin 33 receptor/ST2) in vmPFC samples following the manufacturer's instructions. The same samples were used for these experiments and the MMP arrays. Depending on the assay, 50-100 μg total protein and standards were added to antibody pre-coated wells and after addition of conjugated antibodies specific to the analyte of interest (sandwich ELISA) or conjugated-analyte in the case of CD68 (competitive ELISA) microplates were incubated at 37°C for 60 minutes. Substrate addition led to color development in proportion to the amount of the analyte, except for CD68 kit, where the intensity of the color (optical density, OD) was inversely proportional to the CD68 concentration. The reaction was terminated by addition of acidic stop solution and absorbance was read at 450 nm. A standard curve was plotted relating the OD to the concentration of standards. The analyte concentration in each sample was then interpolated from the corresponding standard curve. Optimal sample protein amounts for each ELISA assay were determined in a pilot experiment to ensure OD values would fall within the range of the corresponding standard curve. A detailed description of the procedure is found on MyBioSource.com.

Western Blotting

The same samples were used for MMP array, ELISA and Western Blotting. Tests were conducted to find out whether chondroitinase ABC (chABC) digestion of the samples was necessary prior to Western Blotting. We observed no discernible differences between samples subjected to various durations of chABC digestion (20h, 1h, 30mins) and those left untreated, and thus did not include this step in order to optimize time. 4-12% stain-free gels (Bio-Rad, Hercules, CA, USA) were used to separate proteins based on size. Blots were probed with an antibody for the N-terminal (DIPEN) neo-epitope of aggrecan core protein cleaved by MMP between amino acids PEN341 and 342FFG (clone BC-4, 1:100, cat # 1042002, MDBioproducts, Oakdale, MN, USA). Prior to gel loading, samples were prepared by adding 1X Laemmli Buffer and incubated at 95°C for 5 minutes, followed by centrifugation and subsequent placement on ice for 3 minutes. Equal volumes of each sample (35 µg) were loaded onto the gradient gels and electrophoresis was conducted for 50 minutes at 135 mV in a Bio-Rad chamber containing 1X running buffer, with constant agitation facilitated by a magnetic stir bar. Preceding the 30-minute semi-dry standard protein transfer from the gel to a nitrocellulose membrane, stain-free gels were activated for 45 seconds on a Chemi-doc to capture a total protein control image. Following a 1-hour blocking step in 5% milk in PBS-tween, the primary antibody, also diluted in the same solution, was incubated with the blot overnight at 4°C under continuous agitation. Post-incubation, three 10-minute washes in PBS-Tween were performed, and a secondary Amersham ECL sheep anti-mouse, horseradish peroxidase linked IgG antibody (1:1000, cat # NA931, Cytvia, Marlborough, MA, USA) was subsequently incubated in 1% milk in PBS-tween for 2 hours at room temperature, again under constant agitation. Blots were subjected to three additional 10-minute washes in PBS-Tween

before being exposed to an enhanced chemiluminescence (ECL) solution (1:1) for 1 minute. The blots were imaged on the Chemi-doc system using predefined settings.

Subsequent blot analyses adhered to the guidelines provided by Bio-Rad. Each blot incorporated a reference lane comprising a composite of all samples, serving as an inter-gel control. To succinctly outline the quantification process, the adjusted volume of the 50 kDa band was used to determine the protein mean intensity on the blot, while the adjusted volume for the entire lane on the stain-free gel provided a measure of total protein. Normalization of each sample was achieved by establishing a normalization factor, computed as the ratio of the total protein content of the sample to the adjusted volume of its corresponding stain-free gel. Subsequently, this factor was divided by the corresponding value for the reference lane, yielding a fold-difference. The resultant fold-differences were then compared between the CTRL and DS-CA.

Statistical analyses

Statistical analyses were conducted using GraphPad Prism v10.1.1 (Boston, MA, USA) and SPSS v 29.0 (IBM Corp, Armonk, New York, USA). Outliers were identified using Grubb's method. Distribution and homogeneity of variances were assessed with Shapiro–Wilk and Levene's tests, respectively. Welch's parametric t-test or analysis of variance (ANOVA) was used to compare CTRL (N=9) subjects to DS-CA (N=14). Age and post-mortem interval (PMI) showed no correlation with any of the presented results (**Supplementary Table 1**). pH was correlated with IL33R and TREM2 levels, while type of antidepressant and number of medications was correlated with CX3CR1 levels. Consequently, a one-way analysis of covariance (ANCOVA) was applied, treating group as a fixed factor and pH or medications as a covariate for these variables. A two-

tailed approach was used for all tests and p-values < 0.05 were considered significant. All data is presented as mean ± standard error of the mean unless otherwise specified.

Results

Downregulation of multiple MMPs in vmPFC grey matter of depressed suicides with a history of child abuse

A representative blot of the high-content screening human MMP antibody array used to assess the relative expression of MMPs and TIMPs in vmPFC grey matter is illustrated in **Fig. 1A**. This approach allowed us to measure a significant overall downregulation of MMPs in DS-CA compared to CTRLs. Notably, gelatinase MMP-9 exhibited a significant downregulation in DS-CA ($P = 0.012$) whereas MMP-2 was similar between groups ($P = 0.43$, **Fig. 1B**). Stromelysin MMP-3 was also significantly downregulated in DS-CA vs CTRL samples ($P = 0.012$, **Fig. 1C**), as was collagenase MMP-8 ($P = 0.0022$). Both MMP-1 ($P = 0.060$) and MMP-13 ($P = 0.12$) remained similar between groups (**Fig. 1D**). Interestingly, all three MMP inhibitors displayed significant downregulation in DS-CA: TIMP-1 ($P = 0.0030$), TIMP-2 ($P < 0.0001$) and TIMP-4 ($P = 0.011$, **Fig. 1E**).

Given the ubiquitous secretion of MMPs and TIMPs from nearly all cell types [26], we selectively isolated microglia with $CD11b^+$ magnetic beads from a subset of samples and processed these cells for the MMP array. These measurements of MMPs and TIMPs in microglia are consistent with the results of a previous study demonstrating the capacity of microglia to produce these enzymes [36]. In human vmPFC samples, gelatinase MMP-9 displayed significant downregulation in DS-CA ($P = 0.0062$), while MMP-2 showed no significant changes ($P = 0.067$, **Fig. 2A**). Stromelysin MMP-3 was significantly downregulated in DS-CA ($P = 0.0083$, **Fig. 2B**).

Collagenase MMP-1 was significantly downregulated (P = 0.0027), whereas MMP-8 (P = 0.85) and MMP-13 (P = 0.14) were similar between groups (**Fig. 2C**). All three inhibitors TIMP-1 (P = 0.030), TIMP-2 (P = 0.0042) and TIMP-4 (P = 0.0085) were downregulated in DS-CA compared to CTRL samples (**Fig. 2D**). In sum, the concurrent downregulation of MMP-9, MMP-3 and TIMP-1, -2, -4 in both whole grey matter and isolated microglia suggested a dampening of microglial ECM degradation in DS-CA samples compared to matched controls.

Canonical microglial markers involved in the regulation of PNNs are dampened in DS-CA samples

We then conducted ELISAs to assess other molecules known to be involved in ECM modulation [18-24]. CX3CR1 (ANCOVA: $F(1,19) = 45.49$, $P < 0.001$, **Fig. 3A**) and IL33R (ANCOVA: $F(1,20) = 12.81$, $P = 0.0020$), **Fig. 3B**) were both significantly downregulated in DS-CA compared to CTRL vmPFC. Conversely, CD68 (P = 0.30, **Fig. 3C**), TREM2 (ANCOVA: $F(1,20) = 0.14$, P = 0.91, **Fig. 3D**) and Cat-S (P = 0.062, **Fig. 3E**) levels were similar between groups. To account for the diurnal rhythm of Cat-S [37], subjects were classified into two categories based on time of death (6:00AM to 5:59PM: Day; 6:00PM-5:59AM: Night). Although there was no significant interaction between group and time of death for Cat-S concentration, a general reduction in Cat-S levels was observed in DS-CA subjects. Notably, individuals who died at night exhibited significantly lower Cat-S concentration (ANOVA: time of death x group $F(1,19) = 1.53$, $P = 0.23$; time of death $F(1,19) = 2.40$, $P = 0.14$; group $F(1,19) = 5.55$, $P = 0.029$; followed by Fisher's LSD post-hoc test, **Fig. 3F**).

Lastly, immunoblotting experiments targeting the neo-epitope of aggrecan cleaved by MMPs at the DIPEN terminal (location of cleavage by MMP-2 and MMP-9) in whole grey matter from

the vmPFC revealed a trend towards a significant reduction in the digestion of aggrecan core proteins by gelatinases in vmPFC samples from DS-CA individuals (P = 0.058, **Fig. 3G**).

Discussion

In this study, we sought to explore potential mechanisms underlying the child abuse-associated increase in vmPFC PNNs recently reported by our group [30]. We focused mainly on microglial factors, and more specifically on MMP-mediated regulation. Our results indicating a significant downregulation of MMPs, TIMPs and other factors involved in intercellular communication in vmPFC samples from DS-CA compared to CTRL are consistent with our previous finding of increased PNN density.

Examining the molecular landscape through the MMP antibody array highlighted a reduction in MMP-9 and MMP-3 in DS-CA compared to CTRL, which was evident in both vmPFC whole grey matter lysate and isolated microglia. Furthermore, the decrease in aggrecan core protein cleavage by MMPs, which was nearly statistically significantly, suggests not only a decline in abundance but also a decrease in enzymatic activity of the MMPs. Interestingly, MMPs are synthesized in a pro-form that remains inactive until proteolytic cleavage. Importantly, this cleavage can be regulated by inflammatory mediators including cytokines, chemokines, free radicals and steroids, or even by other MMPs [25]. We also found reduced TIMPs, which implies a broader dysregulation of the homeostatic system or a negative feedback loop where decreased MMP activity results in the need for fewer inhibitors. While the current study represents the first postmortem assessment of MMPs in child abuse victims, polymorphism in the MMP-9 gene has previously been suggested to increase susceptibility to depression, although conflicting reports on MMP-9 levels in depressed patients suggest a complex relationship [38, 39].

In another set of experiments, we measured the levels of microglial canonical markers implicated in phagocytosis and/or ECM regulation, such as CD68, CX3CR1, IL33R, Cat-S and TREM2. Upon exploring mediators of intercellular communication, particularly through neuronal activation of microglial phagocytosis of ECM components, we observed a strong reduction in the microglial receptors of these signals (CX3CR1 and ILL33R) and no change in microglial activation using CD68 or TREM2 as a proxy. Fractalkine signaling (neural CX3CL1 and microglial CX3CR1 interaction) plays a fundamental role in microglial activity and response to the environment. CX3CR1 deficiency has been shown to impair neuron–microglia communication under chronic unpredictable stress leading to a lack of responsiveness by microglia [40]. Furthermore, chemokine receptor CX3CR1 is involved in microglial activation and induction of phagocytotic activity [41]. In a pioneering study by Tansley et al., CX3CR1 knockout (KO) mice subjected to sciatic nerve injury exhibited diminished PNN degradation and reduced lysosomal glycosaminoglycan accumulation within microglia, a stark contrast to the outcomes observed in wild-type mice [24]. Reduced levels of CX3CR1 in the vmPFC of DS-CA might underlie the increased number of PNNs reported in these subjects [30].

In a similar vein, IL33 signaling through IL33R is necessary for proper central nervous system formation and functioning [42]. During neurodevelopment, astrocytic release of IL33 plays a crucial role in activating microglia to clear excessive synapses [43]. Conversely, the expression of neuronal IL33 is experience-dependent, leading to microglial engulfment of ECM in the adult hippocampus [23]. In our study, we found a child abuse-associated downregulation of IL33R, in a brain area exhibiting a child abuse-associated increase in WFL+ PNNs [30]. This suggests a diminished signaling cascade between IL33 and IL33R, resulting in attenuated ECM digestion, as observed by Nguyen and colleagues (2020) in neuronal IL33 knock-outs [23]. Interestingly, IL-33

also has the capacity to induce polarization of microglia towards an anti-inflammatory phenotype via its interaction with IL33R [44], although the intricacies of this pathway remain only partially defined. Interpreting our findings with this information suggests a plausible diminished anti-inflammatory signaling in our subjects, potentially fostering a tendency towards heightened neuroinflammation—a phenomenon already delineated in the context of depression and ELS [5, 6, 9]. However, this is the first study to examine IL33/IL33R pathways in adults who experienced child abuse, warranting further comprehensive investigations to elucidate these intricate mechanisms.

Another noteworthy enzyme, Cat-S, has been proposed as an ECM regulator influenced by the circadian rhythm [37]. Cat-S secreted from microglia contributes to the diurnal variation in cortical neuron spine density through proteolytic changes of peri-synaptic ECM [45]. Both mouse and human brains exhibit diurnal fluctuations of Cat-S expression in microglia that are antiphase to WFL+ PNN densities, with high Cat-S expression being associated with low WFL+ PNN expression. Interestingly, these rhythms are region-specific, as revealed by human thalamic reticular nucleus expressing more WFL+ PNNs at night and fewer during the day, while the amygdala exhibits an inverse pattern [37]. Furthermore, activated Cat-S incubated with mouse brain sections for just 3 hours reduces WFL+ PNNs, while 24 hours eliminates them completely, highlighting microglial Cat-S specific role in PNN degradation [37]. Interestingly Cat-S can promote the generation of soluble CX3CL1 (the CX3CR1 ligand) [46]. The lower expression of Cat-S in individuals with a history of child abuse suggests a reduced availability of CX3CL1 for CX3CR1, indicating that child adversity is associated with both lower Cat-S expression and diminished availability of CX3CL1 for CX3CR1.

During development, microglia exhibit heightened activity, playing a crucial role in shaping and refining immature neural circuits through the regulation of neurogenesis, synaptogenesis and synaptic pruning [1, 12]. Changes in microglial function during this developmental period have been shown to impact these processes, influencing behavior. However, the specific impact of early-life adversity on microglia has remained largely unexplored until recently [11, 47, 48]. A recent study by the Korosi lab, in collaboration with our group, has shown an enduring effect of early-life stress, induced by limited bedding and nesting, on the microglial transcriptome and function under basal and immune-challenged conditions in mice [9]. These effects were found to persist for up to 6 months after exposure to the stress paradigm. In an *in vitro* assay, this study further revealed that microglia exposed to ELS exhibit a reduced capacity for synaptosome phagocytosis in comparison to control microglia [9]. Intriguingly, the ELISA findings in the current study also indicate that the phagocytic capacity of microglia is attenuated by having experienced childhood adversity, as evidenced by lower expression of CX3CR1 and IL33R in the DS-CA group. This observation adds a layer of complexity to our understanding of the prolonged impact of early-life adversity on microglial function and its potential implications for synaptic dynamics in the developing brain.

Our study is not without limitations. First, because of limited availability of matched well-characterized samples, the sample size of this study was relatively modest, particularly for experiments isolating microglia from fresh brain samples. This might have prevented us from making sex- or age-specific observations. Second, our study could not distinguish between microglial subpopulations, which respond to distinct cell types [49, 50]. For instance, there are microglial subpopulations that specifically respond to inhibitory neurons expressing both *Gabbr1* and *Gabbr2*, revealing $GABA_B$ receptiveness [51]. Furthermore, inhibitory synapse editing in the

visual cortex is mediated by microglial MMP-9 [50]. Given that PNNs predominantly surround parvalbumin-expressing inhibitory interneurons, it raises a compelling question: is there a specific link between these microglial subpopulations and the regulation of PNNs surrounding PV inhibitory neurons in the vmPFC? Despite these limitations, our study provides the first evidence supporting a role for microglia in the child abuse-associated increase in PNNs in the mature vmPFC. Combined with our previous report implicating oligodendrocyte precursor cells in this phenomenon [30], these results further highlight that early-life adversity has a lasting impact on glial cells, with consequences for the neuroplasticity of brain circuitries implicated in cognition and mood.

Author contributions

CB, RR and NM conceived the study. GT participated in the acquisition and clinical characterization of the brain samples. CB, RR, GF and MAD contributed to experiments. BG and NM supervised the study. CB conducted data analysis. CB, RR and NM prepared the manuscript and all other authors contributed and approved of its final version.

Acknowledgments

We are deeply indebted to the next of kin who consented to donating the brains of their loved ones.

Funding

This study was funded by a CIHR Project grant to N.M. R.R. and G.F. received fellowships and C.B. a scholarship from the FRQ-S. The Douglas-Bell Canada Brain Bank is supported in part

by platform support grants from the Réseau Québécois sur le Suicide, les Troubles de l'Humeur et les Troubles Associés (FRQ-S), Healthy Brains for Healthy Lives (CFREF), and Brain Canada.

Conflict of interest

The authors declare no conflict of interest.

Figures and figure legends

A

	A	B	C	D	E	F	G	H
1	POS	POS	NEG	NEG	MMP-1	MMP-2	MMP-3	MMP-8
2								
3	MMP-9	MMP-10	MMP-13	TIMP-1	TIMP-2	TIMP-4	NEG	POS
4								

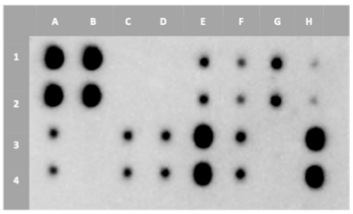

B Gelatinases

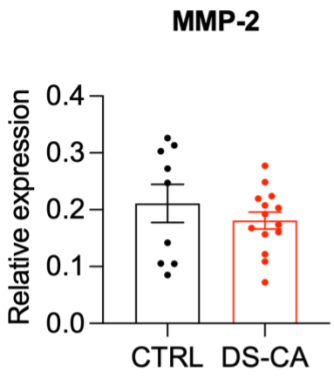

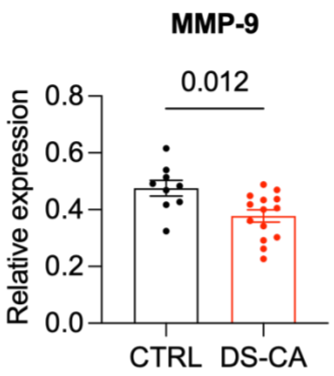

C Stromelysins

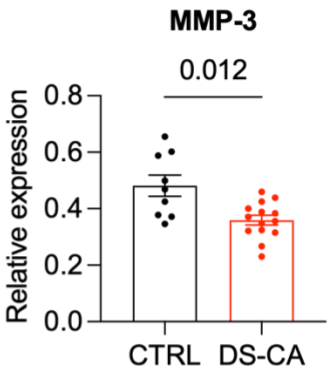

D Collagenases

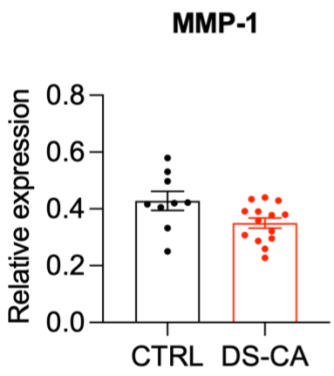

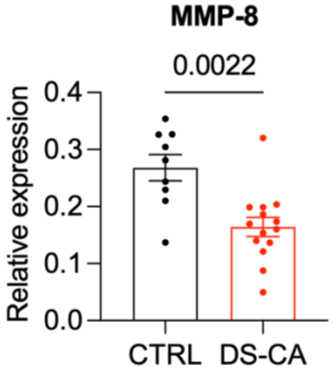

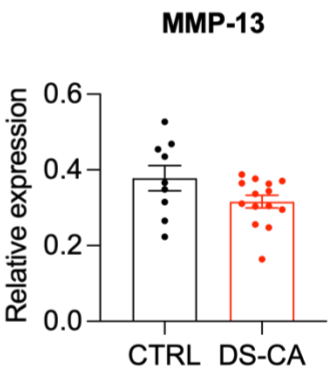

E Endogenous tissue inhibitors

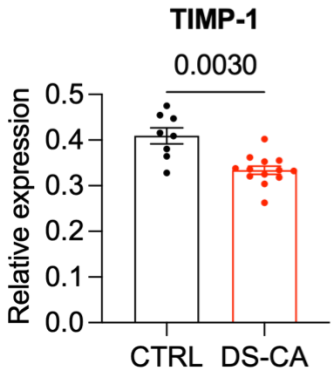

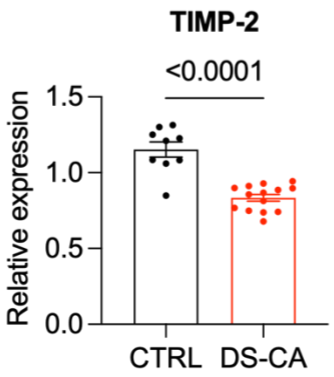

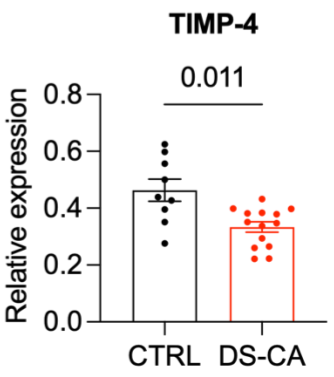

Figure 1: **Most of the examined matrix metalloproteinases and their inhibitors are downregulated in vmPFC grey matter from depressed suicides with a history of child abuse compared to matched controls. A** Map of the human MMP Array (RayBiotec®) used and representative blot. Each antibody is spotted in duplicate on the blot, mean intensity was averaged per antibody as described in the Methods section. **B** MMP-9, **C** MMP-3, **D** MMP-8 and **E** TIMP-1, -2, -4 are significantly decreased in DS-CA compared to CTRL. POS: positive control, NEG: negative control, MMP: matrix metalloproteinase, TIMP: endogenous tissue inhibitor, CTRL: controls, DS-CA: depressed suicides with a history of child abuse

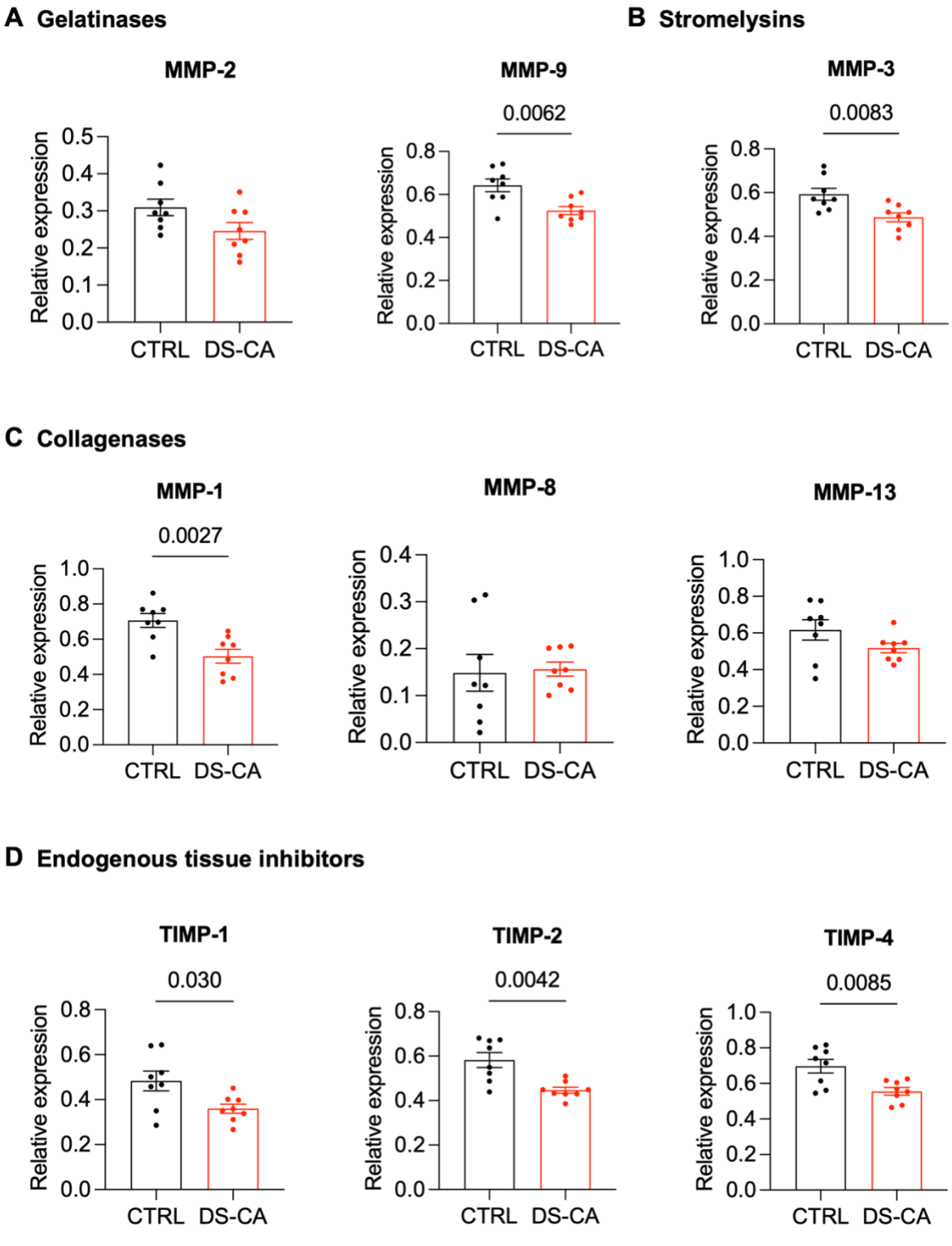
A Gelatinases
B Stromelysins
C Collagenases
D Endogenous tissue inhibitors
MMP-2
MMP-9
MMP-3
MMP-1
MMP-8
MMP-13
TIMP-1
TIMP-2
TIMP-4
0.0062
0.0083
0.0027
0.030
0.0042
0.0085
Relative expression
CTRL
DS-CA

Figure 2: **Microglia secrete less MMPs and TIMPs in vmPFC samples from depressed suicides with a history of child abuse compared to matched controls. A** MMP-9, **B** MMP-3, **C** MMP-1, and **D** TIMP-1, -2, -4 are significantly decreased in microglia isolated from the vmPFC of DS-CA compared to CTRL. MMP: matrix metalloproteinase, TIMP: endogenous tissue inhibitor, CTRL: controls, DS-CA: depressed suicide with a history of child abuse.

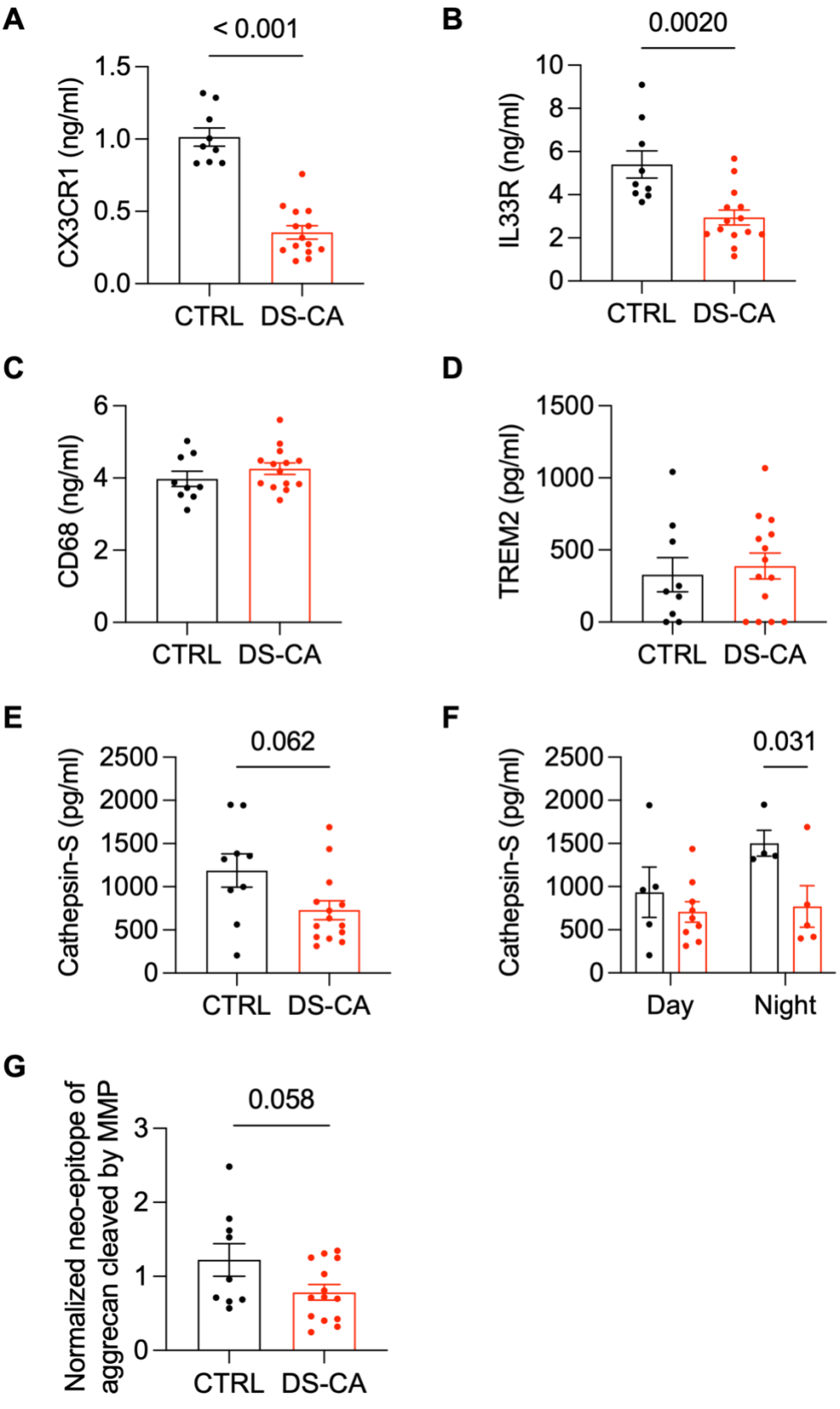
A
< 0.001
CX3CR1 (ng/ml)
1.5
1.0
0.5
0.0
CTRL
DS-CA
B
0.0020
IL33R (ng/ml)
10
8
6
4
2
0
CTRL
DS-CA
C
CD68 (ng/ml)
6
4
2
0
CTRL
DS-CA
D
TREM2 (pg/ml)
1500
1000
500
0
CTRL
DS-CA
E
0.062
Cathepsin-S (pg/ml)
2500
2000
1500
1000
500
0
CTRL
DS-CA
F
0.031
Cathepsin-S (pg/ml)
2500
2000
1500
1000
500
0
Day
Night
G
0.058
Normalized neo-epitope of aggrecan cleaved by MMP
3
2
1
0
CTRL
DS-CA

Figure 3: **Intercellular communication between neurons and microglia is dampened in vmPFC samples from depressed suicides with a history of child abuse compared to matched controls. A** CX3CR1 and **B** IL33R are significantly decreased in DS-CA compared to CTRL as investigated by ELISA. **C** CD68 and **D** TREM2 are not associated with changes associated with child abuse. **E-F** Cathepsin-S levels are significantly lower in DS-CA that died at night (between 6:00PM-5:59AM) **G** The cleavage of aggrecan core protein in DS-CA by MMPs is showing a slight reduction compared to CTRL. CX3CR1: CX3C motif chemokine receptor 1, IL33R: interleukin 33 receptor, CD68: cluster of differentiation 68, TREM2: triggering receptor expressed on myeloid cells 2), ELISA: enzyme-linked immunosorbent assay, MMP: matrix metalloproteinase, CTRL: control, DS-CA: depressed suicide with a history of child abuse.

Tables

Table 1: Group characteristics			
	CTRL	**DS-CA**	**p-value**
N = 23	9	14	
Axis 1 diagnosis	0	MDD (8); DD-NOS (6)	
Age (years)	51.11 ± 12.72	50.07 ± 12.86	0.85
Sex (M/F)	6/3	10/4	
PMI (hours)	58.59 ± 14.62	57.94 ± 14.89	0.92
Tissue pH	6.17 ± 0.23	6.26 ± 0.29	0.44
Substance dependence	0	Alcohol (1); Cannabis (2)	
Medication prescribed in past three months	Benzodiazepines (1)	Benzodiazepines (1); SNRI (2); SSRI (4); SARI (1); Antipsychotic (2); TCA (2); Opioid (1); Anxiolytic (1); GABA analog (1)	
Data presented as mean ± standard deviation			

Supplementary Information

Supplementary Table 1

Spearman's Rho		**MMP1**	**MMP2**	**MMP3**	**MMP8**	**MMP9**	**MMP13**	**TIMP1**	**TIMP2**	**TIMP4**	**CX3CR1**	**IL33R**	**CD68**	**TREM2**	**Cat-S**	**Cleaved aggrecan**
Age	Coef	-0.04	-0.17	-0.07	0.21	-0.0033	-0.19	0.07	0.22	-0.01	0.02	0.35	-0.37	-0.36	-0.12	0.026
	Sig.	0.87	0.46	0.77	0.35	0.99	0.41	0.75	0.34	0.97	0.94	0.10	0.08	0.09	0.59	0.91
PMI	Coef	0.04	0.04	-0.02	0.16	-0.03	-0.15	-0.01	0.09	0.01	-0.02	0.15	0.23	-0.20	0.16	0.15
	Sig.	0.85	0.86	0.93	0.50	0.89	0.53	0.96	0.70	0.98	0.92	0.49	0.29	0.36	0.47	0.49
pH	Coef	-0.10	-0.10	-0.13	-0.31	-0.17	0.01	-0.01	0.06	-0.28	-0.08	-0.52	0.26	0.78	-0.19	-0.27
	Sig.	0.67	0.65	0.58	0.17	0.47	0.96	0.95	0.80	0.21	0.72	0.01	0.23	< 0.00001	0.38	0.21
Type of antidepressants	Coef	-0.20	0.19	-0.21	-0.21	-0.16	-0.018	-0.30	-0.35	-0.18	-0.65	-0.28	0.0080	0.037	-0.35	-0.33
	Sig.	0.38	0.40	0.35	0.35	0.47	0.94	0.18	0.12	0.41	< 0.001	0.20	0.97	0.87	0.12	0.13
Number of medications	Coef	-0.19	0.18	-0.19	-0.24	-0.16	-0.055	-0.32	-0.49	-0.16	-0.59	-0.31	-0.15	-0.13	-0.29	-0.41
	Sig.	0.41	0.41	0.39	0.28	0.47	0.81	0.15	0.021	0.49	0.004	0.16	0.49	0.55	0.19	0.06

Correlation coefficients and P values for Spearman's rho non-parametric measure of association between co-variates and dependent variables. Red = correlation is significant at the 0.05 level (2-tailed).

References

1. Wright-Jin, E.C. and D.H. Gutmann, *Microglia as Dynamic Cellular Mediators of Brain Function.* Trends in Molecular Medicine, 2019. **25**(11): p. 967-979.

2. Javanmehr, N., et al., *Microglia dynamics in aging-related neurobehavioral and neuroinflammatory diseases.* Journal of Neuroinflammation, 2022. **19**(1): p. 273.

3. Li, B., et al., *Stress induced microglial activation contributes to depression.* Pharmacol Res, 2022. **179**: p. 106145.

4. Troubat, R., et al., *Neuroinflammation and depression: A review.* Eur J Neurosci, 2021. **53**(1): p. 151-171.

5. Rahimian, R., et al., *The emerging tale of microglia in psychiatric disorders.* Neurosci Biobehav Rev, 2021. **131**: p. 1-29.

6. Rahimian, R., et al., *Microglial Inflammatory-Metabolic Pathways and Their Potential Therapeutic Implication in Major Depressive Disorder.* Front Psychiatry, 2022. **13**: p. 871997.

7. Torres-Platas, S.G., et al., *Evidence for increased microglial priming and macrophage recruitment in the dorsal anterior cingulate white matter of depressed suicides.* Brain Behav Immun, 2014. **42**: p. 50-9.

8. Schramm, E. and A. Waisman, *Microglia as Central Protagonists in the Chronic Stress Response.* Neurol Neuroimmunol Neuroinflamm, 2022. **9**(6).

9. Reemst, K., et al., *Early-life stress lastingly impacts microglial transcriptome and function under basal and immune-challenged conditions.* Translational Psychiatry, 2022. **12**(1): p. 507.

10. Catale, C., et al., *Microglial Function in the Effects of Early-Life Stress on Brain and Behavioral Development.* J Clin Med, 2020. **9**(2).

11. Bolton, J.L., et al., *Early stress-induced impaired microglial pruning of excitatory synapses on immature CRH-expressing neurons provokes aberrant adult stress responses.* Cell reports, 2022. **38**(13).

12. Crapser, J.D., et al., *Microglia as hackers of the matrix: sculpting synapses and the extracellular space.* Cell Mol Immunol, 2021. **18**(11): p. 2472-2488.

13. Dzyubenko, E. and D.M. Hermann, *Role of glia and extracellular matrix in controlling neuroplasticity in the central nervous system.* Seminars in Immunopathology, 2023. **45**(3): p. 377-387.

14. Pearson, C.S., et al., *Identification of a critical sulfation in chondroitin that inhibits axonal regeneration.* Elife, 2018. **7**.

15. Monnier, P.P., et al., *The Rho/ROCK pathway mediates neurite growth-inhibitory activity associated with the chondroitin sulfate proteoglycans of the CNS glial scar.* Mol Cell Neurosci, 2003. **22**(3): p. 319-30.

16. Tsien, R.Y., *Very long-term memories may be stored in the pattern of holes in the perineuronal net.* Proc Natl Acad Sci U S A, 2013. **110**(30): p. 12456-61.

17. Sigal, Y.M., et al., *Structural maturation of cortical perineuronal nets and their perforating synapses revealed by superresolution imaging.* Proc Natl Acad Sci U S A, 2019. **116**(14): p. 7071-7076.

18. Venturino, A., et al., *Microglia enable mature perineuronal nets disassembly upon anesthetic ketamine exposure or 60-Hz light entrainment in the healthy brain.* Cell Rep, 2021. **36**(1): p. 109313.

19. Sun, J., et al., *Microglia shape AgRP neuron postnatal development via regulating perineuronal net plasticity.* Molecular Psychiatry, 2023.

20. Crapser, J.D., et al., *Microglia facilitate loss of perineuronal nets in the Alzheimer's disease brain.* EBioMedicine, 2020. **58**: p. 102919.

21. Arreola, M.A., et al., *Microglial dyshomeostasis drives perineuronal net and synaptic loss in a CSF1R+/- mouse model of ALSP, which can be rescued via CSF1R inhibitors.* Science Advances, 2021. **7**(35): p. eabg1601.

22. Crapser, J.D., et al., *Microglial depletion prevents extracellular matrix changes and striatal volume reduction in a model of Huntington's disease.* Brain, 2020. **143**(1): p. 266-288.

23. Nguyen, P.T., et al., *Microglial Remodeling of the Extracellular Matrix Promotes Synapse Plasticity.* Cell, 2020. **182**(2): p. 388-403.e15.

24. Tansley, S., et al., *Microglia-mediated degradation of perineuronal nets promotes pain.* Science, 2022. **377**(6601): p. 80-86.

25. Laronha, H. and J. Caldeira, *Structure and Function of Human Matrix Metalloproteinases.* Cells, 2020. **9**(5).

26. Könnecke, H. and I. Bechmann, *The role of microglia and matrix metalloproteinases involvement in neuroinflammation and gliomas.* Clin Dev Immunol, 2013. **2013**: p. 914104.

27. Bitanihirwe, B.K.Y. and T.-U.W. Woo, *A conceptualized model linking matrix metalloproteinase-9 to schizophrenia pathogenesis.* Schizophrenia Research, 2020. **218**: p. 28-35.

28. Wen, T.H., et al., *Genetic Reduction of Matrix Metalloproteinase-9 Promotes Formation of Perineuronal Nets Around Parvalbumin-Expressing Interneurons and Normalizes Auditory Cortex Responses in Developing Fmr1 Knock-Out Mice.* Cerebral Cortex, 2017. **28**(11): p. 3951-3964.

29. Alaiyed, S., et al., *Venlafaxine stimulates PNN proteolysis and MMP-9-dependent enhancement of gamma power; relevance to antidepressant efficacy.* J Neurochem, 2019. **148**(6): p. 810-821.

30. Tanti, A., et al., *Child abuse associates with increased recruitment of perineuronal nets in the ventromedial prefrontal cortex: a possible implication of oligodendrocyte progenitor cells.* Molecular Psychiatry, 2022. **27**(3): p. 1552-1561.

31. Teicher, M.H., et al., *The effects of childhood maltreatment on brain structure, function and connectivity.* Nat Rev Neurosci, 2016. **17**(10): p. 652-66.

32. Hiser, J. and M. Koenigs, *The Multifaceted Role of the Ventromedial Prefrontal Cortex in Emotion, Decision Making, Social Cognition, and Psychopathology.* Biol Psychiatry, 2018. **83**(8): p. 638-647.

33. A. Dumais, B.Sc. ,, et al., *Risk Factors for Suicide Completion in Major Depression: A Case-Control Study of Impulsive and Aggressive Behaviors in Men.* American Journal of Psychiatry, 2005. **162**(11): p. 2116-2124.

34. Bifulco, A., G.W. Brown, and T.O. Harris, *Childhood Experience of Care and Abuse (CECA): a retrospective interview measure.* J Child Psychol Psychiatry, 1994. **35**(8): p. 1419-35.

35. Juergen Mai, M.M., George Paxinos, *Atlas of the Human Brain. 4th Ed*. 2016: Elseiver.

36. Boutej, H., et al., *Diverging mRNA and Protein Networks in Activated Microglia Reveal SRSF3 Suppresses Translation of Highly Upregulated Innate Immune Transcripts.* Cell Rep, 2017. **21**(11): p. 3220-3233.

37. Pantazopoulos, H., et al., *Circadian Rhythms of Perineuronal Net Composition.* eNeuro, 2020. **7**(4).

38. Li, H., et al., *Matrix Metalloproteinase-9 as an Important Contributor to the Pathophysiology of Depression.* Front Neurol, 2022. **13**: p. 861843.

39. Beroun, A., et al., *MMPs in learning and memory and neuropsychiatric disorders.* Cell Mol Life Sci, 2019. **76**(16): p. 3207-3228.

40. Milior, G., et al., *Fractalkine receptor deficiency impairs microglial and neuronal responsiveness to chronic stress.* Brain Behav Immun, 2016. **55**: p. 114-125.

41. Müller, C.E. and T. Claff, *Activated microglia nibbling glycosaminoglycans from spinal cord perineural nets: a new mechanism for neuropathic pain.* Signal Transduct Target Ther, 2022. **7**(1): p. 333.

42. Dwyer, G.K., L.M. D'Cruz, and H.R. Turnquist, *Emerging Functions of IL-33 in Homeostasis and Immunity.* Annu Rev Immunol, 2022. **40**: p. 15-43.

43. Vainchtein, I.D., et al., *Astrocyte-derived interleukin-33 promotes microglial synapse engulfment and neural circuit development.* Science, 2018. **359**(6381): p. 1269-1273.

44. Jia, Z., et al., *IL-33/ST2 Axis: A Potential Therapeutic Target in Neurodegenerative Diseases.* Biomolecules, 2023. **13**(10): p. 1494.

45. Nakanishi, H., *Cathepsin regulation on microglial function.* Biochim Biophys Acta Proteins Proteom, 2020. **1868**(9): p. 140465.

46. Fonović, U.P., Z. Jevnikar, and J. Kos, *Cathepsin S generates soluble CX3CL1 (fractalkine) in vascular smooth muscle cells.* Biol Chem, 2013. **394**(10): p. 1349-52.

47. Johnson, F.K. and A. Kaffman, *Early life stress perturbs the function of microglia in the developing rodent brain: New insights and future challenges.* Brain Behav Immun, 2018. **69**: p. 18-27.

48. Dayananda, K.K., et al., *Early life stress impairs synaptic pruning in the developing hippocampus.* Brain Behav Immun, 2023. **107**: p. 16-31.

49. Ngozi, Z. and J.L. Bolton, *Microglia Don't Treat All Neurons the Same: The Importance of Neuronal Subtype in Microglia-Neuron Interactions in the Developing Hypothalamus.* Frontiers in Cellular Neuroscience, 2022. **16**.

50. Hashimoto, A., et al., *Microglia enable cross-modal plasticity by removing inhibitory synapses*. Cell Rep, 2023. **42**(5): p. 112383.

51. Favuzzi, E., et al., *GABA-receptive microglia selectively sculpt developing inhibitory circuits*. Cell, 2021. **184**(15): p. 4048-4063.e32.

Chapter V: Discussion

Summary of key findings

Overall, our investigations reveal that child abuse leaves lasting cellular and molecular imprints on the developing human brain. Although longitudinal studies at the molecular level in humans are unfeasible, we sought insights through post-mortem brain analysis. The overall findings indicate a child abuse-related increase in WFL+ PNN density and intensity in the vmPFC of depressed suicides. We propose that this phenomenon may be mediated by the upregulation of canonical PNN components in oligodendrocyte precursor cells within the same region, reflecting a precocious maturation often observed in maltreated children.

Furthermore, we provide, for the first time, a detailed account of the sulfation code as detected by LC-MS/MS in the vmPFC, EC, and HPC of healthy individuals who died accidentally. Surprisingly, child abuse doesn't seem to alter the long-lasting composition of PNNs, as evidenced by consistent labeling patterns regardless of abuse status or mood disorder. Our study also suggests a pivotal role for microglia in the enduring increase in PNNs observed in the vmPFC. This is supported by a downregulation in communication between microglia and neurons, along with a decrease in the production of MMPs and their inhibitors in cases of abuse.

Additionally, our examination of a mouse model of ELS mirrors the persistent neuroplasticity issues seen in humans. Notably, mice subjected to limited bedding and nesting from PD2-9 exhibited significantly more WFL+ PNNs in the mPFC. Analysis of the sulfation code and labeling pattern in the mPFC, EC, and vHPC of these animals further underscored their resilience to ELS in terms of PNN composition.

Integration of key findings

Perineuronal net stability

Within the scientific community, the prevailing consensus has been that once formed, PNNs maintain stability throughout life [54, 56, 133]. However, recent research has introduced a new layer of complexity by highlighting the dynamic nature of PNNs. A 2023 pre-print, from the lab of Nobel Prize winner Roger Tsien, suggests that PNN components—ACAN, brevican, HAPLN1, versican and TnR—are as stable as histone H4 and myelin basic protein, both considered to be highly stable, based on ^{15}N isotope labeling experiments [134]. Furthermore, the work by Pantazopolous et al. (2020) reveals that WFL+ PNNs exhibit density variations with the circadian rhythm, primarily due to microglial modulation of Cathepsin-S, evident across multiple regions in the mouse and human brain [135]. This information challenges the previously held belief and implies a level of dynamism in PNNs beyond initial understanding. While the idea of dismantling and reconstructing entire PNNs daily might appear energetically unfavorable, this phenomenon could be attributed to variations in sulfation patterns, leading to differences in WFL labeling. Alternatively, it may involve the turnover of glycosaminoglycan (GAG) side chains without a complete dismantling of the entire PNN structure. This would align with previous studies demonstrating that chABC digestion reduces WFL+ labeling, yet PNN visibility returns after 4-weeks and fully recovers after 5 months post injection in the rat brain, suggesting complete turnover of the GAG side chains [136]. Although, numerous studies suggest that PNNs play a crucial role in long-term memory and circuit stability, with processes from various cell types entering their holes to synapse on the encapsulated neuron [75, 99, 137]. Thus, this evolving perspective raises a fundamental question: if PNNs are indeed undergoing daily changes, how do we reconcile this with the fact that cellular processes enter PNN holes to establish enduring

synaptic connections with the underlying cell? These shifts in understanding prompt an exploration of the intricate mechanisms that may govern the stability and adaptability of PNNs, challenging conventional views and opening new avenues for research in neural plasticity. Although intriguing, studying this intricacy in the postmortem brain proves challenging and is better suited for in vivo imaging or cell culture experiments.

Our discovery of a persistent impact of child abuse on PNNs, when compared to both a healthy control group and a psychopathology group without a history of abuse, yields two crucial insights. Firstly, it highlights that regardless of whether PNNs maintain complete stability throughout life, their maintenance and regulation are susceptible to disruption, leading to enduring alterations in these nets. Secondly, the findings emphasize the significance of stress timing in influencing the disturbance of PNNs. This assertion is grounded in our examination of PNNs in individuals who, despite experiencing no signs of severe abuse during their regular upbringing, experienced life stresses and depression leading to suicide and showed no changes in PNNs. It is striking that we observe an upregulation of PNNs decades after the abuse because there are routine activities that humans take part in that are associated with changes in PNNs. For example, exercising has been associated with a decrease in PNNs throughout the brain [138], while vitamin-D deficiency has been linked to impaired hippocampal memory and decreased PNNs [139]. This underscores the possibility of mitigating the effects of child abuse through intentional changes in daily practices.

Glial regulation of perineuronal nets

Microglia

In this thesis, we explored the regulation of PNNs by microglia through MMPs and intercellular communication with neurons. While our focus centered on these mechanisms, it is essential to acknowledge the existence of potential alternative pathways at play. Notably, the complement pathway plays a crucial role in synaptic restructuring and pruning by microglia [140]. Although no specific evidence has been published on this topic, a study investigating C1q in neurodegenerative brains revealed intriguing findings. C1q mRNA was not only sequestered in activated microglia but was also localized with CSPG (aggrecan) surrounding neurons in the deep cerebellar nucleus and hippocampal CA2 [141]. This discovery raises the possibility that PNNs are actively involved in sequestering C1q, potentially safeguarding the synapses they stabilize or it may suggest that the PNN itself is marked for degradation. This intriguing dual possibility warrants further investigation.

Oligodendrocyte lineage

Our investigation unveiled the involvement of oligodendrocytes in the production of components incorporated into PNNs. This is evident from the exclusive presence of VCAN mRNA in oligodendrocyte precursor cells and the protein's localization within PNNs. However, this revelation opens the door to further exploration of how child abuse impacts myelination. Notably, child abuse has been linked to significant issues in the white matter of the vmPFC in analogous brain samples [19, 20]. Additionally, the interplay between myelin and PNNs, crucial elements in neurodevelopment, remains largely uncharted territory, particularly in the context of their susceptibility to the effects of child abuse.

Astrocytes

While astrocytes are conventionally assumed to play a primary role in producing PNN components [142-145] it's essential to recognize the multifaceted nature of reactive astrocytes. Beyond their conventional functions, reactive astrocytes are capable of phagocytosis [146, 147], suggesting a potential role in PNN degradation under specific circumstances. This complexity underscores the intricacies of the regulatory network involving microglia, PNNs, and other glial components in the aftermath of child abuse.

Limitations

While we explored molecular markers of microglia-PNN interaction, it is imperative to further investigate their spatial relationship within the same brain area through immunohistochemistry. Challenges arise due to the differential staining preferences of microglia and PNNs in distinct tissue preparation methods. Notably, microglia staining in frozen-unfixed tissue lacks reliability, whereas PNN labeling in the same tissue is dependable. While microglia stain well in long-term fixed formalin-stored tissue, many PNN markers in our lab are incompatible with this method. Consequently, we are required to use fresh-fixed brain tissue. This is a process that entails immediate fixation for 24h as samples arrive at the Douglas-Bell Canada Brain Bank. The subsequent characterization of the brain samples spans over 1.5 years. Effectively, we find ourselves navigating this intricate process somewhat blindly, only to discover two years later that certain samples are unsuitable for use. This limitation is a pivotal factor contributing to the small sample size in the microglia isolation (Chapter IV), as it necessitates the use of fresh brain samples. Currently, our lab is engaged in an ongoing follow-up study, exploring the distribution of PNNs

and microglia within said tissue. This investigation aims to discern if their spatial relationship can contribute valuable insights to our overarching narrative.

An additional constraint inherent to using postmortem human brain, particularly those derived from suicide cases, resides in the extended postmortem interval and the inherent variability in tissue quality. In response to this challenge, our studies consistently incorporate meticulous consideration when matching the subjects between groups. The prospect of stratifying our groups based on types of maltreatment is enticing as there is ample evidence suggesting various forms of abuse reveal distinctive long-lasting effects [12, 14, 21, 25]. However, the inherent heterogeneity in lived experiences and the scarcity of brains possessing well-documented histories of abuse that align precisely with all other inclusion criteria renders this impossible. Consequently, we focus exclusively on the most severe cases of child abuse, comparing them to meticulously selected, pristine controls. Moreover, the elevated likelihood of suicide completion among males relative to females in Canada [36] introduces an imbalance in the Douglas-Bell Canada Brain Bank, meaning that obtaining female brain tissue is exceptionally challenging. Thus, our studies contain limited number of female brains, a recognized limitation. Despite this limitation, noteworthy initiatives within the MGSS are dedicated to elucidating sex differences [148, 149]. These endeavors specifically aim to characterize sex-specific distinctions with a shared objective of enhancing our understanding of depression, suicide, and predisposing factors such as child abuse.

Conclusion and future directions

In conclusion, our investigation reveals significant alterations in PNNs following experiences of child abuse. This collection of manuscripts represents an original effort in examining the enduring impact of child abuse on PNNs in the postmortem human brain, with a

specific focus on microglial regulation. For the first time, we characterize the composition of PNNs across both mouse and human brains, conducting a comparative analysis of sulfation code and labeling patterns under both healthy and child abuse conditions. Additionally, our group is the first to delineate the phenotypes of cells enwrapped by WFL+ PNNs in the human brain. Our findings align with rodent literature, indicating that most PNNs surround PV inhibitory interneurons, while a substantial population envelop other inhibitory neurons and some excitatory neurons [150].

An intriguing and yet unanswered question, both in humans and rodents, pertains to the selective formation of PNNs around specific cells. While literature suggest that experience dependent cellular activity triggers PNN formation [151, 152], a comprehensive understanding of why a particular cell recruits a PNN remains elusive. To facilitate this investigation, we have successfully optimized a short staining protocol, enabling the collection of neurons with and without PNNs through laser capture microdissection (LCM). LCM emerges as the optimal method, given the impracticality of using fluorescent-mediated sorting of cells or nuclei for investigating the ECM. Many available protocols rely on protein digestion, specifically designed to degrade the ECM, allowing for the capture and analysis of intracellular information. Moreover, it is noteworthy that, as outlined in this thesis, a universal pan-PNN marker exclusive to PNNs is yet to be identified for sorting purposes. Markedly, WFL labels blood vessels and ACAN is present within neurons and occasionally within glial cells. Additionally, single-nucleus RNA sequencing methods would face challenges in differentiating neurons based on PNN status. LCM serves as a viable approach for identifying PNN status around neurons before embarking on transcriptomic analyses. The ideal scenario would involve specific staining for PV cells, however, the loss of PV antigenicity in frozen non-fixed tissue necessitates the use of either fresh of fixed tissue. However, working with fixed tissue poses challenges in maintaining optimal conditions for RNA health and fresh tissue

entails a prolonged characterization process, as previously mentioned. Despite these complexities, our ongoing efforts are directed towards conducting transcriptomics to enhance our comprehension of PNN formation within the human brain.

The recently published atlas showcasing WFL+ PNNs surrounding PV interneurons throughout the adult mouse brain stands as an incredible asset to the scientific community [153]. However, a comparable resource is currently absent in the characterization of the postmortem human brain. Future studies should focus on creating a similar atlas for the human brain, encompassing neurons more broadly and not solely limited to PV cells. Additionally, the development of such atlases for multiple antibodies against PNN components would be a valuable endeavor for advancing our understanding in this field.

Finally, this thesis represents an original contribution to the field of molecular psychiatry, shedding light on novel factors in the brain that may be implicated in depression, suicide and the enduring consequences of child abuse. Beyond its scientific implications, this research also provides strong arguments when advocating for child protection in various forms. Indeed, I've gained substantial experience in communicating my research to the lay public during my graduate studies and have observed first-hand that the public is even more sensitized to the effect of childhood maltreatment when it learns that cells and connections in the brain are lastingly affected by this type of early-life adversity. This evidence further serves as a valuable resource for policymakers, underscoring the importance of proactive measures to address a healthy and nurturing environment for all children.

References

1. Poggi, G., et al., *NG2-glia: rising stars in stress-related mental disorders?* Molecular Psychiatry, 2023. **28**(2): p. 518-520.
2. Belliveau, C., N. Mechawar, and A. Tanti, *Reply to: "NG2-glia: rising stars in stress-related mental disorders?".* Molecular Psychiatry, 2023. **28**(2): p. 521-522.
3. Bader, D.F., Kristyn, *What do we know about physical and non-physical childhood maltreatment in Canada?*, in *Economic and Social Reports*. 2023.
4. Organization, W.H., *Child maltreatment: Fact Sheet.* 2016.
5. Targum, S.D. and C.B. Nemeroff, *The Effect of Early Life Stress on Adult Psychiatric Disorders.* Innov Clin Neurosci, 2019. **16**(1-2): p. 35-37.
6. Buckingham, E.T. and P. Daniolos, *Longitudinal outcomes for victims of child abuse.* Curr Psychiatry Rep, 2013. **15**(2): p. 342.
7. Dhar, A.K. and D.A. Barton, *Depression and the Link with Cardiovascular Disease.* Frontiers in Psychiatry, 2016. **7**.
8. Jaffee, S.R., *Child Maltreatment and Risk for Psychopathology in Childhood and Adulthood.* Annual Review of Clinical Psychology, 2017. **13**(1): p. 525-551.
9. Afifi, T.O., et al., *Child abuse and mental disorders in Canada.* Canadian Medical Association Journal, 2014. **186**(9): p. E324.
10. Nemeroff, C., *Paradise Lost: The Neurobiological and Clinical Consequences of Child Abuse and Neglect.* Neuron, 2016. **89**(5): p. 892-909.
11. Gerin, M.I., et al., *A systematic review of childhood maltreatment and resting state functional connectivity.* Dev Cogn Neurosci, 2023. **64**: p. 101322.

12. Shrivastava, A.K., et al., *Child sexual abuse and the development of psychiatric disorders: a neurobiological trajectory of pathogenesis.* Ind Psychiatry J, 2017. **26**(1): p. 4-12.

13. Heim, C., et al., *The link between childhood trauma and depression: insights from HPA axis studies in humans.* Psychoneuroendocrinology, 2008. **33**(6): p. 693-710.

14. Noll, J.G., et al., *Childhood Sexual Abuse and Early Timing of Puberty.* J Adolesc Health, 2017. **60**(1): p. 65-71.

15. Richardson, R., et al., *Effects of early-life stress on fear memory in the developing rat.* Current Opinion in Behavioral Sciences, 2016. **7**: p. 15-20.

16. Ibrahim, P., et al., *Molecular impacts of childhood abuse on the human brain.* Neurobiol Stress, 2021. **15**: p. 100343.

17. Warhaftig, G., D. Almeida, and G. Turecki, *Early life adversity across different cell-types in the brain.* Neurosci Biobehav Rev, 2023. **148**: p. 105113.

18. Barnett Burns, S., D. Almeida, and G. Turecki, *The Epigenetics of Early Life Adversity: Current Limitations and Possible Solutions.* Prog Mol Biol Transl Sci, 2018. **157**: p. 343-425.

19. Lutz, P.E., et al., *Association of a History of Child Abuse With Impaired Myelination in the Anterior Cingulate Cortex: Convergent Epigenetic, Transcriptional, and Morphological Evidence.* Am J Psychiatry, 2017. **174**(12): p. 1185-1194.

20. Tanti, A., et al., *Child abuse associates with an imbalance of oligodendrocyte-lineage cells in ventromedial prefrontal white matter.* Mol Psychiatry, 2018. **23**(10): p. 2018-2028.

21. Teicher, M.H., et al., *The effects of childhood maltreatment on brain structure, function and connectivity.* Nat Rev Neurosci, 2016. **17**(10): p. 652-66.

22. van Harmelen, A.L., et al., *Reduced medial prefrontal cortex volume in adults reporting childhood emotional maltreatment.* Biol Psychiatry, 2010. **68**(9): p. 832-8.

23. van Harmelen, A.L., et al., *Hypoactive medial prefrontal cortex functioning in adults reporting childhood emotional maltreatment.* Soc Cogn Affect Neurosci, 2014. **9**(12): p. 2026-33.

24. Ansell, E.B., et al., *Cumulative adversity and smaller gray matter volume in medial prefrontal, anterior cingulate, and insula regions.* Biol Psychiatry, 2012. **72**(1): p. 57-64.

25. Choi, J., et al., *Preliminary evidence for white matter tract abnormalities in young adults exposed to parental verbal abuse.* Biol Psychiatry, 2009. **65**(3): p. 227-34.

26. Hanson, J.L., et al., *Early Neglect Is Associated With Alterations in White Matter Integrity and Cognitive Functioning.* Child Development, 2013. **84**(5): p. 1566-1578.

27. van Harmelen, A.L., et al., *Childhood emotional maltreatment severity is associated with dorsal medial prefrontal cortex responsivity to social exclusion in young adults.* PLoS One, 2014. **9**(1): p. e85107.

28. Underwood, M.D., et al., *Early-Life Adversity, but Not Suicide, Is Associated With Less Prefrontal Cortex Gray Matter in Adulthood.* Int J Neuropsychopharmacol, 2019. **22**(5): p. 349-357.

29. Organization, W.H., *Depression: Fact Sheet.* 2020.

30. Kessler, R.C., *The costs of depression.* Psychiatr Clin North Am, 2012. **35**(1): p. 1-14.

31. Macqueen, G., et al., *Systematic Review of Clinical Practice Guidelines for Failed Antidepressant Treatment Response in Major Depressive Disorder, Dysthymia, and*

Subthreshold Depression in Adults. The Canadian Journal of Psychiatry, 2017. **62**(1): p. 11-23.

32. Ormel, J., et al., *More treatment but no less depression: The treatment-prevalence paradox.* Clinical Psychology Review, 2022. **91**: p. 102111.
33. Sansone, R.A. and L.A. Sansone, *Antidepressant adherence: are patients taking their medications?* Innovations in clinical neuroscience, 2012. **9**(5-6): p. 41-46.
34. Heim, C. and C.B. Nemeroff, *The role of childhood trauma in the neurobiology of mood and anxiety disorders: preclinical and clinical studies.* Biol Psychiatry, 2001. **49**(12): p. 1023-39.
35. Organization, W.H., *Depressive disorder (depression)*. 2023.
36. Canada, G.o., *Suicide in Canada: Key Statistics*. 2023.
37. Wiesel, T.N. and D.H. Hubel, *EFFECTS OF VISUAL DEPRIVATION ON MORPHOLOGY AND PHYSIOLOGY OF CELLS IN THE CATS LATERAL GENICULATE BODY.* J Neurophysiol, 1963. **26**: p. 978-93.
38. Wiesel, T.N., *Postnatal development of the visual cortex and the influence of environment.* Nature, 1982. **299**(5884): p. 583-91.
39. Van der Loos, H. and T.A. Woolsey, *Somatosensory cortex: structural alterations following early injury to sense organs.* Science, 1973. **179**(4071): p. 395-8.
40. Kilgard, M.P., et al., *Sensory input directs spatial and temporal plasticity in primary auditory cortex.* J Neurophysiol, 2001. **86**(1): p. 326-38.
41. Takesian, A.E. and T.K. Hensch, *Balancing plasticity/stability across brain development.* Prog Brain Res, 2013. **207**: p. 3-34.

42. Rudy, B., et al., *Three groups of interneurons account for nearly 100% of neocortical GABAergic neurons.* Developmental Neurobiology, 2011. **71**(1): p. 45-61.

43. Tremblay, R., S. Lee, and B. Rudy, *GABAergic Interneurons in the Neocortex: From Cellular Properties to Circuits.* Neuron, 2016. **91**(2): p. 260-92.

44. Rudy, B., et al., *Three groups of interneurons account for nearly 100% of neocortical GABAergic neurons.* Dev Neurobiol, 2011. **71**(1): p. 45-61.

45. Hensch, T.K., *Critical period plasticity in local cortical circuits.* Nat Rev Neurosci, 2005. **6**(11): p. 877-88.

46. Ferguson, B.R. and W.-J. Gao, *PV Interneurons: Critical Regulators of E/I Balance for Prefrontal Cortex-Dependent Behavior and Psychiatric Disorders.* Frontiers in Neural Circuits, 2018. **12**: p. 37.

47. Hu, H., J. Gan, and P. Jonas, *Interneurons. Fast-spiking, parvalbumin(+) GABAergic interneurons: from cellular design to microcircuit function.* Science, 2014. **345**(6196): p. 1255263.

48. Marin, O., *Developmental timing and critical windows for the treatment of psychiatric disorders.* Nat Med, 2016. **22**(11): p. 1229-1238.

49. Daw, N.W., *Critical periods and amblyopia.* Arch Ophthalmol, 1998. **116**(4): p. 502-5.

50. Ruoslahti, E., *Brain extracellular matrix.* Glycobiology, 1996. **6**(5): p. 489-492.

51. Novak, U. and A.H. Kaye, *Extracellular matrix and the brain: components and function.* J Clin Neurosci, 2000. **7**(4): p. 280-90.

52. Vitellaro-Zuccarello, L., S. De Biasi, and R. Spreafico, *One hundred years of Golgi's "perineuronal net": history of a denied structure.* Ital J Neurol Sci, 1998. **19**(4): p. 249-53.

53. Bruckner, G., et al., *Postnatal development of perineuronal nets in wild-type mice and in a mutant deficient in tenascin-R.* J Comp Neurol, 2000. **428**(4): p. 616-29.

54. Rogers, S.L., et al., *Normal Development of the Perineuronal Net in Humans; In Patients with and without Epilepsy.* Neuroscience, 2018. **384**: p. 350-360.

55. Fawcett, J.W., T. Oohashi, and T. Pizzorusso, *The roles of perineuronal nets and the perinodal extracellular matrix in neuronal function.* Nat Rev Neurosci, 2019. **20**(8): p. 451-465.

56. Mauney, S.A., et al., *Developmental pattern of perineuronal nets in the human prefrontal cortex and their deficit in schizophrenia.* Biol Psychiatry, 2013. **74**(6): p. 427-35.

57. Celio, M.R., et al., *Perineuronal nets: past and present.* Trends Neurosci, 1998. **21**(12): p. 510-5.

58. Balmer, T.S., et al., *Modulation of Perineuronal Nets and Parvalbumin with Developmental Song Learning.* Journal of Neuroscience, 2009. **29**(41): p. 12878-12885.

59. van 't Spijker, H.M. and J.C.F. Kwok, *A Sweet Talk: The Molecular Systems of Perineuronal Nets in Controlling Neuronal Communication.* Frontiers in Integrative Neuroscience, 2017. **11**(33).

60. Lensjø, K.K., et al., *Differential Expression and Cell-Type Specificity of Perineuronal Nets in Hippocampus, Medial Entorhinal Cortex, and Visual Cortex Examined in the Rat and Mouse.* eNeuro, 2017. **4**(3).

61. Engel, M., et al., *Chondroitin sulfate proteoglycans in the developing central nervous system. I. cellular sites of synthesis of neurocan and phosphacan.* J Comp Neurol, 1996. **366**(1): p. 34-43.

62. Schwartz, N.B. and M.S. Domowicz, *Proteoglycans in brain development and pathogenesis.* FEBS Lett, 2018. **592**(23): p. 3791-3805.

63. Deepa, S.S., et al., *Specific molecular interactions of oversulfated chondroitin sulfate E with various heparin-binding growth factors. Implications as a physiological binding partner in the brain and other tissues.* J Biol Chem, 2002. **277**(46): p. 43707-16.

64. Oohashi, T., et al., *The hyaluronan and proteoglycan link proteins: Organizers of the brain extracellular matrix and key molecules for neuronal function and plasticity.* Experimental Neurology, 2015. **274**: p. 134-144.

65. Miyata, S. and H. Kitagawa, *Chondroitin 6-Sulfation Regulates Perineuronal Net Formation by Controlling the Stability of Aggrecan.* Neural Plasticity, 2016. **2016**: p. 1305801.

66. Alonge, K.M., et al., *Quantitative analysis of chondroitin sulfate disaccharides from human and rodent fixed brain tissue by electrospray ionization-tandem mass spectrometry.* Glycobiology, 2019. **29**(12): p. 847-860.

67. Miyata, S., et al., *Persistent cortical plasticity by upregulation of chondroitin 6-sulfation.* Nat Neurosci, 2012. **15**(3): p. 414-22, s1-2.

68. Dick, G., et al., *Semaphorin 3A binds to the perineuronal nets via chondroitin sulfate type E motifs in rodent brains.* J Biol Chem, 2013. **288**(38): p. 27384-95.

69. de Winter, F., et al., *The Chemorepulsive Protein Semaphorin 3A and Perineuronal Net-Mediated Plasticity.* Neural Plast, 2016. **2016**: p. 3679545.

70. Bernard, C. and A. Prochiantz, *Otx2-PNN Interaction to Regulate Cortical Plasticity.* Neural Plast, 2016. **2016**: p. 7931693.

71. Beurdeley, M., et al., *Otx2 Binding to Perineuronal Nets Persistently Regulates Plasticity in the Mature Visual Cortex.* The Journal of Neuroscience, 2012. **32**(27): p. 9429-9437.

72. Lundell, A., et al., *Structural Basis for Interactions between Tenascins and Lectican C-Type Lectin Domains: Evidence for a Crosslinking Role for Tenascins.* Structure, 2004. **12**(8): p. 1495-1506.

73. Kwok, J.C., et al., *Extracellular matrix and perineuronal nets in CNS repair.* Dev Neurobiol, 2011. **71**(11): p. 1073-89.

74. Tsien, R.Y., *Very long-term memories may be stored in the pattern of holes in the perineuronal net.* Proceedings of the National Academy of Sciences, 2013. **110**(30): p. 12456.

75. Tewari, B.P., et al., *Perineuronal nets support astrocytic ion and glutamate homeostasis at tripartite synapses.* Res Sq, 2023.

76. Sigal, Y.M., et al., *Structural maturation of cortical perineuronal nets and their perforating synapses revealed by superresolution imaging.* Proc Natl Acad Sci U S A, 2019. **116**(14): p. 7071-7076.

77. Foscarin, S., et al., *Experience-Dependent Plasticity and Modulation of Growth Regulatory Molecules at Central Synapses.* PLoS ONE, 2011. **6**(1): p. e16666.

78. Lipachev, N., et al., *Quantitative changes in perineuronal nets in development and posttraumatic condition.* Journal of Molecular Histology, 2019. **50**(3): p. 203-216.

79. Laboratories, V., *Wisteria Floribunda Lectin (WFA, WFL), Biotynilated Data Sheet*. 2020.

80. Nadanaka, S., et al., *Reconsideration of the Semaphorin-3A Binding Motif Found in Chondroitin Sulfate Using Galnac4s-6st-Knockout Mice.* Biomolecules, 2020. **10**(11).

81. Härtig, W., et al., *Chondroitin sulfate proteoglycan-immunoreactivity of lectin-labeled perineuronal nets around parvalbumin-containing neurons.* Brain Res, 1994. **635**(1-2): p. 307-11.

82. Matthews, R.T., et al., *Aggrecan glycoforms contribute to the molecular heterogeneity of perineuronal nets.* J Neurosci, 2002. **22**(17): p. 7536-47.

83. Härtig, W., et al., *Update on Perineuronal Net Staining With Wisteria floribunda Agglutinin (WFA).* Front Integr Neurosci, 2022. **16**: p. 851988.

84. Ueno, H., et al., *Expression of aggrecan components in perineuronal nets in the mouse cerebral cortex.* IBRO Rep, 2018. **4**: p. 22-37.

85. Miyata, S., et al., *Structural Variation of Chondroitin Sulfate Chains Contributes to the Molecular Heterogeneity of Perineuronal Nets.* Front Integr Neurosci, 2018. **12**: p. 3.

86. Frischknecht, R., et al., *Brain extracellular matrix affects AMPA receptor lateral mobility and short-term synaptic plasticity.* Nat Neurosci, 2009. **12**(7): p. 897-904.

87. Morawski, M., et al., *Ion exchanger in the brain: Quantitative analysis of perineuronally fixed anionic binding sites suggests diffusion barriers with ion sorting properties.* Sci Rep, 2015. **5**: p. 16471.

88. Wingert, J.C. and B.A. Sorg, *Impact of Perineuronal Nets on Electrophysiology of Parvalbumin Interneurons, Principal Neurons, and Brain Oscillations: A Review.* Front Synaptic Neurosci, 2021. **13**: p. 673210.

89. Balmer, T.S., *Perineuronal Nets Enhance the Excitability of Fast-Spiking Neurons.* eNeuro, 2016. **3**(4): p. ENEURO.0112-16.2016.

90. Dityatev, A., et al., *Activity-dependent formation and functions of chondroitin sulfate-rich extracellular matrix of perineuronal nets.* Developmental neurobiology, 2007. **67**(5): p. 570-588.

91. Christensen, A.C., et al., *Perineuronal nets stabilize the grid cell network.* Nature Communications, 2021. **12**(1): p. 253.

92. Lensjo, K.K., et al., *Removal of Perineuronal Nets Unlocks Juvenile Plasticity Through Network Mechanisms of Decreased Inhibition and Increased Gamma Activity.* J Neurosci, 2017. **37**(5): p. 1269-1283.

93. Carceller, H., et al., *Perineuronal Nets Regulate the Inhibitory Perisomatic Input onto Parvalbumin Interneurons and γ Activity in the Prefrontal Cortex.* J Neurosci, 2020. **40**(26): p. 5008-5018.

94. Suttkus, A., et al., *Aggrecan, link protein and tenascin-R are essential components of the perineuronal net to protect neurons against iron-induced oxidative stress.* Cell Death & Disease, 2014. **5**(3): p. e1119-e1119.

95. Cabungcal, J.H., et al., *Perineuronal nets protect fast-spiking interneurons against oxidative stress.* Proc Natl Acad Sci U S A, 2013. **110**(22): p. 9130-5.

96. Pizzorusso, T., et al., *Reactivation of ocular dominance plasticity in the adult visual cortex.* Science, 2002. **298**(5596): p. 1248-51.

97. Shi, W., et al., *Perineuronal nets protect long-term memory by limiting activity-dependent inhibition from parvalbumin interneurons.* Proc Natl Acad Sci U S A, 2019.

98. Sanchez, B., et al., *From molecules to behavior: Implications for perineuronal net remodeling in learning and memory.* J Neurochem, 2023.

99. Gogolla, N., et al., *Perineuronal nets protect fear memories from erasure.* Science, 2009. **325**(5945): p. 1258-61.

100. Callaghan, B.L. and R. Richardson, *Early-life stress affects extinction during critical periods of development: an analysis of the effects of maternal separation on extinction in adolescent rats.* Stress, 2012. **15**(6): p. 671-9.

101. Slaker, M.L., et al., *Cocaine Exposure Modulates Perineuronal Nets and Synaptic Excitability of Fast-Spiking Interneurons in the Medial Prefrontal Cortex.* eNeuro, 2018. **5**(5).

102. Blacktop, J.M., R.P. Todd, and B.A. Sorg, *Role of perineuronal nets in the anterior dorsal lateral hypothalamic area in the acquisition of cocaine-induced conditioned place preference and self-administration.* Neuropharmacology, 2017. **118**: p. 124-136.

103. Blacktop, J.M. and B.A. Sorg, *Perineuronal nets in the lateral hypothalamus area regulate cue-induced reinstatement of cocaine-seeking behavior.* Neuropsychopharmacology, 2019. **44**(5): p. 850-858.

104. Hensch, T.K. and P.M. Bilimoria, *Re-opening Windows: Manipulating Critical Periods for Brain Development.* Cerebrum : the Dana forum on brain science, 2012. **2012**: p. 11-11.

105. Kohnke, S., et al., *Nutritional regulation of oligodendrocyte differentiation regulates perineuronal net remodeling in the median eminence.* Cell Rep, 2021. **36**(2): p. 109362.

106. Beroun, A., et al., *MMPs in learning and memory and neuropsychiatric disorders.* Cell Mol Life Sci, 2019. **76**(16): p. 3207-3228.

107. Vafadari, B., A. Salamian, and L. Kaczmarek, *MMP-9 in translation: from molecule to brain physiology, pathology, and therapy.* Journal of Neurochemistry, 2016. **139**(S2): p. 91-114.

108. Alaiyed, S., et al., *Venlafaxine stimulates PNN proteolysis and MMP-9-dependent enhancement of gamma power; relevance to antidepressant efficacy.* J Neurochem, 2019. **148**(6): p. 810-821.

109. Alaiyed, S., et al., *Venlafaxine stimulates an MMP-9-dependent increase in excitatory/inhibitory balance in a stress model of depression.* J Neurosci, 2020.

110. Wen, T.H., et al., *Genetic Reduction of Matrix Metalloproteinase-9 Promotes Formation of Perineuronal Nets Around Parvalbumin-Expressing Interneurons and Normalizes Auditory Cortex Responses in Developing Fmr1 Knock-Out Mice.* Cerebral Cortex, 2017. **28**(11): p. 3951-3964.

111. Mascio, G., et al., *Perineuronal nets are under the control of type-5 metabotropic glutamate receptors in the developing somatosensory cortex.* Translational Psychiatry, 2021. **11**(1): p. 109.

112. Bitanihirwe, B.K.Y. and T.W. Woo, *A conceptualized model linking matrix metalloproteinase-9 to schizophrenia pathogenesis.* Schizophr Res, 2020.

113. Pantazopoulos, H., et al., *Extracellular matrix-glial abnormalities in the amygdala and entorhinal cortex of subjects diagnosed with schizophrenia.* Arch Gen Psychiatry, 2010. **67**(2): p. 155-66.

114. Yukawa, T., et al., *Pathological alterations of chondroitin sulfate moiety in postmortem hippocampus of patients with schizophrenia.* Psychiatry Res, 2018. **270**: p. 940-946.

115. Beroun, A., et al., *MMPs in learning and memory and neuropsychiatric disorders.* Cellular and Molecular Life Sciences, 2019. **76**(16): p. 3207-3228.

116. Crapser, J.D., et al., *Microglial depletion prevents extracellular matrix changes and striatal volume reduction in a model of Huntington's disease.* Brain, 2020. **143**(1): p. 266-288.

117. Crapser, J.D., et al., *Microglia facilitate loss of perineuronal nets in the Alzheimer's disease brain.* EBioMedicine, 2020. **58**: p. 102919.

118. Liu, Y.J., et al., *Microglia Elimination Increases Neural Circuit Connectivity and Activity in Adult Mouse Cortex.* J Neurosci, 2021. **41**(6): p. 1274-1287.

119. Spijker, S., M.K. Koskinen, and D. Riga, *Incubation of depression: ECM assembly and parvalbumin interneurons after stress.* Neurosci Biobehav Rev, 2020. **118**: p. 65-79.

120. Riga, D., et al., *Hippocampal extracellular matrix alterations contribute to cognitive impairment associated with a chronic depressive-like state in rats.* Sci Transl Med, 2017. **9**(421).

121. Yu, Z., et al., *Decreased Density of Perineuronal Net in Prelimbic Cortex Is Linked to Depressive-Like Behavior in Young-Aged Rats.* Frontiers in Molecular Neuroscience, 2020. **13**: p. 4.

122. Ohira, K., et al., *Chronic fluoxetine treatment reduces parvalbumin expression and perineuronal nets in gamma-aminobutyric acidergic interneurons of the frontal cortex in adult mice.* Mol Brain, 2013. **6**: p. 43.

123. Fitzgerald, P.J. and B.O. Watson, *Gamma oscillations as a biomarker for major depression: an emerging topic.* Translational Psychiatry, 2018. **8**(1).

124. Fitzgerald, M.L. and S.A. Anderson, *Casting a (Perineuronal) Net: Connecting Early Life Stress to Neuropathological Changes and Enhanced Anxiety in Adults.* Biol Psychiatry, 2019. **85**(12): p. 981-982.

125. Umemori, J., et al., *Distinct effects of perinatal exposure to fluoxetine or methylmercury on parvalbumin and perineuronal nets, the markers of critical periods in brain development.* Int J Dev Neurosci, 2015. **44**: p. 55-64.

126. Santiago, A.N., et al., *Early life trauma increases threat response of peri-weaning rats, reduction of axo-somatic synapses formed by parvalbumin cells and perineuronal net in the basolateral nucleus of amygdala.* J Comp Neurol, 2018. **526**(16): p. 2647-2664.

127. Murthy, S., et al., *Perineuronal Nets, Inhibitory Interneurons, and Anxiety-Related Ventral Hippocampal Neuronal Oscillations Are Altered by Early Life Adversity.* Biol Psychiatry, 2019. **85**(12): p. 1011-1020.

128. Gildawie, K.R., J.A. Honeycutt, and H.C. Brenhouse, *Region-specific Effects of Maternal Separation on Perineuronal Net and Parvalbumin-expressing Interneuron Formation in Male and Female Rats.* Neuroscience, 2020. **428**: p. 23-37.

129. Guadagno, A., et al., *It Is All in the Right Amygdala: Increased Synaptic Plasticity and Perineuronal Nets in Male, But Not Female, Juvenile Rat Pups after Exposure to Early-Life Stress.* J Neurosci, 2020. **40**(43): p. 8276-8291.

130. Catale, C., et al., *Early-life social stress induces permanent alterations in plasticity and perineuronal nets in the mouse anterior cingulate cortex.* Eur J Neurosci, 2022. **56**(10): p. 5763-5783.

131. Young, L., et al., *Damage to ventromedial prefrontal cortex impairs judgment of harmful intent.* Neuron, 2010. **65**(6): p. 845-51.

132. Brown, V.M., et al., *Ventromedial prefrontal value signals and functional connectivity during decision-making in suicidal behavior and impulsivity.* Neuropsychopharmacology, 2020. **45**(6): p. 1034-1041.

133. Tsien, R.Y., *Very long-term memories may be stored in the pattern of holes in the perineuronal net.* Proc Natl Acad Sci U S A, 2013. **110**(30): p. 12456-61.

134. Lev-Ram, V., et al., *Do perineuronal nets stabilize the engram of a synaptic circuit?* bioRxiv, 2023.

135. Pantazopoulos, H., et al., *Circadian Rhythms of Perineuronal Net Composition.* eNeuro, 2020. **7**(4).

136. Brückner, G., et al., *Acute and long-lasting changes in extracellular-matrix chondroitin-sulphate proteoglycans induced by injection of chondroitinase ABC in the adult rat brain.* Exp Brain Res, 1998. **121**(3): p. 300-10.

137. Pyka, M., et al., *Chondroitin sulfate proteoglycans regulate astrocyte-dependent synaptogenesis and modulate synaptic activity in primary embryonic hippocampal neurons.* Eur J Neurosci, 2011. **33**(12): p. 2187-202.

138. Smith, C.C., et al., *Differential regulation of perineuronal nets in the brain and spinal cord with exercise training.* Brain Res Bull, 2015. **111**: p. 20-6.

139. Mayne, P.E. and T.H.J. Burne, *Vitamin D in Synaptic Plasticity, Cognitive Function, and Neuropsychiatric Illness.* Trends Neurosci, 2019. **42**(4): p. 293-306.

140. Presumey, J., A.R. Bialas, and M.C. Carroll, *Complement System in Neural Synapse Elimination in Development and Disease.* Adv Immunol, 2017. **135**: p. 53-79.

141. Lopez, M.E., A.D. Klein, and M.P. Scott, *Complement is dispensable for neurodegeneration in Niemann-Pick disease type C.* Journal of Neuroinflammation, 2012. **9**(1): p. 216.

142. Carulli, D., et al., *Composition of perineuronal nets in the adult rat cerebellum and the cellular origin of their components.* J Comp Neurol, 2006. **494**(4): p. 559-77.

143. Giamanco, K. and R. Matthews, *Deconstructing the perineuronal net: cellular contributions and molecular composition of the neuronal extracellular matrix.* Neuroscience, 2012. **218**: p. 367-384.

144. Dzyubenko, E., C. Gottschling, and A. Faissner, *Neuron-Glia Interactions in Neural Plasticity: Contributions of Neural Extracellular Matrix and Perineuronal Nets.* Neural Plasticity, 2016. **2016**: p. 5214961.

145. Faissner, A., et al., *Contributions of astrocytes to synapse formation and maturation - Potential functions of the perisynaptic extracellular matrix.* Brain Res Rev, 2010. **63**(1-2): p. 26-38.

146. Hobohm, C., et al., *Decomposition and long-lasting downregulation of extracellular matrix in perineuronal nets induced by focal cerebral ischemia in rats.* J Neurosci Res, 2005. **80**(4): p. 539-48.

147. Konishi, H., S. Koizumi, and H. Kiyama, *Phagocytic astrocytes: Emerging from the shadows of microglia.* Glia, 2022. **70**(6): p. 1009-1026.

148. Maitra, M., et al., *Cell type specific transcriptomic differences in depression show similar patterns between males and females but implicate distinct cell types and genes.* Nat Commun, 2023. **14**(1): p. 2912.

149. Labonté, B., et al., *Sex-specific transcriptional signatures in human depression.* Nat Med, 2017. **23**(9): p. 1102-1111.

150. Tanti, A., et al., *Child abuse associates with increased recruitment of perineuronal nets in the ventromedial prefrontal cortex: a possible implication of oligodendrocyte progenitor cells.* Molecular Psychiatry, 2022. **27**(3): p. 1552-1561.

151. McRae, P.A., et al., *Sensory deprivation alters aggrecan and perineuronal net expression in the mouse barrel cortex.* Journal of Neuroscience, 2007. **27**(20): p. 5405-5413.

152. Lander, C., et al., *A family of activity-dependent neuronal cell-surface chondroitin sulfate proteoglycans in cat visual cortex.* Journal of Neuroscience, 1997. **17**(6): p. 1928-1939.

153. Lupori, L., et al., *A comprehensive atlas of perineuronal net distribution and colocalization with parvalbumin in the adult mouse brain.* Cell Rep, 2023. **42**(7): p. 112788.

Appendix

A. Permission from co-first-authors

Arnaud TANTI
UMR INSERM 1253 – iBrain
Equipe 2 : Experimental and Translational Psychiatry
UFR Sciences et Techniques
Parc Grandmont
37200 TOURS

FRANCE
Tours,
January 15th 2024

Subject : Permission to use authorship

To Whom it May Concern,

I confirm that Claudia Belliveau, PhD candidate in Dr Naguib Mechawar's laboratory (McGill), can use the following published article: *Child abuse associates with increased recruitment of perineuronal nets in the ventromedial prefrontal cortex: a possible implication of oligodendrocyte progenitor cells* (*link to publication*), which she co-first authored, as part of her manuscript-based thesis. I also confirm that this material will not be used as part of another manuscript-based thesis.

Arnaud TANTI,

January 17, 2024

To whom it may concern,

I am Reza Rahimian, a post-doctoral fellow in Dr. Mechawar lab at Douglas Mental Health University Institute. Here I give the permission to Claudia Belliveau (my colleague and PhD student in IPN) to use the manuscript entiltled “Postmortem evidence of a microglial involvement in the child abuse-associated increase of perineuronal nets in the ventromedial prefrontal cortex” as a part of her manuscript-based thesis. Furthermore, I will not use the same manuscript in a thesis anytime in the future.

Please don’t hesitate to contact me if you have any questions in this context.

Best,

Reza Rahimian, Pharm.D, Ph.D

Email: reza.rahimian@mail.mcgill.ca

REZA

B. Significant contribution of thesis author to other works

- Théberge, S., **Belliveau, C.**, Xie, D., Khalaf, R., Perlman, K., Rahimian, R., Davoli, M.A., Turecki, G., Mechawar, N. (2024) Parvalbumin interneurons in human ventromedial prefrontal cortex: a comprehensive post-mortem study of myelination and perineuronal nets in neurotypical individuals and depressed suicides with and without a history of child abuse. *Under review*
- **Belliveau, C.,** Mechawar, N., Tanti, A. (2022) Reply to: "NG2-glia: rising stars in stress-related mental disorders?". *Molecular Psychiatry*.
- Rahimian, R.**, **Belliveau, C**.**, Chen, R., Mechawar, N. (2022) Microglial inflammatory-metabolic pathways and their potential therapeutic implication in major depressive disorder. *Frontiers in Psychiatry*.

  ** shared first authorship
- **Belliveau, C.**, Nagy, C., Escobar, S., Mechawar, N., Turecki, G., Rej, S.*, Torres-Platas, S.G*. (2021) Effects of Mindfulness-Based Cognitive Therapy on Peripheral Markers of Stress and Inflammation in Older-Adults With Depression and Anxiety: A Parallel Analysis of a Randomized Controlled Trial. *Frontiers in Psychiatry: Aging Psychiatry*

  * shared last authorship
- Guadagno, A., **Belliveau, C**., Mechawar, N., Walker, C-D. (2021) Effects of Early Life Stress on the Developing Basolateral Amygdala-Prefrontal Cortex Circuit: The Emerging Role of Local Inhibition and Perineuronal Nets. *Frontiers in Human Neuroscience*.
- O'Leary, L.A., **Belliveau, C.**, Davoli, M.A., Ma, J.C., Tanti, A., Turecki, G., Mechawar, N. (2021) Widespread decease of cerebral vimentin-immunoreactive astrocytes in depressed suicides. *Frontiers in Psychiatry*.

- O'Leary, L.A., Davoli, M.A., **Belliveau, C**., Tanti, A., Ma, J.C., Farmer, W., Murai, K., Mechawar, N. (2020) Characterization of vimentin-immunoreactive astrocytes in the human brain. *Frontiers in Neuroanatomy*.
- Torres-Platas S.G.**, Escobar S.**, **Belliveau C.**, Wu J., Sasi N., Fotso J., Potes A., Thomas Z., Goodman A., Looper K., Segal M., Berlim M., Vasudev A., Moscovitz N., Rej S. (2019) Mindfulness-Based Cognitive Therapy Intervention for the Treatment of Late-Life Depression and Anxiety Symptoms in Primary Care: A Randomized Controlled Trial. *Psychotherapy & Psychosomatics*.

** shared first authorship